EFFECTS OF TITANOCENE DICHLORIDE ON THE FORMATION OF FREE RADICALS IN THE HYDROTREATMENT OF A COAL LIQUID

By

HAROLD HERBERT WANDKE II

Bachelor of Science

in Chemical Engineering

Oklahoma State University

Stillwater, Oklahoma

1984

Submitted to the Faculty of the
Graduate College of the
Oklahoma State University
in partial fulfillment of
the requirements for
the Degree of
MASTER OF SCIENCE
December, 1987

EFFECTS OF TITANOCENE DICHLORIDE ON

THE FORMATION OF FREE RADICALS

IN THE HYDROTREATMENT OF A

COAL LIQUID

Thesis Approved:

Mayis Seapan

Thesis Adviser

Larry E. Halliburton

Robert S. Robinson Jr.

Norman N. Durham

Dean of the Graduate College

ABSTRACT

In hydrotreatment, coking is a major mechanism for catalyst deactivation. Titanocene dichloride has been shown to reduce catalyst coking and to increase hydrotreatment activity. In this study, the effects of titanocene dichloride upon the hydrotreatment of an SRC-II Middle Distillate were investigated, with special attention paid to the phenomenon of product free radical concentration during the catalytic and non-catalytic hydrotreatment processes. The hydrotreated products were analyzed for elemental composition, boiling point distribution, free radical concentration, and iron and titanium concentration. Spent catalyst was analyzed for coke content, surface area, pore volume, and titanium distribution. Variables investigated included the effects of sulfidation time, feed doping with titanocene dichloride, reaction temperature, space time, and gas type upon the hydrotreatment process.

Titanocene dichloride increased the efficiency of the hydrogenation, hydrodenitrogenation, and hydrodeoxygenation reactions during catalytic hydrotreatment, while increasing the amount of the low-boiling fractions of the product. During non-catalytic hydrotreatment, titanocene dichloride decreased the amount of the high-boiling fractions in the product. Monitoring of the presence of free radicals in the

product indicated that the relative concentration of free radicals was constant from room temperature up to 250 C; increased significantly from 250 C to 350 C; and decreased from 350 C to 400 C. The presence of catalyst in the reactor significantly reduced product free radical concentration. Titanocene dichloride in the presence of molecular hydrogen significantly increased the free radical concentration at 250-350 C in a non-catalytic environment. No titanium survived catalytic hydrotreatment. Titanium concentration of the non-catalytic hydrotreated product remained constant from room temperature up to 250 C, and decreased drastically above 250 C.

ACKNOWLEDGEMENTS

This study is not the work of one man; rather, it is the summation of effort exerted by many people for my benefit. I wish to express my gratitude to everyone who assisted me in my work and in my stay here at Oklahoma State University. In particular, I am indebted to my major adviser, Dr. Mayis Seapan, for his guidance, concern, and encouragement during my study. I am also indebted to Jirdsak Tscheikuna for the assistance and guidance that he gave me.

I am also thankful to the other committee members, Dr. Robert L. Robinson, Jr. and Dr. Larry Halliburton, for their advisement during the course of this work. I would like to express my appreciation to Dr. Halliburton and Dr. Chen for their help with all the e.s.r. analysis that was performed.

I would like to thank my co-workers and assistants who rendered invaluable aid to my study: Mark Springer, Robert Newton, J.L. Liu, Raul Adarme, Hasan Qabazard, Mark Williams, Carlos Ruiz, Dan Friedeman, Larry Crynes, David Tice, Gary Martin, Mike Gibson, Randy Smejkal, Kimbra Gaines, Ann Ogglesby, Chad Stewart, and John Carroll.

Special thanks are due to the Department of Energy, the OSU School of Chemical Engineering, and the Phillips Petroleum Corporation for the funding this project and

financial assistance that I recieved during the course of this work.

My wife, Salli, was crucial in encouraging me, supporting me, and aiding me in this work. She drove me to the lab at 4 in the morning; she fed me when I was too busy to feed myself, and she was generally a "second right hand" during my work.

My mother, my step-father, my sisters, and the rest of my family deserve my deepest appreciation for their support, encouragement, and understanding. A special note of thanks goes to Father Jerry Miller, Charlie Vestey, David Duncan, Eric Long, Andy Shook, and Tony Gray for their support and encouragement. And lastly, a special "thank you" goes to my brother-in-law, Brant Sears, for the computer that I used extensively during my work.

This work is dedicated to my mother, JoAnn, and my wife, Salli.

TABLE OF CONTENTS

LIST OF TABLES

LIST OF FIGURES

Figure Page

Figure Page

CHAPTER I

INTRODUCTION

A major problem in catalytic hydrotreatment is the degradation of catalyst activity and selectivity over a long time period. Deactivation takes place due to various mechanisms (Tscheikuna, 1984). One of the major deactivation mechanisms is the coking of catalyst by deposition of carbonaceous materials upon the catalyst surface. Chan (1982) studied the catalyst deactivation in the hydrotreatment of an SRC-II Light Oil doctored with small amounts of bis(cyclopentadienyl) titanium dichloride (commonly known as titanocene dichloride) and hydrotreated over a nickel/molybdenum on alumina catalyst. He observed large improvements in catalyst activity and a decrease in catalyst coking when the feed contained titanocene dichloride.

Tscheikuna (1984) followed up Chan's study by doctoring low- and high-coking model hydrocarbon compounds with minute amounts of titanocene dichloride and hydrotreating the mixture over a nickel/molybdenum on alumina catalyst in a two-stage trickle-bed reactor. He determined that titanocene dichloride affects the catalyst activity and the amount of coking on the catalyst. He also discovered that

titanocene dichloride slowly reacts with Tetralin (tetrahydronapthalene), the low-coking model compound used in his study that is also a common component of coal liquids. He concluded that the differences in hydrogenation activity and coke formation were possibly due to free radicals being generated by titanocene dichloride.

This present study investigated the effects of titanocene dichloride upon the catalytic and non-catalytic hydrotreatment of an SRC-II Middle Distillate. Special attention was paid to the phenomenon of free radical formation during hydrotreatment by using electron spin resonanace (e.s.r.) spectroscopy. Catalytic hydrotreatment with and without titanocene dichloride in the coal liquid feedstock was first investigated, and then temperature-dependent non-catalytic hydrotreatment with and without titanocene dichloride in the coal liquid feedstock was observed. The free radical phenomenon was investigated at all times. Several new instruments and/or methodologies were utilized; including electron spin resonance spectroscopy, simulated distillation via gas chromatography, and sulfur analysis via x-ray fluorescence.

The addition of 50 ppm of titanium as titanocene dichloride to the SRC-II Middle Distillate and hydrotreatment over Shell 324 catalyst improved the hydrogenation, hydrodesulfurization, hydrodenitrogenation, and hydrodeoxygenation of the coal liquid, and had no significant effect upon catalyst coking. Complete

hydrodesulfurization was achieved during all catalytic runs with and without titanocene dichloride. In a non-catalytic environment, the presence of titanocene dichloride or molecular hydrogen had no effect upon the hydrotreatment of the SRC-II Middle Distillate between the temperatures of 25 C and 400 C at 10.44 MPa. Monitoring of the presence of free radicals in the Middle Distillate indicated that the relative concentration of free radicals was constant from room temperature up to 250 C; increased significantly from 250 C to 350 C; and then decreased from 350 C to 400 C. The presence of catalyst in the reactor significantly reduced product free radical concentration. Titanocene dichloride in the presence of molecular hydrogen significantly increased the free radical concentration at 250-350 C in a non-catalytic environment. No titanium survived catalytic hydrotreatment. Titanium concentration of the non-catalytic hydrotreated product remained constant from room temperature up to 250 C, and decreased drastically above 250 C.

CHAPTER II

LITERATURE REVIEW

Current literature on the following topics will be discussed: 1) coal liquids; 2) coal liquid hydrotreatment; 3) electron spin resonance spectroscopy studies of coal liquids; 4) free radicals in hydrotreatment; 5) titanocene dichloride; and 6) role of additives in hydrotreatment.

Coal Liquids

Coal liquids are composed of mostly aromatic and heterocyclic (S-, N-, and O-containing cyclic) compounds. Coal liquids contain various metals, either in organometallic or inorganic form. Major metals in coal liquids include iron, titanium and potassium. Coal liquids can be divided into several different fractions. These fractions are defined as oil (pentane-solubles), asphaltenes (pentane-insolubles/ toluene solubles), preasphaltenes (toluene insolubles/ THF solubles), and residue (THF insolubles) (Monier and Kriz,1985).

There have been many attempts to simulate coal liquids by using various model compounds. Investigators, such as Pratt and Christoverson (1983), Salim and Bell (1984), Girgis and Gates (1985), and Tscheikuna (1984) have used

model compounds to investigate various hydrotreatment reactions.

There have been many attempts to characterize coal liquids and other hydrocarbon feedstocks. These methods include electron spin resonance spectroscopy (Graham, 1986), nuclear magnetic resonance spectroscopy (Thompson and Holmes, 1985), high performance liquid chromatography (Boduszynski, 1985), and mass spectroscopy (Boduszynski, 1985). Results show the complex and diverse composition of coal liquids and that their compositions vary widely according to the type of coal and liquefaction process used.

Coal Liquid Hydrotreatment

There are several methods available to upgrade heavy oils, such as hydrotreatment, high-pressure extraction, and pyrolysis (Beazer,1984). However, the preferred method for upgrading coal liquids is hydrotreatment.

Hydrotreatment is typically carried out in trickle-bed reactors at 300-425 C and 10-20 MPa. A history of trickle-bed reactors is presented by Bhan (1983). He discusses various aspects of trickle-bed reactors, such as the gas-liquid distribution, catalyst wetting, and axial dispersion in the reactor.

When coal liquids are hydrotreated, there occurs a number of reactions that reduce the feed aromaticity and eliminate heterocyclic S-, N-, and O-compounds, as well as

the metals content. The basic reactions are as follows:

Hydrogenation (HYD): Unsaturates--> Saturates;

Hydrodemetallization (HDM):

Organometallics--> Metal Deposits + Hydrocarbons;

Hydrodenitrogenation (HDN):

N-compounds--> Hydrocarbons + Ammonia;

Hydrodesulfurization (HDS):

S-compounds--> Hydrocarbons + Hydrogen Sulfide;

Hydrodeoxygenation (HDO):

O-compounds--> Hydrocarbons + Water.

The catalysts used for hydrotreatment are usually cobalt/molybdenum on alumina or nickel/molybdenum on alumina, with cobalt/molybdenum on alumina being preferred for HDS, and nickel/molybdenum on alumina for HDN. Hydrotreatment catalysts are porous gamma-alumina supports with molybdenum as the active metal and cobalt or nickel as the promoter. As the catalyst is calcined, the promoter ions penetrate the superficial alumina layers and interact with the molybdenum ions (Hallie, 1982). Extremely high calcination temperatures (650-700 C) tend to diminish the catalyst activity, however.

Tischer et. al. (1985) found that catalysts with high metal loadings and wide pores would enhance the conversion of the heavy fraction of an unspecified coal liquid feedstock. They found that nickel/molybdenum on alumina catalysts are superior to nickel/tungsten on alumina catalysts for upgrading coal liquids, and that the optimum

nickel/(molybdenum + nickel) atomic ratio is 0.4. They also found that changing the nickel/molybdenum ratio would not affect the oil conversion or the amount of coke deposition on the catalysts.

Muchnick et al. (1985) found that wide-pore catalysts give better conversion and HDS activity for coal liquids than their conventional counterparts. For sulfided catalysts, the order of ease of reaction is HDS >> HDN > HDO (Pratt and Christoverson, 1983).

The main difficulty of coal liquid hydrotreatment is the lack of any catalyst able to remove heteroatomics and unsaturated compounds from the coal liquids for an extended period of time. In general, catalyst deactivation takes place by 4 basic mechanisms: chemical poisoning, fouling, thermal degradation, and vapor formation (Bartholemew, 1984). For hydrotreatment, catalyst poisoning, coking, and fouling by metals deposition are the primary means of catalyst deactivation.

Heterogenous catalysis involves the adsorption of the reactants onto the catalyst surface, reaction, and then the desorption of the products. Catalyst poisoning is the strong chemisorption of reactants, products, or impurities upon active catalyst sites. Catalyst poisons can be classifed by the chemical species absorbed or the types of reactions poisoned. In coal liquid hydrotreatment, basic nitrogen-compounds can attach to the acidic sites and deactivate the catalyst.

Catalyst fouling, or coking, is produced by the decomposition and condensation of hydrocarbons on the catalyst surface. Much heavier coking is produced when coal liquids, rather than petroleum feedstocks, are hydrotreated. This is due to the higher level of aromaticity of the coal liquid feed, and the tendency for higher operating temperatures during coal liquid hydrotreatment (Haynes, Jr.,1984). Catalyst fouling during coal liquid hydrotreatment is also due to the deposition of metals on the catalyst, blocking the active catalyst sites.

Catalyst poisoning can be prevented by removing the poisoning impurities from the feed prior to hydrotreating the feed. Catalyst coking is due to free radical reactions (Bartholemew, 1984), and can be prevented by using free radical traps, by avoiding coke precursors in the feed, by using additives, and by reducing the acidity of the catalyst surface. Catalyst deactivation due to metals deposition can be prevented by the use of a guard bed (Beazer, 1984) or some other means of removing the metals before hydrotreatment.

Reactor plugging problems due to coking can be avoided by using large-pore catalysts, and by using larger catalyst pellets (Bartholemew, 1984). Wide-pore catalysts also enhance the hydrotreatment reactions (Maloletnev et al., 1984).

Coked catalysts can be regenerated by burning the coke off of the catalyst. The gasification of the coke is

greatly enhanced by the metals on the catalyst surface.

According to Scaroni and Jenkins (1985), nitrogen-containing heterocyclic compounds act as coking precursors because of the preferential adsorption on the acid sites and their prolonged attachment to the catalyst surface. The apparent importance of acid sites on the catalyst surface supports the role of radical cations in the coking process.

Parera et al. (1985) affirmed the role of condensation/dehydrogenation in coking. They state that one way of decreasing these type of reactions is to increase the hydrogen partial pressure, and thus prevent the formation and dehydrogenation of heavy aromatics.

Rudnick and Sinclair (1985) state that the coking tendency of a coker feed is related to the asphaltene and polyaromatic contents of the feed. They found that the coking tendency of the coker feeds were related to their radical concentrations.

The hydrotreatment catalysts are usually much more active with the catalyst metals in the sulfided state, rather than the oxide state (Hallie, 1982). Shell Chemical Company (1981) recommends that sulfiding an oxide catalyst take place in 2 steps. The first step consists of contacting the catalyst with hydrogen sulfide or an organic sulfur compound at low temperatures until the exit gas stream has a hydrogen sulfide concentration of 1000 ppm. The second step consists of increasing the catalyst bed

temperature gradually until the desired operating temperature is reached, while maintaining the exit gas hydrogen sulfide concentration at a level above 1000 ppm. Shell hydrotreatment catalysts are not fully sulfided until they contain 8-10 weight percent sulfur. They recommend that the catalyst be calcined before sulfiding to remove any moisture from the catalyst bed.

Shell also warns that prior to pre-sulfiding, any contact of the catalyst with a hydrogen-rich gas at temperatures above 260 C will result in the reduction of the catalyst metals to a basic state; contact of the oil feedstock with the base metal can result in a high cracking rate, and a high rate of catalyst coking.

Presulfiding can be done using various sulfiding compounds. Presulfiding with a non-spiked sulfur-containing hydrocarbon feedstock is a very time-consuming method, and results in only a moderately-sulfided catalyst. Alternatively, a mixture of 3 to 10 volume percent of hydrogen sulfide in hydrogen can be used to sulfide the catalyst; this method is commonly used in laboratory situations. Finally, a hydrocarbon feedstock can be spiked with a sulfur-containing compound that decomposes at low temperatures, such as carbon disulfide. Best results are obtained using the spiked feedstock method (Hallie, 1982).

Shah (1979) discussed the modelling of trickle-bed reactors. Under certain conditions (no mass-transfer resistance between phases, effective catalyst wetting, no

radial or axial dispersion in the liquid phase across the reactor), a plug-flow kinetics model can be assumed. Jones and Frieman (1970) studied the HDN of a COED oil and observed first-order kinetics. For a plug flow first-order irreversible reaction, the kinetic rate is given by

$$kt=-\ln(C_{out}/C_{in})$$

where

k = first order rate constant, 1/hr

t = space-time, hr

C_{out} = concentration of reactant at outlet

C_{in} = concentration of reactant at inlet.

The rate constant "k" is given by

$$k=k_o \exp[-E/RT]$$

where

k_o = Arrhenius pre-exponential constant, 1/hr

E = activation energy, kcal/mol

R = 0.00198 kcal/(mol*K)

T = reaction temperature, K.

In conclusion, coal liquid hydrotreatment results in the removal of sulfur-, nitrogen-, and oxygen-heterocyclic compounds, the enhancement of the hydrogen/carbon ratio, and removal of metallic compounds in the coal liquid. However, the catalyst can be deactivated by poisoning, coking, and metals-deposition. The coke on the catalyst may be burned off of the catalyst; however, the poisoning and metals deposition are not easily reversed. Finally, the method of

sulfiding the hydrotreatment catalyst is very important to the performance of the catalyst.

E.S.R. Studies of Coal Liquids

Electron spin resonance (e.s.r.) takes place because electrons have a spin angular momentum, and thus, have a spin magnetic moment. The two spin levels (alpha and beta) correspond to two different energy levels, the alpha spin possessing a higher energy level than the beta spin. When a magnetic field is applied across a sample containing unpaired electrons, the sample absorbs energy of a particular wavelength. This absorbance occurs when unpaired electrons with the lower energy level spin flip to the higher energy level spin.

In e.s.r. spectroscopy, a sample is bombarded with microwave radiation of a specific frequency and a varying magnetic field is applied across the sample. The absorbance of the microwave energy is measured and the first derivative of the absorbance versus the magnetic field is plotted.

From the e.s.r. spectrum, information about the free radicals can be obtained. This information includes: 1) whether or not free radicals are present in the sample; 2) what the concentration of the free radicals is; and possibly 3) what the structure of the free radical is.

E.S.R. spectroscopy will detect unpaired electrons in free radicals having one unpaired electron, unpaired electrons in transition-metal complexes, and molecules in

the triplet state (possessing two unpaired electrons). If the sample absorbs microwave energy during a run, an e.s.r. spectrum similar to Figure 1 will be obtained. If no free radicals are present, then no energy will be absorbed, and the spectrum will consist of a horizontal line (Figure 2).

The e.s.r. spectrum is a plot of the derivative dS/dB versus B, where S is the signal (proportional to the amount of energy absorbed by the sample), and B is the applied magnetic field. A relative number of unpaired electron spins can be obtained from the e.s.r spectrum. This number can be compared to a standard containing a known number of unpaired spins and the total number of unpaired spins in the sample can be determined.

The structure of the free radical may be inferred from the g-value of the unpaired electron and the hyperfine structure of the spectrum. The g-value of the electron depends upon the local magnetic field, which can differ from the applied magnetic field. Inorganic free radicals have a g-value in the vicinity of 1.97 to 2.02, organic free radicals at around 2.00, and transition metal ions from 0 to 4 (Atkins, 1978).

The hyperfine structure of the spectrum refers to the splitting of the spectrum into a number of lines (centered on the position of single resonance) due to the different nuclear magnetic moments present around the unpaired electron. These moments can add to or subtract from the local field at the electron. The more magnetic nuclei

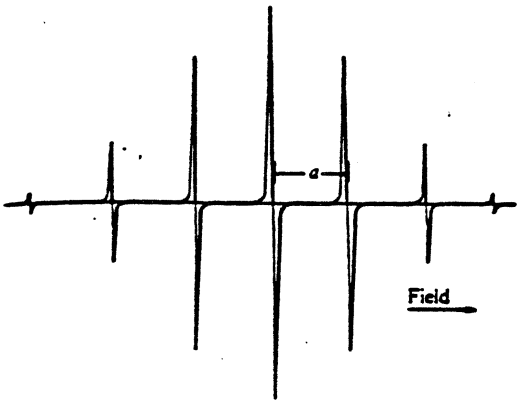

Figure 1. E.S.R. Spectrum for Sample Containing Free Radicals

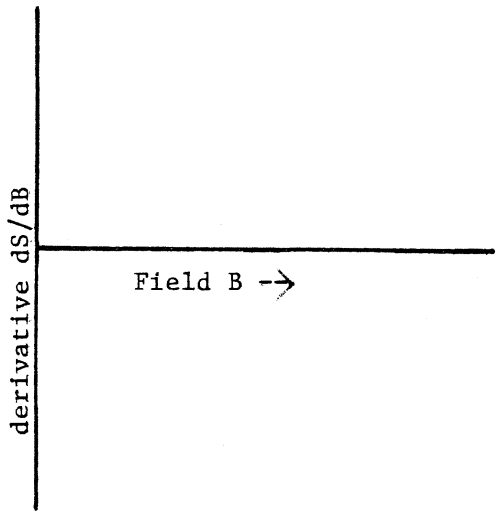

Figure 2. E.S.R. Spectrum for Sample Containing No Free Radicals

present and the greater their spin quantum number, the greater the splitting. From the knowledge of the g-value of the electron and the hyperfine structure of the spectrum, the identity of the free radical can be inferred (Atkins, 1978).

Electron spin resonance spectroscopy is a technique used to examine substances in order to detect unpaired electrons in the substance being examined. Electron spin resonance spectroscopy is often used to examine free radicals and transition metal complexes present in coals and coal liquids. While not all the literature involving e.s.r. and coal liquids can be presented here, the following is representative of recent work in the field.

Stenberg (1985) used e.s.r. while investigating the catalysis mechanism of coal liquefaction by hydrogen sulfide to identify the radicals formed during coal liquefaction. He discovered that the 316 stainless steel reactor walls were acting as a sulfur radical scaveneger during the liquefaction process. The steel wall also promoted the production of unidentifiable high molecular weight compounds.

Dack et. al. (1985) used e.s.r. to study the presence of free radicals and paramagnetic metal ions in Victorian Brown coal. Signals at a g-value around 2 were attributed to organic free radicals, and those at a g-value of about 4.3 were attributed to Fe(III). The Mn(II) ion was also detected in the coal. Metal ion signals were reduced to 0

by the removal of the metal ions by acid washing. The amplitudes of the metal ion signals were changed when the coals were dried. Other paramagnetic ions, such as Mn(II) and Cu(II) when exchanged onto the coal produced their characteristic metal ion spectra. Various different forms of free radicals were found during the investigation.

Graham (1986) used e.s.r. to study the paramagnetic metal species in petroleum and in tar sands. He was able to verify the presence of vanadium, manganese, and iron ions in the samples. He found that e.s.r. is especially useful for detecting metal ions in concentrations of a few ppm, and that the derived magnetic constants are useful in probing the characterization of metals in organic complexes and minerals.

Stenberg et. al. (1985) used e.s.r. to measure the increase in free radical concentration during the pyrolysis of 12 coals of varying ranks between the temperatures of 140 and 400 C. No correlation was found between the net quantity of radicals produced on thermolysis and the percentage conversion to THF-soluble material in liquefaction using either a hydrogen-donor or non-hydrogen-donor solvent. Decker lignite produced a high steady state radical concentration at all temperatures (150-450 C). Wyodak subbituminous and Martin Lake lignite gave large steady state radical concentrations at lower reaction temperatures and low to modest levels at the higher temperatures. Zap, San Mighel and Gascoyne lignites

exhibited reduced levels of radical concentrations at lower temperatures and increasing levels at higher temperatures.

Rudnick and Sinclair (1985) used e.s.r. to measure the free radical concentration of various petroleum-based commercial coker feeds that were heated before analysis, with the temperature ranging from 25 to 350 C; they found that the feeds showed a maximum free radical concentration around 150 to 200 C.

Yamada et al. (1984) used e.s.r. to identify free radicals formed during the heating of a hydrotreated middle distillate. As the oil was heated in an argon atmosphere, the free radical concentration increased, reaching a maximum between 130 and 150 C, and then decreased at higher temperatures. The radical was very stable for the mildly-hydrotreated samples, but the radical in the severely-hydrotreated samples disappeared at temperatures higher than 150 C. When oxygen was introduced in the oil, the radical was converted into semiquinone and/or aryloxy radicals and stable molecules.

Cole et al. (1985) studied the pyrolysis and oxidation of two different coals using e.s.r to measure the free radicals generated as a function of time. They found that initial increases in the organic free radical concentrations were observed at all temperatures, but at the higher temperatures termination reactions caused the increases to be transient. Unweathered coals produced a larger number of radicals than the weathered coals.

Yokono et al. (1985) used in-situ e.s.r. to study the effect of liquefaction catalysts upon coal pyrolysis. They found that the presence of the catalysts increased the concentration of radicals generated during pyrolysis. The order of activity of the catalysts with respect to increase in spin concentration was $ZnCl_2$ (impregnated) >= $ZnCl_2$ (dispersed) > $ZnCl_2$/KCl > $SnCl_2$ > $SbCl_3$ = $AlCl_3$ = $CaCl_2$ > coal alone.

Kim et al. (1984) performed an in-situ free radical quenching experiment inside the e.s.r microwave cavity using a solution flow system to study the quenching of radicals produced by 1,1,2,2-tetraphenylethane by several donor solvents. They found that indane quenched the radicals most quickly, followed by hydrophenanthrene, Tetralin, and cumene, in descending order of quenching rate.

Rudnick and Tueting (1984) carried out coal liquefaction experiments using low- and high-hydrogen content donor solvents, periodically withdrawing samples from the reactor, storing them at cryogenic temperatures, and examining them by e.s.r. They found that the hydrogen-rich solvent was more effective in quenching the radicals produced during liquefaction than the hydrogen-poor solvent was.

In conclusion, many studies have confirmed the use of e.s.r. in identifying and quantifying the presence of free radicals and certain metal ions in coals and coal liquids during pyrolysis, liquefaction, and hydrotreatment.

Free Radicals in Hydrotreatment

The role of free radicals in the hydrotreatment process has been investigated for quite some time. However, the extent of that role is still not known. The following review is representative of recent investigative work.

Ouchi et. al. (1984) heat-treated asphaltenes from coal and coal tar pitch under nitrogen and hydrogen gas. Under nitrogen, thermal decomposition of the asphaltenes produced free radicals that abstracted hydrogen atoms from other molecules to stabilize and produce smaller molecules and gases. Some of the radicals condensed to form heavier solvent-insoluble fractions. Under hydrogen gas, the free radicals were stabilized by the hydrogen to produce smaller molecules and also avoid production of the heavier fraction. The higher the partial pressure of the hydrogen gas was, the lower the yield of the heavier fraction and the greater the yield of the lighter fraction. Higher temperatures accelerated the production of the heavier fractions, while the presence of donor solvents reduced the production of the heavier fractions.

In coal pyrolysis, various types of free radicals are produced. If these free radicals are not quenched quickly by hydrogen-donor solvents, the free radicals will recombine and form heavier molecules (Kim et. al., 1984). Disappearance of the free radicals is generally due to hydrogen abstraction, incorporation with the donor solvent,

or disproportionation.

Suzuki et. al. (1985) found that during coal hydroliquifaction, direct hydrogen transfer from gaseous hydrogen to the coal fragment free radicals on the catalyst surface was much faster than hydrogen abstraction from Tetralin.

The role of carbenes and metal carbene complexes in transition metal-catalyzed reactions is suspected to be quite extensive (Labinger, 1979).

Using model compounds to study the pyrolysis of Tetralin in the presence of molecular hydrogen, Vernon (1980) confirmed the role that molecular hydrogen plays in stabilizing thermally-produced free radicals under coal liquefaction conditions. He found that under some conditions, molecular hydrogen can compete with a good donor solvent in stabilizing free radicals.

In conclusion, the presence of free radicals in coal liquids has a marked effect upon the catalytic hydrotreatment process.

Titanocene Dichloride

Titanium is one of the trace elements found in coal. Although the presence of discrete organic Ti complexes in coals has not been established, there is strong evidence for the formation of organic Ti complexes in coal liquids.

Titanocene dichloride is an organometallic compound with the chemical name of bis(cyclopentadienyl) titanium

dichloride. It is a ferrocene-type molecule, with a titanium atom attached to two chlorine atoms substituted for the iron atom (see Table I). It reacts with water and with polar organic solvents, and is decomposed on silica or glass (Pez and Armor,1981).

Filby et al. (1976) suggest that the formation of organometallic compounds, such as titanocene dichloride, could form during the coal liquefaction process. However, Tscheikuna (1984) found that titanocene dichloride is not stable in Tetralin and other organic compounds commonly found in coal liquids; therefore titanocene dichloride could not be one of the natural organometallic compounds in coal liquids.

Titanium complexes, and titanocene dichloride in particular, catalyze certain isomerization and polymerization reactions (Pez and Armor,1981, Bonds et al.,1975, Labinger,1979). The presence of titanium on Shell 324 catalyst has been found to increase the hydrodenitrogenation of indole without deactivating the catalyst (Lynch,1985).

Chan (1982) doctored an SRC-II Light Oil with titanocene dichloride and hydrotreated the coal liquid over Shell 324 catalyst. The addition of titanocene dichloride improved the hydrodenitrogenation, hydrodesulfurization, hydrodeoxygenation, and hydrogenation activities of the catalyst, and decreased the catalyst coking.

Tscheikuna (1984) doctored model hydrocarbons with

TABLE I

PROPERTIES OF TITANOCENE DICHLORIDE*

Formula	$(C_5H_5)_2TiCl_2$
Structure	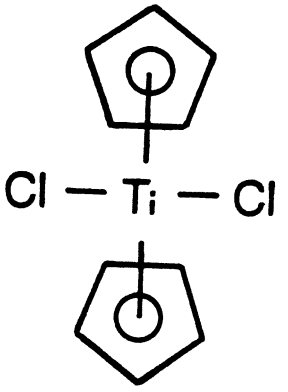
Chemical Name	Bis(cyclopentadienyl) titanium dichloride
Physical Properties	
Molecular Weight	249.0
Form	Crystalline solid
Color	Red
Melting Point	287-289 C (with decomposition)
Titanium Content (weight %)	19.24%
Chlorine Content (weight %)	28.48%

*From Tscheikuna (1984).

titanocene dichloride and hydrotreated the mixture over Shell 324 catalyst. He observed changes in catalyst activity and coking when titanocene dichloride was added to the feedstock. The changes depended upon the type of feedstock used. When the oil feedstock was pure Tetralin, the presence of titanocene dichloride increased the hydrogenation reaction rate but also increased the coking of the catalyst. When the oil feedstock was 95% Tetralin (by weight) and 5% phenanthrene, the presence of titanocene dichloride decreased the hydrogenation reaction rate but reduced the coking of the catalyst.

In conclusion, the presence of minute amounts of titanocene dichloride (and other titanium compounds) in coal liquids has a marked effect upon the catalytic hydrotreatment of the coal liquids.

Role of Additives in Hydrotreatment

The role of trace amounts of additives to hydrocarbon feedstocks for the promotion of hydrotreatment has been investigated by many authors. The types of additives can range from transition metal complexes (Garg and Givens, 1984) to simple acidic and basic compounds (Salim and Bell, 1984).

Salim and Bell (1984) found that the addition of hydrochloric acid or water promoted the hydrogenation of 3-ring aromatiac and hydroaromatic model compounds over Lewis-acid catalysts such as $ZnCl_2$ or $AlCl_3$; the

catalysts were otherwise inactive without the promoters.

Kukes et al. (1986) added 750 ppm of phosphorous to a hydrocarbon feedstock and then hydrotreated the oil over alumina in a trickle-bed reactor; they discovered an enhancement in the removal of vanadium from the feed by both a homogenous reaction occuring in the feed, and a heterogenous reaction on the catalyst surface.

Garg and Givens (1984) added trace amounts of molybdenum-, nickel-, and cobalt-complexes to a coal liquefaction process and found that the addition of the metals increased coal conversion, oil yield, and solvent quality.

Bearden, Jr. et al. (1979) patented a process that utilizes the dissolving of oil-soluble metal compounds in the hydrocarbon feedstock and converting the compounds into a solid, non-colloidal catalyst that enhanced the catalytic hydrotreatment of the oil. The preferred metal was molybdenum, and best results were achieved by the addition of 10 to 950 ppm of the metal.

Lynch (1985) studied catalyst deactivation by a single titanium compound using an organic (titanium porphyrin) dissolved in a hydrogenated creosote oil. He first deactivated the catalyst with carbonaceous material and metal under coal liquefaction conditions, using the creosote oil (with and without the titanium porphyrin). He then hydrotreated model compounds (dibenzothiophene, indole, napthalene, and dibenzofuran) using the aged catalysts in

order to determine the extent of deactivation. Very little or no catalyst deactivation was noted between the aged catalysts, either with or without titanium, for dibenzothiophene, napthalene, and dibenzofuran; however, the presence of titanium on the aged catalyst actually increased indole conversion over that of the aged catalyst without titanium.

In conlusion, the presence of minute amounts of certain additives to hydrocarbon feedstocks (including coal liquids) before hydrotreatment has been found to enhance the hydrotreatment process.

Summary

1) Characterization by methods such as electron spin resonance spectroscopy, high performance liquid chromatography, mass spectroscopy, and nuclear magnetic resonance spectroscopy show the complex and diverse composition of coal liquids and that their compositions vary widely according to the type of coal and liquefaction process used.

2) Coal liquid hydrotreatment results in the removal of sulfur-, nitrogen-, and oxygen heterocyclic compounds, the enhancement of the hydrogen/carbon ratio, and removal of metal compounds in the coal liquid. However, the catalyst can be deactivated by poisoning, coking, and metals-deposition. The coke on the catalyst may be burned off of the catalyst; however, the poisoning and metals

deposition are not easily reversed. Finally, the method of sulfiding the hydrotreatment catalyst is very important to the performance of the catalyst.

3) Many studies have confirmed the value of using e.s.r. in identifying and quantifying the presence of free radicals and certain metal ions in coals and coal liquids during pyrolysis, liquefaction, and hydrotreatment.

4) The presence of free radicals in coal liquids have a marked effect upon their catalytic hydrotreatment.

5) The presence of small amounts of titanocene dichloride has a marked effect on the catalytic hydrotreatment of the coal liquids.

6) The presence of minute amounts of certain additives to hydrocarbon feedstocks (including coal liquids) before hydrotreatment has been found to enhance the hydrotreatment process.

CHAPTER III

EXPERIMENTAL METHODS AND ANALYSIS

The reactor system used during this study will be described, followed by a discussion of the analysis techniques used to characterize the liquid products and spent catalysts generated during hydrotreatment.

Reactor System

Figure 3 is the flow-diagram of the trickle-bed reactor system used in this study. The system was designed by an earlier investigator (Bhan, 1983) and has been used by several others at Oklahoma State University (Tscheikuna, 1984; Beazer, 1984; Newton, 1985). It can be used as either a one- or two-stage reactor; only the top reactor was utilized in this study.

Hydrogen gas flows into the top of the top reactor from a hydrogen cylinder. The incoming hydrogen (reactor) pressure is held constant by a pressure regulator at the hydrogen cylinder. The gas flow rate into the reactor is measured by a high pressure flow meter. The reactor gas pressure is monitored by a Heise pressure gauge. Oil is charged from the feed tank into the Ruska pump, and from the pump into the reactor. The pump pressure is monitored by

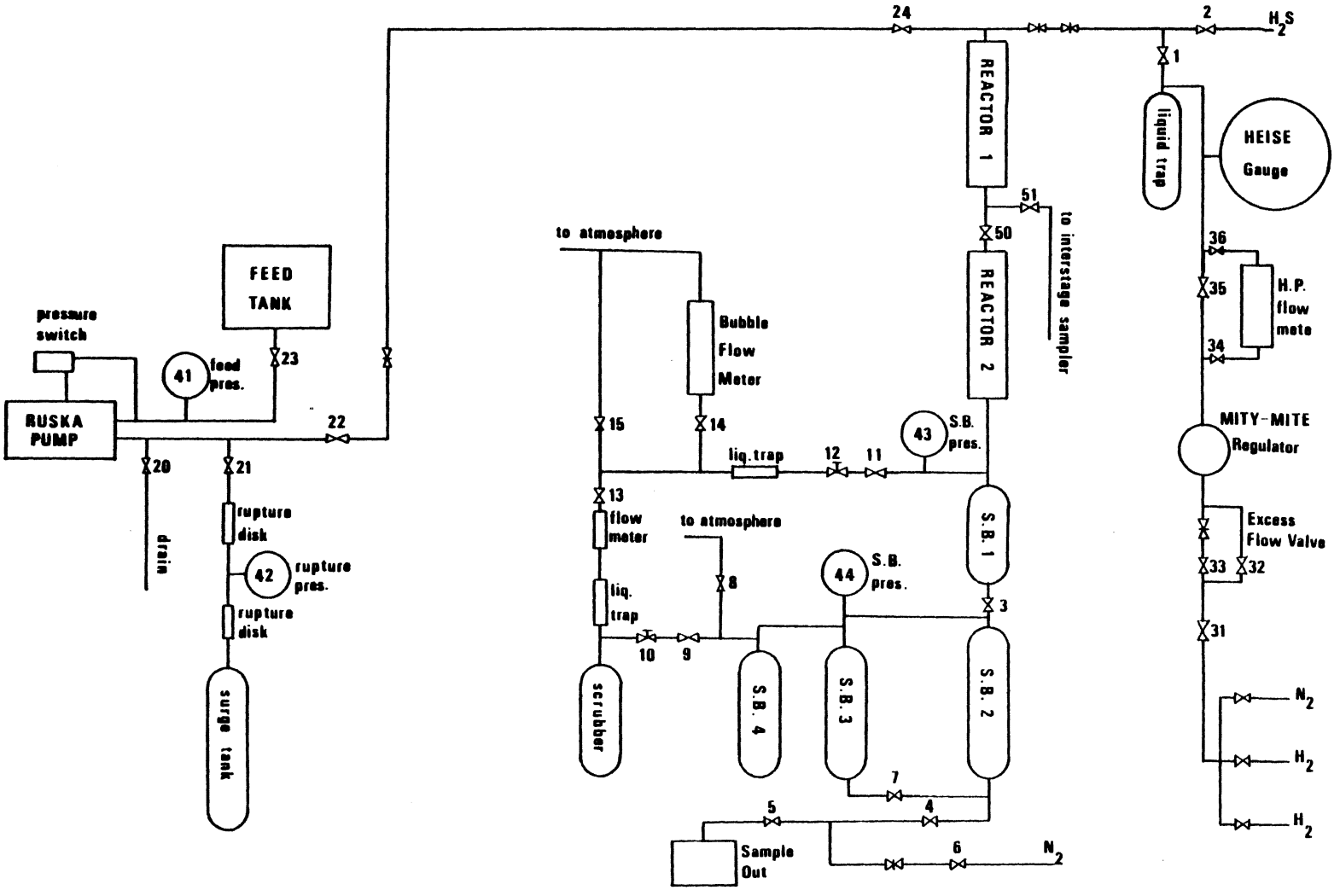

Figure 3. Reactor Diagram

pressure gauge 41. Oil and gas flow cocurrently downward through reactor 1, which is packed with catalyst and/or clipped tubing. An interstage sampling system, capable of taking small liquid samples without disturbing reactor operation is installed at the bottom of the top reactor. Product oil and gas flow through sample bomb 1 into sample bomb 2, and are separated. The pressure of the first sample bomb, which is the reactor downstream pressure, is monitored by pressure gauge 43. Pressure gauge 44 measures the pressure of the second sample bomb.

The third sample bomb is used to collect the liquid. Sample bomb 4 is used to knock out any leftover liquid in the gas stream. Valve 10 controls the outlet gas flow rate. A scrubber filled with an ethanolamine solution is used to remove hydrogen sulfide from the outlet gas stream. The outlet gas flow rate can be measured either by a bubble flow meter or a low pressure rotameter. The temperatures of the two reactors are controlled separately by two temperature programmer/controllers, or by a system of variacs, and are measured inside the catalyst beds and outside the reactor walls by a digital temperature readout.

Detailed descriptions of the main components of the system and experimental procedures are given in Appendixes A and B.

Oil samples were taken at regular, predetermined times during each experiment. The samples from the interstage sampling system were called E.S.R. samples and were analyzed

by e.s.r. spectroscopy. The accumulated product oil collected in the sample bombs were called the product. After each catalytic run, the reactor was cut and the catalyst was divided into 5 sections, ranging from top to bottom. Each oil sample and catalyst sample was labelled and analyzed.

Sample Analysis

Catalyst samples were analyzed for pore volume, surface area, and coke content; all measurements were made with the coke still on the catalyst. The metal profile inside the catalyst pellets were observed by EDAX. The product samples were analyzed for carbon, hydrogen, and nitrogen (CHN) content by an elemental analyzer and for sulfur content by an x-ray fluorescence sulfur analyzer. Relative boiling point distributions for the liquid samples were obtained by gas chromatography. Atomic absorption was used to determine Fe and Ti content in the liquid samples. E.S.R. samples were analyzed by e.s.r. spectroscopy for Fe(III) and free radical concentrations.

Catalyst Characterization

The catalyst from each reactor was separated into 5 different sections, ranging from top section (numbered zone 1) to the bottom section (numbered zone 5). Each sample was extracted with tetrahydrofuran in a Soxhlet extraction unit for at least 24 hours.

During surface area/pore volume determination, each sample had to be dried under a vacuum for 5-6 hours at 110 C. After drying, the catalyst was weighed, and placed in a small sample cell. When the sample was evacuated to 200 microns Hg pressure, the sample cell was filled with mercury. The sample cell was then placed in the porisimeter for evaluation. The porosimeter forced the mercury into the pores of the catalyst, measuring the amount of mercury intruded, and thus the sample pore volume was determined. The surface area was calculated by the analyzer from the sample pore volume and pore size distribution.

The coke content for this study was defined as the weight percent of loss of carbonaceous material by burning the catalyst at 600 C for at least 72 hours. The catalyst samples were weighed at room temperature, placed into a crucible, and then placed into the furnace to burn off the coke. After at least 72 hours in the oven, the samples were allowed to cool to room temperature and were then weighed. The amount of coke on the catalyst was calculated by:

weight % coke = [(W1-W2)/W2] X 100%

where

W1=weight of spent catalyst;

W2=weight of burned catalyst.

For catalytic runs, three pellets were decoked for each sample examined; for a few samples, six pellets were decoked to check the precision of the method. The steel pellets that filled the reactor during non-catalytic runs were also

examined for coke; two pellets were decoked for each sample examined. The steel pellets were not extracted before decoking.

EDAX of Catalyst

A JEOL Model JFM-35 Electron Scanning Microscope equipped with an Energy Dispersive X-ray Analyzer was used to determine metals distributions in the spent catalysts. In Energy Dispersive Analysis by X-ray (EDAX), an electron beam is focused to a small diameter (typically 100 Angstroms) and systematically scanned over the area of the specimen under investigation. Collision of the primary beam with the surface of the specimen produces x-rays whose individual energies are characteristic of the elements from which they originate. The X-rays are analyzed to identify each element present and to give a measure of the amount present. Because the beam diameter is small, a profile across the catalyst surface may be obtained.

Product Characterization: Carbon, Hydrogen, and Nitrogen Analysis

A Perkin Elemer elemental analyzer Model 240B was used to determine the weight percent carbon, hydrogen, and nitrogen in the product samples. The elemental analyzer consists of three major sections: combustion furnace, reduction furnace, and detection system. In the combustion furnace, the oil sample is burned at about 960 C in a purified oxygen atmosphere catalyzed by silver tungstate and

magnesium oxide. The gases are carried through the combustion tube by purified helium gas. Sulfur oxides and halogens are removed in the combustion tube by silver vandate, silver oxide, and silver tungstate. The gases are passed through a reduction tube operating at 600 C, where the nitrogen oxides are reduced to N_2. The remaining gases (carbon dioxide, molecular nitrogen, water vapor, and helium) are collected in a mixing volume at a constant temperature until equilibrium is reached. The gases then pass through a series of gas traps and thermal conductivity cells.

Water is trapped by magnesium perchlorate and the difference of thermal conductivity before and after the trap gives the the water content, which corresponds to the hydrogen content of the sample. Carbon dioxide is trapped in Colorcarb absorbent and the carbon reading is read. The remaining gases (molecular nitrogen and helium) are passed through a thermal conductivity cell where the nitrogen content is measured by comparing the signal with that of another cell measuring the thermal conductivity of pure helium.

The elemental analyzer was periodically calibrated with acetanilide to insure proper response at all times.

Sulfur Analysis

A Horiba Model SCFA-200 Sulfur Analyzer was used to determine the amount of sulfur in the accumulated oil

samples. The analyzer operates by X-ray fluorescence. A primary X-ray is generated and is radiated upon the measuring sample or the reference samples, and the X-ray energy (called fluorescence X-ray) specific to each element contained in the sample (such as sulfur) is excited in intensities proportional to each element's concentration. Only the fluorescence X-ray of the sulfur is picked up by an X-ray filter and then converted into an electric pulse proportional to the energy. This pulse is measured over a pre-determined time period.

For each sample, seven readings were taken: two reference standards were analyzed first, then the sample was analyzed three times, and finally the two reference samples were re-analyzed. The readings for each of the two standards were then averaged; then, linear interpolation was used to determine the sulfur concentration for each of the 3 sample readings. Finally, the average of the 3 sample readings was taken to determine the sulfur concentration of the sample.

GC Simulated Distillations

A simulated distillation of coal liquids via gas chromatography was developed and utilized to examine the boiling point behavior of the coal liquids before and after hydrotreatment. The procedure used was similar to ASTM Method D2887-84, where a mixture of normal hydrocarbons is used to calibrate g.c. retention times with the boiling

points of the hydrocarbons. When a complex feedstock, e.g. a coal liquid, is then injected into the g.c. column, the retention time of each component is used to calculate its boiling point, and the boiling point versus cummulative percent area of the chromatogram is calculated. A true boiling point curve of the oil can then be constructed; or, the boiling point distribution may be tabulated. The results may be used to compare the products of one run to another, although they should not be compared to results obtained by other distillation methods.

A Hewlett-Packard Model 5880A gas chromatograph equipped with a Level 4 control terminal was used to simulate the distillations. The column used was a 2-meter 1/8-inch diameter column packed with 10% OV-101 on Chromasorb W-HP, 80/100. Approximately 0.7 microliters of coal liquid sample was injected into the g.c. at the start of each run, and the oven temperature was varied from 40 C to 230 C at a rate of 5 C/minute.

Atomic Absorption

Atomic Absorption (AA) was used to determine the concentrations of iron and titanium in the samples. In AA, a small portion of the sample is vaporized in a flame, and light of a specific wavelength (dependent upon the element of interest) is passed through the flame and absorbed by the element of interest. Generally, the amount of absorbance is proportional to the concentration of the element in the

sample.

During analysis, the samples were diluted with methyl-isobutyl-ketone (MIBK). Standards were prepared with Conostan metallo-organic standards dissolved in MIBK. Pure MIBK was used as a blank to zero the Perkin-Elmer Model 503 AA unit. An air-acetylene mixture was used as the oxidant/fuel combination during iron analysis, and a nitrous oxide-acetylene flame was used during titanium analysis in order to prevent the chemical interferences present in lower temperature flames when air is used as the oxidant.

E.S.R. Analysis

E.S.R. spectroscopy was used to determine relative concentrations of free radicals and Fe(III) ions in the E.S.R. samples, which were obtained directly from the reactor. After sampling, each E.S.R. sample was immediately injected into a quartz tube and then the tube was placed into a dewar filled with liquid nitrogen at 77 K. Cryogenic temperatures were required to "freeze" the free radicals and prevent their concentrations from changing between the time of sampling and time of analysis (Rudnick and Tueting, 1984). When a sufficient number of samples had been collected, they were taken to the E.S.R. lab of the Physics Department of OSU and analyzed by e.s.r. spectroscopy. The instruments used were a Bruker ER200D-SRC console, a Bruker ER082 (155/45) field modulator, a Bruker BE-25 electromagnet, and an IBM ER044 MRDH microwave bridge.

These instruments are located at the Physics Department of the Oklahoma State University and the experiments were conducted under the supervision of Professor Halliburton. The instrument settings were as follows: microwave frequency 9.7 GHz, microwave power 200 mW, modulator frequency 100 kHz, field modulation intensity 10 G, and the time constant 0.2 seconds. The instrument gain, scan range, and scan time were varied to obtain the best reading possible.

CHAPTER IV

RESULTS AND DISCUSSION OF EXPERIMENTAL RUNS

Description of Runs

The objectives of this study were twofold: 1) to determine the effect of titanocene dichloride upon the catalytic and non-catalytic hydrotreatment of a coal liquid; and 2) to determine the relationship between the free radical concentration of the coal liquid during reaction and the results of hydrotreatment.

Eight catalytic and 10 non-catalytic runs were performed for this study. Run E1 was aborted after 12 hours of operation due to a reactor leak. Runs E2 through E4 were undoped catalytic runs designed to determine the kinetics of undoctored hydrotreatment, and to determine suitable reaction conditions for the doctored runs. Runs E5 was aborted at the start due to a valve leak. Run E6 was an aborted run due to a pump breakdown. Run E7 was an 'on/off' run where the oil feedstock was periodically doctored with 50 ppm of titanium as titanocene dichloride in order to test doctored and non-doctored hydrotreatment using the same catalyst. Run E8 was a 60-hour non-catalytic run in which the SRC-II Middle Distillate was periodically doctored with

25 and 50 ppm of titanium as titanocene dichloride in order to test doctored and non-doctored non-catalytic hydrotreatment under the same conditions. Run E9 was performed under same conditions as run E4, except that the feedstock was doctored with 50 ppm of titanium as titanocene dichloride in order to determine the kinetics of doctored hydrotreatment. The conditions of runs E2-E9 are listed in Table II.

Run E8, and runs E10 through E18 were all non-catalytic. Runs E10 through E18 were experiments in which the effects of reaction temperature, type of gas flowing through the reactor, and presence of titanocene dichloride were investigated. The conditions for runs E10-E18 are listed in Table III.

Liquid samples were analyzed for elemental composition (carbon, hydrogen, nitrogen, and sulfur contents; and by difference, oxygen content), metals analysis, and gas chromatographic simulated distillation. ESR samples were analyzed for relative free radical content and relative iron(III) content. The spent catalysts were analyzed for surface area/pore volume, coke content, and titanium distribution. The results of these analyses will be presented and discussed below.

The oil in all these experiments was a Solvent Refined Coal (SRC-II) Middle Distillate which was obtained from the SRC Coal Liquefaction plant of Wilsonville Alabama. The same oil was used from two different containers. Even

TABLE II

REACTION CONDITIONS FOR RUNS
E2 TO E9

RUN E2: CATALYST: 13 G OF SHELL 324
REACTION TEMPERATURE: 375 C
LIQUID FEED RATE: 30 CC/HR
SULFIDING: 1 HOUR @ 250 C
FEED: NO TI
PRESSURE: 10.44 MPa
GAS TYPE: HYDROGEN
GAS FLOW RATE: 400 CC/MIN

RUN E3: CATALYST: 13 G OF SHELL 324
REACTON TEMPERATURE: 350 C
LIQUID FEED RATE: 30 CC/HR
SULFIDING: 1 HOUR @ 250 C
FEED: NO TI
PRESSURE: 10.44 MPa
GAS TYPE: HYDROGEN
GAS FLOW RATE: 400 CC/MIN

RUN E4: CATALYST: 13 G OF SHELL 324
REACTION TEMPERATURE: 350 C (0-50 HRS)
325 C (50-60 HRS)
LIQUID FEED RATE: 30 CC/HR (0-40 HRS)
60 CC/HR (40-60 HRS)
SULFIDING: 200-250 C @ 1 C/HR, 1 HOUR @ 250 C
FEED: NO TI
PRESSURE: 10.44 MPa
GAS TYPE: HYDROGEN
GAS FLOW RATE: 400 CC/MIN

RUN E7: CATALYST: 13 G OF SHELL 324
REACTION TEMPERATURE: 350 C
LIQUID FEED RATE: 30 CC/HR
SULFIDING: 250-350 C @ 1 C/HR, 2 HOURS @ 350 C
FEED: NO TI (0-24 HRS)
50 PPM TI (24-36 HRS)
NO TI (36-48 HRS)
50 PPM TI (48-60 HRS)
PRESSURE: 10.44 MPa
GAS TYPE: HYDROGEN
GAS FLOW RATE: 400 CC/MIN

TABLE II, (CONTINUED)

RUN E8:	CATALYST: NONE REACTION TEMPERATURE: 350 C LIQUID FEED RATE: 30 CC/HR SULFIDING: NONE FEED: NO TI (0-24 HRS) 50 PPM TI (24-36 HRS) NO TI (36-48 HRS) 25 PPM TI (48-60 HRS) PRESSURE: 10.44 MPa GAS TYPE: HYDROGEN GAS FLOW RATE: 400 CC/MIN
RUN E9:	CATALYST: 13 G OF SHELL 324 REACTION TEMPERATURE: 350 C (0-50 HRS) 325 C (50-60 HRS) LIQUID FEED RATE: 30 CC/HR (0-40 HRS) 60 CC/HR (40-60 HRS) SULFIDING: 200-250 C @ 1 C/HR, 1 HOUR @ 250 C FEED: 50 PPM TI PRESSURE: 10.44 MPa GAS TYPE: HYDROGEN GAS FLOW RATE: 400 CC/MIN

TABLE III

CONDITIONS OF RUNS E10-E18

FIRST SET:

TEMPERATURE: 300-400 C
PRESSURE: 10.44 MPa
OIL FEED RATE: 30 CC/HR
GAS FEED RATE: 400 CC/MIN
GAS TYPE AND FEED DOCTORING:
RUN E10: NITROGEN, NO TITANOCENE DICHLORIDE
RUN E11: HYDROGEN, NO TITANOCENE DICHLORIDE
RUN E12: NITROGEN, 50 PPM TI AS TITANOCENE DICHLORIDE
RUN E13: HYDROGEN, 50 PPM TI AS TITANOCENE DICHLORIDE

SECOND SET:

TEMPERATURE: 50-400 C
PRESSURE: 10.44 MPa
OIL FEED RATE: 30 CC/HR
GAS FEED RATE: 400 CC/MIN
GAS TYPE AND FEED DOCTORING:
RUN E14: NITROGEN, 50 PPM TI AS TITANOCENE DICHLORIDE
RUN E15: HYDROGEN, 50 PPM TI AS TITANOCENE DICHLORIDE
RUN E16: HYDROGEN, 200 PPM TI AS TITANOCENE DICHLORIDE
RUN E17: HYDROGEN, NO TITANOCENE DICHLORIDE
RUN E18: NITROGEN, NO TITANOCENE DICHLORIDE

though they were expected to be identical oils, their analysis was slightly different. In runs E2 through E8 the oil from the first 5-gallon container was used. In runs E9 through E18 the oil from the second container was used. An average analysis of the oil is shown in Table IV.

Titanocene dichloride was obtained from the Alfa Chemical Company. The catalyst in all catalytic runs was a commercial Shell 324 Ni-Mo/alumina catalyst. Analysis of the fresh Shell 324 catalyst is presented in Table V.

In non-catalytic runs, the reactor was packed with pieces of 316 stainless steel 1/8-inch (0.32-cm) and 1/4-inch (0.64-cm) outer diameter tubing cut into 1/4-inch lengths by a bolt cutter, effectively sealing off the ends of each piece.

Elemental Analysis

The liquid products from all catalytic runs were analyzed for elemental composition. The results are listed in Table VI, and presented in Figures 4 through 13.

Runs E2 through E4 were preliminary runs and were used to establish the temperature and space-time conditions for the remaining catalytic runs. The temperature and space-time of runs E2 through E4 were varied in order to determine the kinetics of non-doctored hydrotreatment.

Figures 4 through 6 compare the HYD, HDN, and HDO for runs E2 and E3. For run E2, at 375 C, 10.44 MPa and 0.44 hours space-time, a constant nitrogen conversion (about 75%)

TABLE IV

PROPERTIES OF SRC-II MIDDLE
DISTILLATE FEEDSTOCK

	Container #1*	Container #2**
Elemental Analysis		
Carbon	82.1%	85.6%
Hydrogen	9.49%	10.1%
Nitrogen	0.83%	1.1%
Sulfur	0.15%	0.15%
Oxygen (by difference)	7.4%	3.1%
Trace Metal		
Iron (micrograms/liter)	45	30
Titanium (micrograms/liter)	0.	0.
Distillation by Gas Chromatography		
Boiling Fraction	Area %	
<100 C	4.5	
100-150 C	1.0	
150-200 C	25.0	
200-250 C	43.8	
250-300 C	19.8	
300 C+	5.9	

*Sample from E2-Feed
**Sample from E9-Feed

TABLE V

PROPERTIES OF SHELL 324 CATALYST

Chemical Composition (weight %)	
NiO	3.4
MoO3	19.3
Physical Properties	
Geometry	1.6 mm (1/16") extrudate
Surface area, m**2/g	146 (reported)* 191 (measured)
Pore Volume, m**3/g	0.42 (reported)* 0.48 (measured)
Pore size distribution,	
% pore volume in pore diameter, nm	
6	3.6-6.0
11	6.0-8.0
39	8.0-10.0
37	10.0-14.0
8	14.0+

*From Tscheikuna (1984).

TABLE VI

ELEMENTAL ANALYSIS OF RUNS E2-E9

Sample	%N	%C	%H	%S	%O	H/C
E2-FD	0.83	82.1	9.49	0.15	7.4	1.39
E2-12*	0.26	86.0	10.5	0.00	3.2	1.47
-24	0.17	85.5	10.5	0.00	3.8	1.47
-36	0.23	84.5	10.8	0.00	4.5	1.53
-48	0.19	82.3	10.1	0.00	7.4	1.47
-60	0.19	81.1	10.4	0.00	8.3	1.53
E3-12	0.59	82.3	10.6	0.00	6.5	1.55
-24	0.46	87.4	10.7	0.00	1.4	1.47
-36	0.52	85.8	10.2	0.00	3.5	1.43
-48	0.38	84.9	10.0	0.00	4.7	1.41
-60	0.39	86.8	10.8	0.00	2.0	1.49
E4-12	0.61	83.1	10.3	0.98	5.0	1.49
-24	0.37	85.3	10.3	0.03	4.0	1.45
-36	0.20	85.9	10.5	0.00	3.4	1.47
-40	0.27	84.1	10.7	0.00	4.9	1.53
-50	0.60	84.4	9.6	0.00	5.4	1.36
-60	0.85	84.9	9.42	0.00	4.8	1.33
E7-FD	0.73	83.3	8.87	0.15	6.9	1.27
-6	0.81	84.8	11.0	0.34	3.1	1.56
-12	0.16	88.6	11.8	0.00	0.00	1.60
-18	0.17	86.8	11.5	0.00	1.53	1.59
-24	0.20	85.4	11.2	0.00	3.2	1.57
-30	0.21	85.7	11.3	0.00	2.8	1.58
-36	0.28	86.2	10.8	0.00	2.7	1.50
-42	0.22	83.9	10.6	0.00	5.3	1.52
-48	0.27	88.8	10.6	0.00	0.3	1.43
-54	0.24	86.2	10.8	0.00	2.8	1.50
-60	0.29	86.5	10.5	0.00	2.7	1.46
E8-6	0.59	82.3	8.49	0.12	8.5	1.24
-12	0.49	81.9	8.74	0.18	8.7	1.28
-18	0.78	83.1	9.63	0.09	6.4	1.39
-24	0.67	84.4	9.25	0.12	5.6	1.32
-30	0.65	83.	9.13	0.08	6.9	1.32
-36	0.64	83.	9.04	0.08	7.2	1.31
-42	0.55	83.9	8.84	0.03	6.7	1.26
-48	0.64	83.9	8.90	0.04	6.5	1.27
-54	0.66	83.9	8.87	0.04	6.5	1.27
-60	0.73	85.8	9.12	0.10	4.3	1.28
E9-FD	1.1	85.6	10.1	0.15	3.1	1.42

TABLE VI (CONTINUED)

Sample	%N	%C	%H	%S	%O	H/C
-6	0.2	89.2	10.0	0.04	0.6	1.35
-12	0.1	88.8	11.1	0.00	0.00	1.50
-18	0.06	87.6	11.4	0.00	0.9	1.56
-24	0.07	90.0	11.9	0.00	0.00	1.59
-30	0.13	87.3	11.9	0.00	0.7	1.64
-36	0.01	85.9	11.3	0.00	2.8	1.58
-40	0.03	87.3	11.1	0.00	1.6	1.53
-50	0.25	86.3	11.7	0.00	1.8	1.63
-55	0.5	86.0	10.6	0.00	2.9	1.48
-60	0.5	84.9	10.4	0.00	4.2	1.47

*Samples are designated by a code identifying run number and time on line; thus, E2-12 would be the 12-hour sample for run E2.

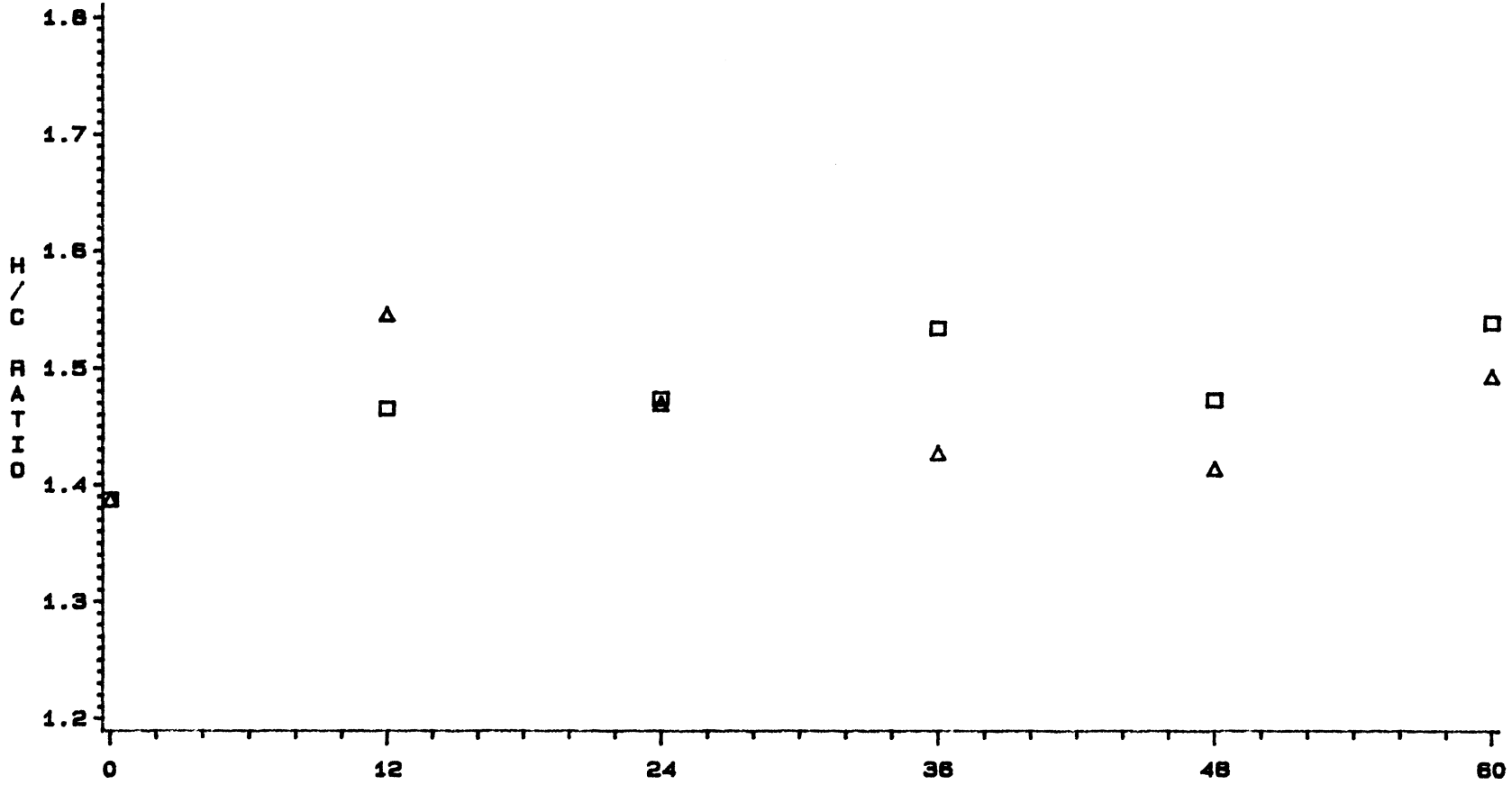

FIGURE 4. EFFECT OF REACTION TEMPERATURE ON H/C RATIO FOR RUNS E2 AND E3

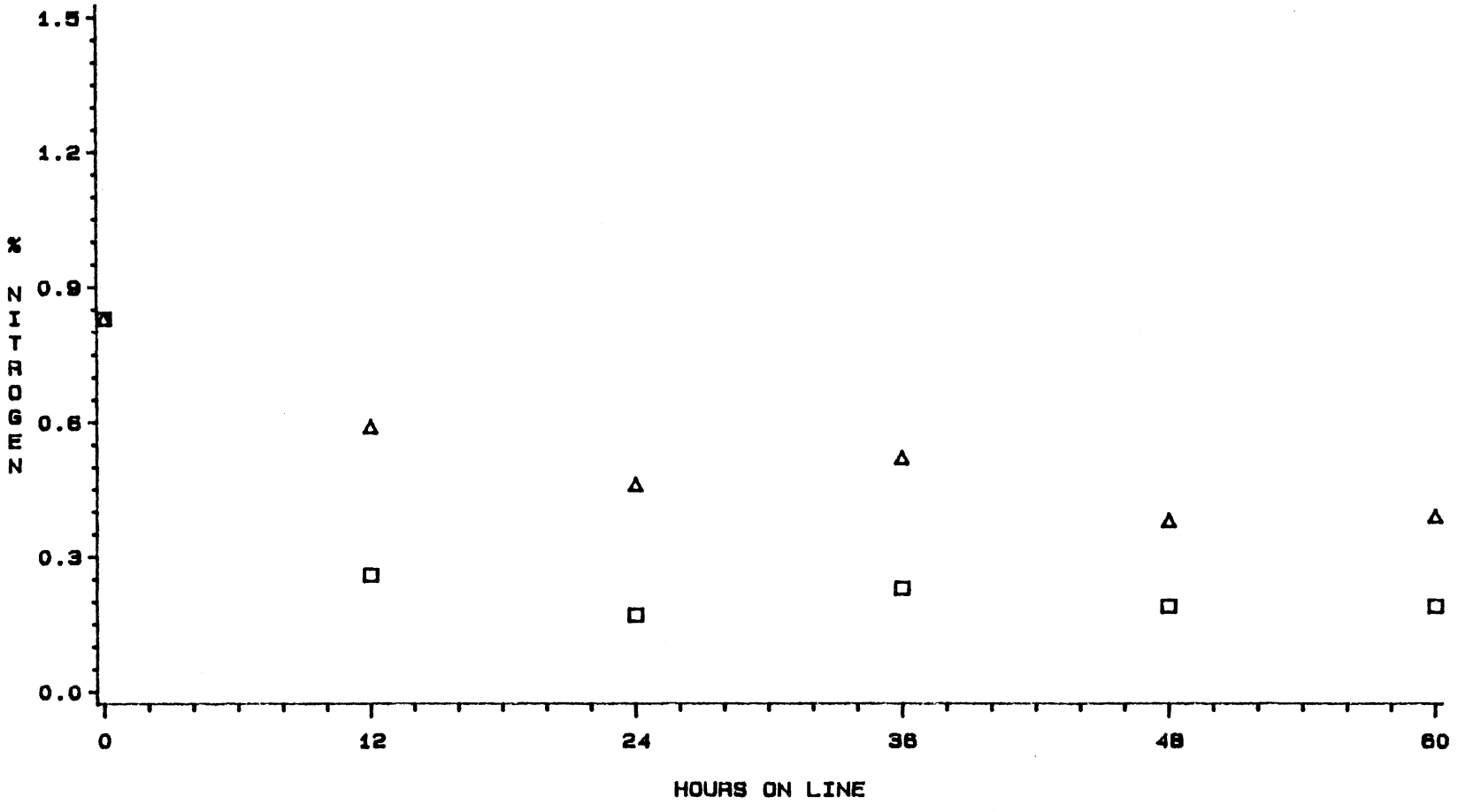

FIGURE 5. EFFECT OF REACTION TEMPERATURE ON NITROGEN CONCENTRATION FOR RUNS E2 AND E3

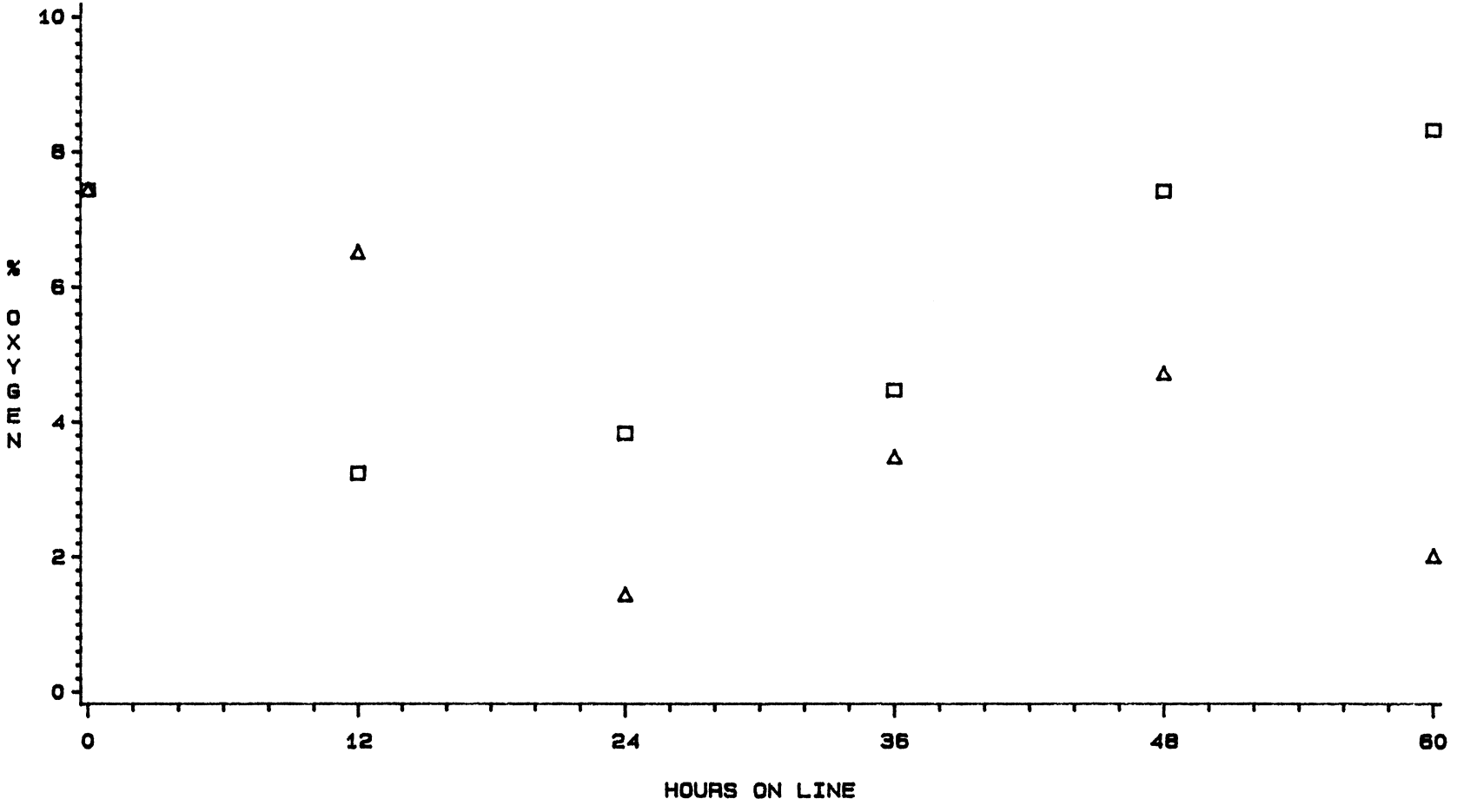

FIGURE 6. EFFECT OF REACTION TEMPERATURE ON OXYGEN CONCENTRATION FOR RUNS E2 AND E3

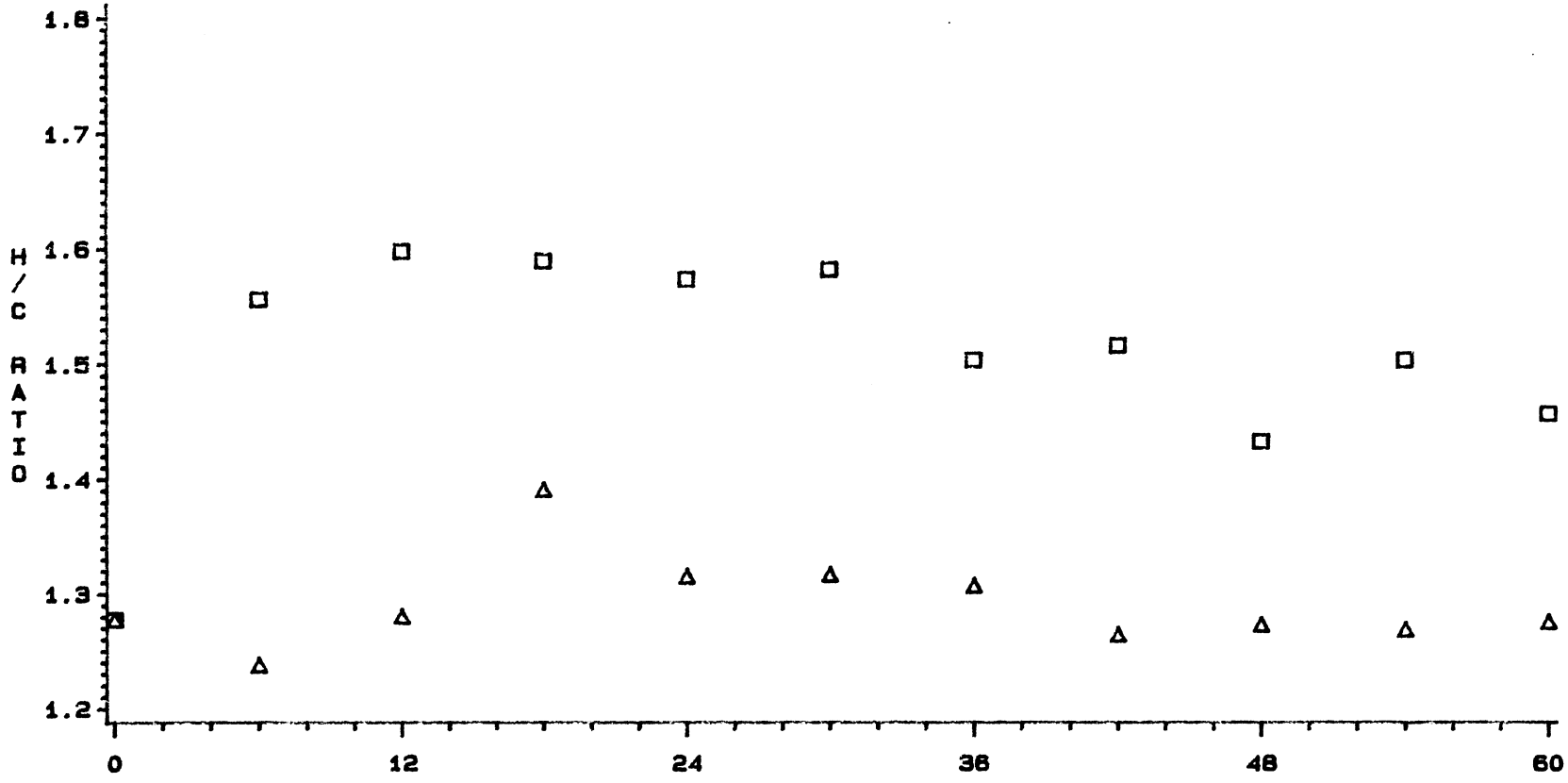

KEY: E7 (CATALYTIC) E8 (NON-CATALYTIC)
0-24 HRS (NO TI); 24-36 HRS (50 PPM TI); 36-48 HRS (NO TI)
48-60 HRS (50 PPM TI-E7; 25 PPM TI-E8)

FIGURE 7. EFFECT OF CATALYST ON H/C RATIO FOR RUNS E7 AND E8

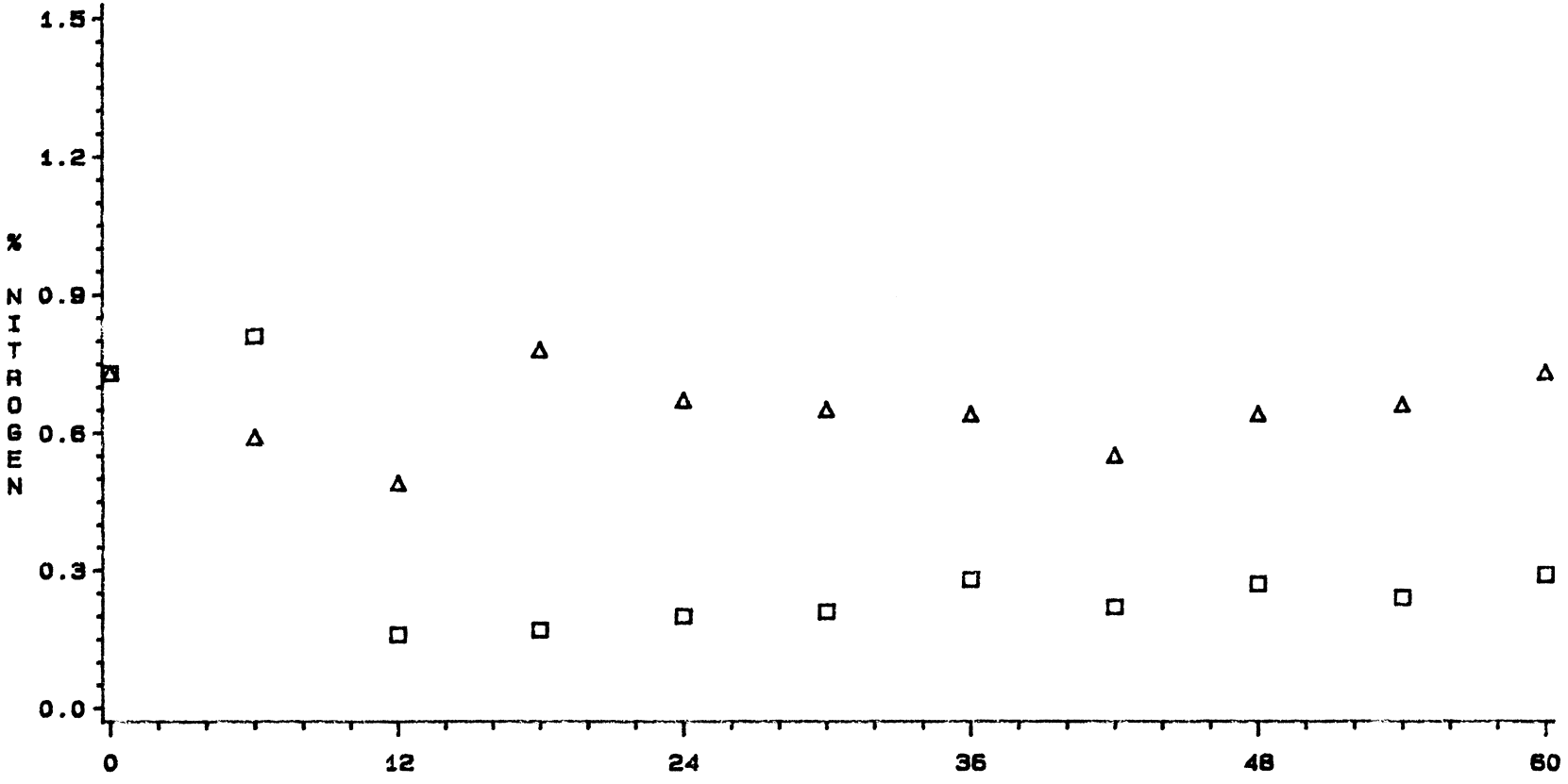

KEY: E7 (CATALYTIC) E8 (NON-CATALYTIC)
0-24 HRS (NO TI); 24-36 HRS (50 PPM TI); 36-48 HRS (NO TI)
48-60 HRS (50 PPM TI-E7; 25 PPM TI-E8)

FIGURE 8. EFFECT OF CATALYST ON NITROGEN CONCENTRATION FOR RUNS E7 AND E8

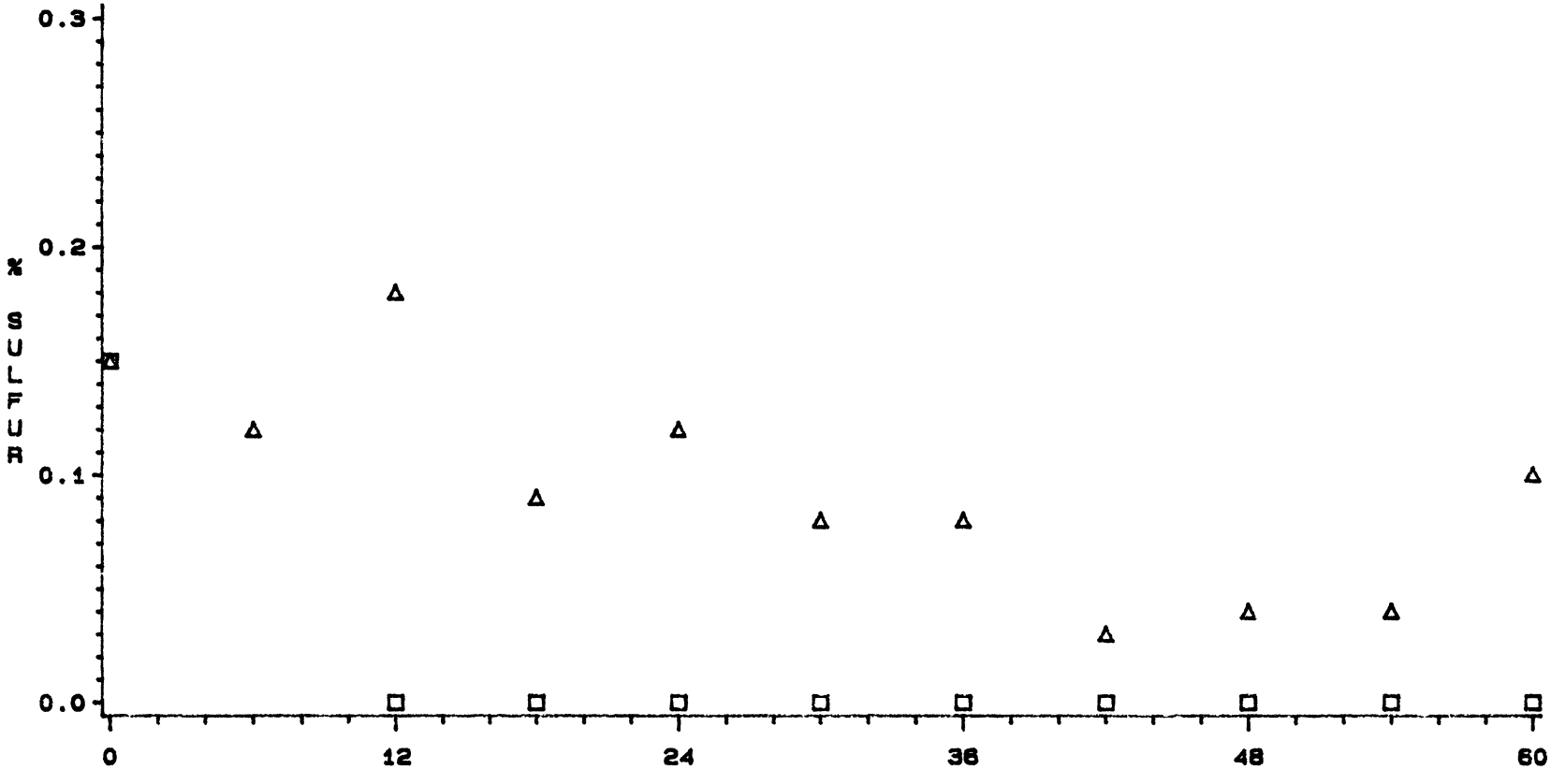

KEY: E7 (CATALYTIC) E8 (NON-CATALYTIC)
0-24 HRS (NO TI); 24-36 HRS (50 PPM TI); 36-48 HRS (NO TI)
48-60 HRS (50 PPM TI-E7; 25 PPM TI-E8)

FIGURE 9. EFFECT OF CATALYST ON SULFUR CONCENTRATION FOR RUNS E7 AND E8

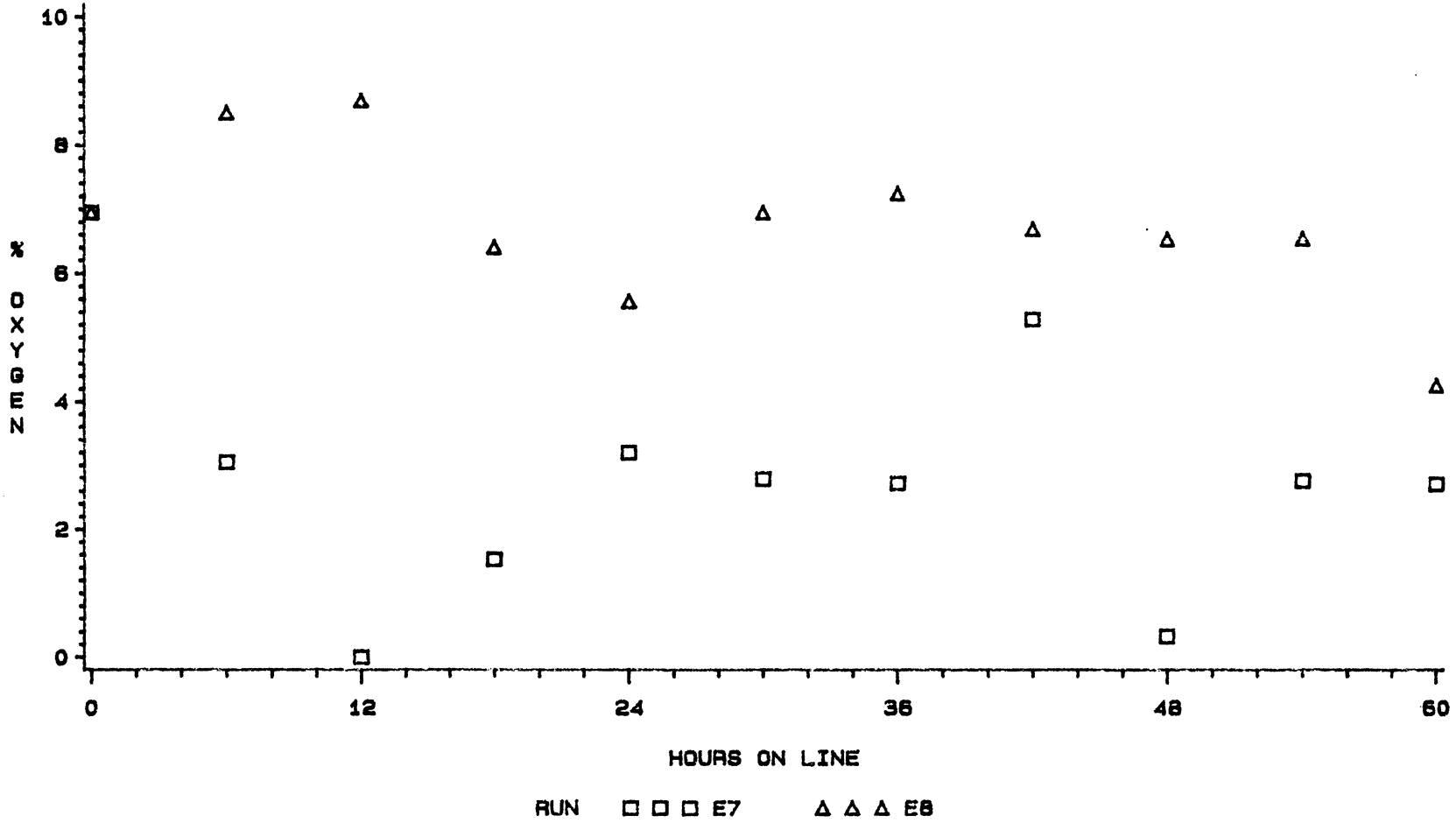

KEY: E7 (CATALYTIC) E8 (NON-CATALYTIC)
0-24 HRS (NO TI); 24-36 HRS (50 PPM TI); 36-48 HRS (NO TI)
48-60 HRS (50 PPM TI-E7; 25 PPM TI-E8)

FIGURE 10. EFFECT OF CATALYST ON OXYGEN CONCENTRATION FOR RUNS E7 AND E8

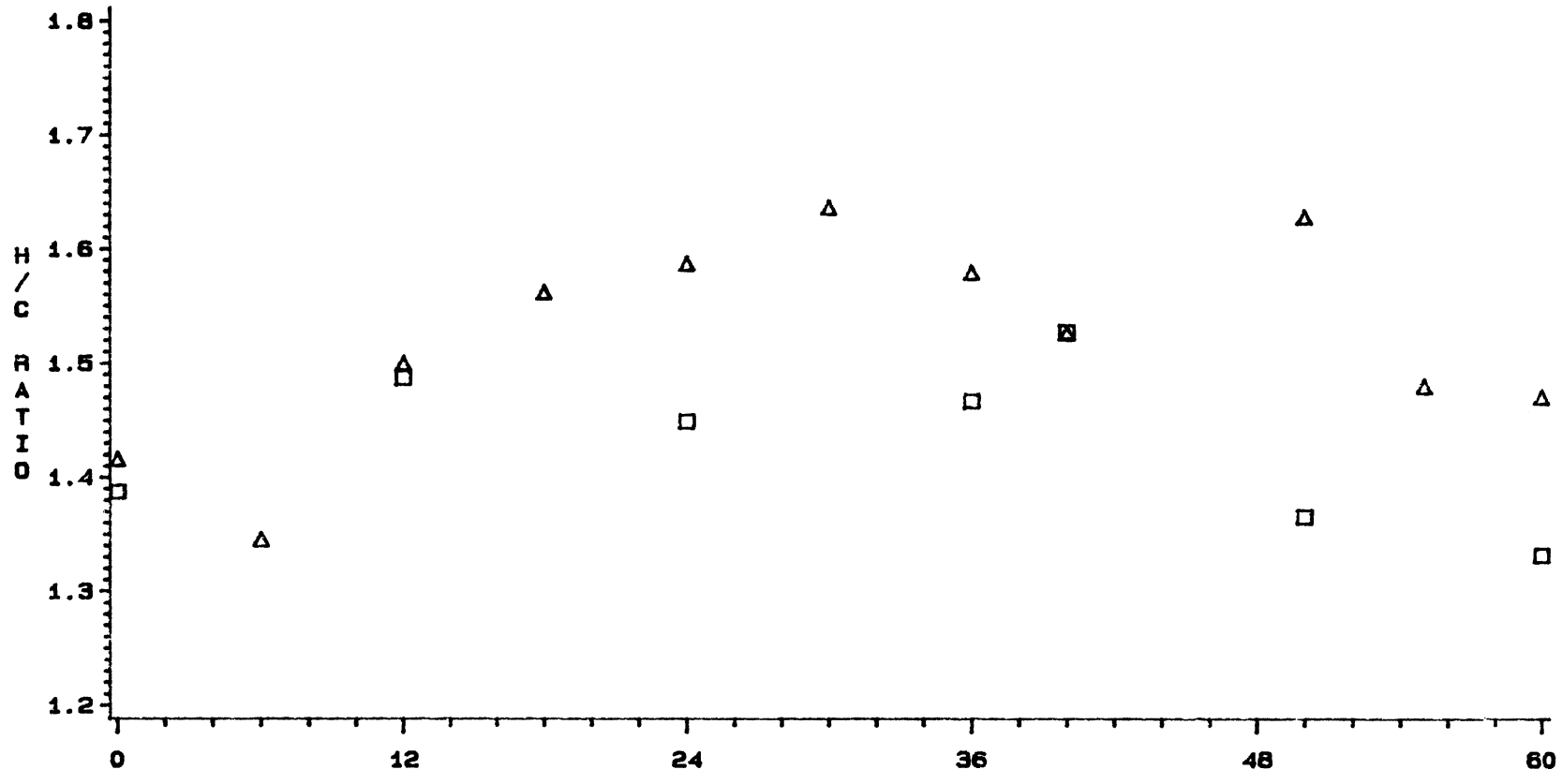

KEY: E4 (0 PPM TI) E9 (50 PPM TI)
0-40 HRS (350 C, 0.44 HR); 40-50 HRS (350 C, 0.22 HR)
50-60 HRS (325 C, 0.22 HR)

FIGURE 11. EFFECT OF TDC ON H/C RATIO FOR RUNS E4 AND E9

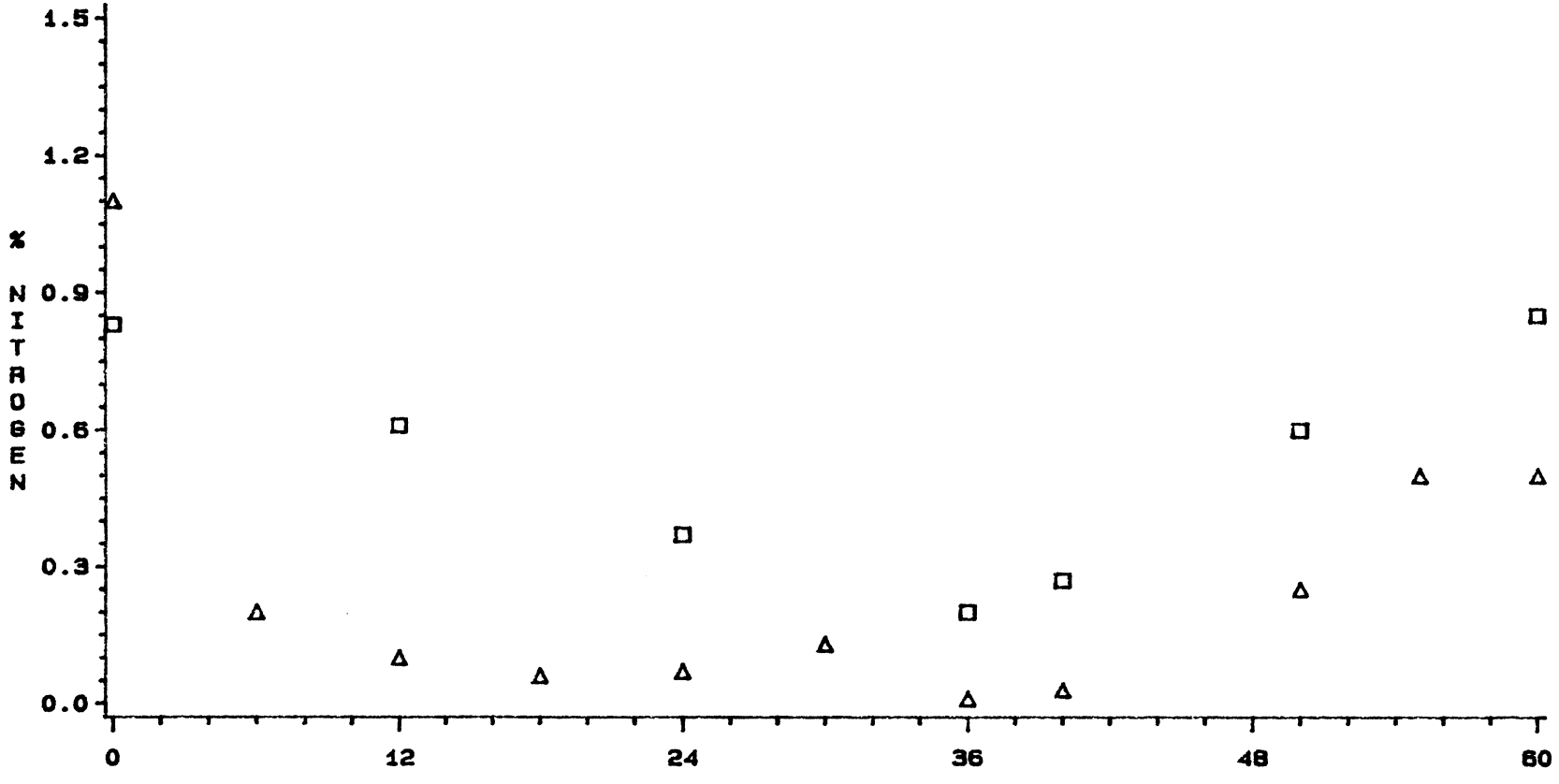

KEY: E4 (0 PPM TI) E9 (50 PPM TI)
0-40 HRS (350 C, 0.44 HR); 40-50 HRS (350 C, 0.22 HR)
50-60 HRS (325 C, 0.22 HR)

FIGURE 12. EFFECT OF TDC ON NITROGEN CONCENTRATION FOR RUNS E4 AND E9

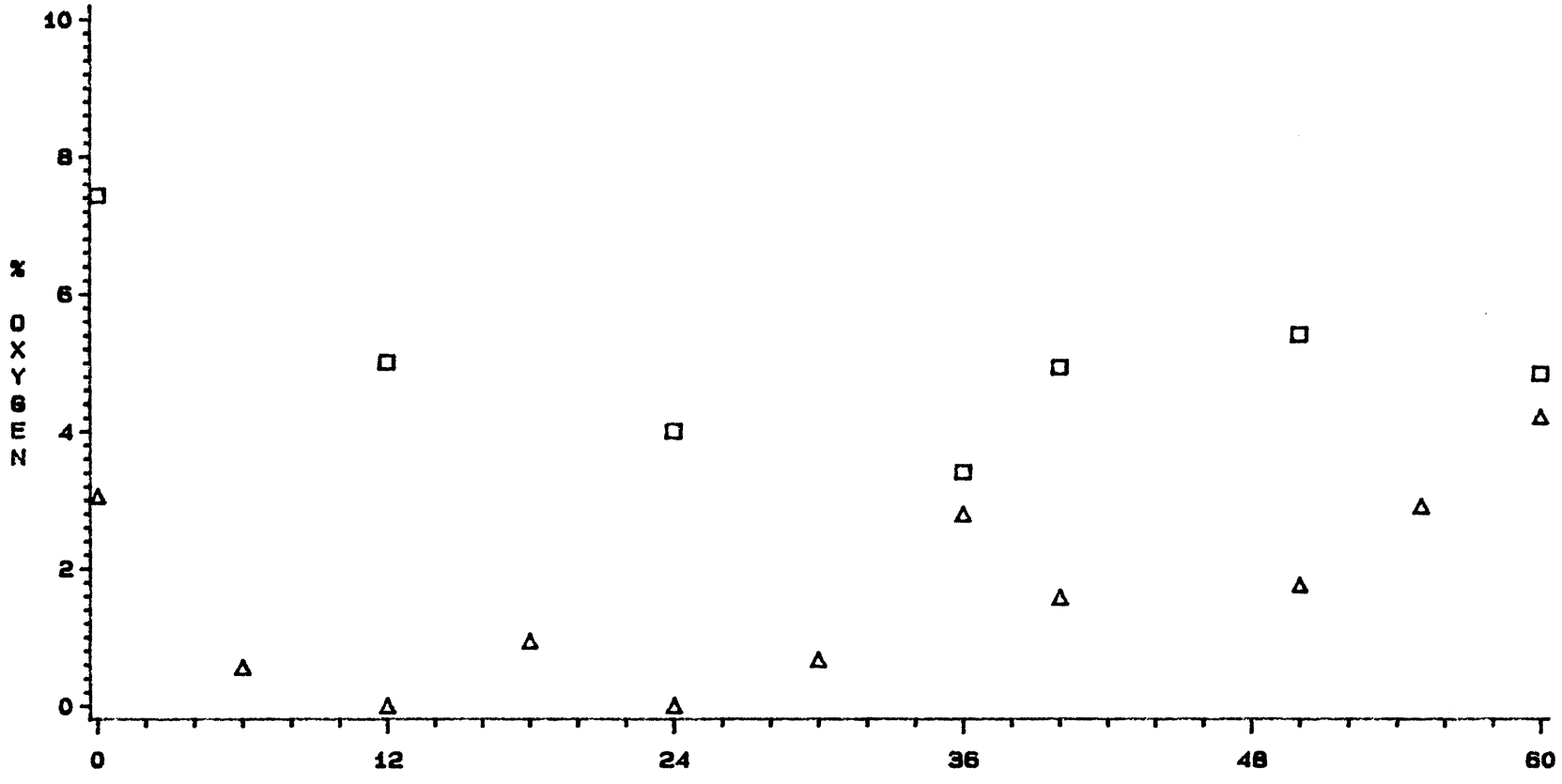

KEY: E4 (0 PPM TI) E9 (50 PPM TI)
0-40 HRS (350 C, 0.44 HR); 40-50 HRS (350 C, 0.22 HR)
50-60 HRS (325 C, 0.22 HR)

FIGURE 13. EFFECT OF TDC ON OXYGEN CONCENTRATION FOR RUNS E4 AND E9

was established, but the H/C ratio increased with time from 1.47 (12 hours) to 1.53 (36 and 60 hours). No catalyst deactivation was noted. For run E3, when the temperature was lowered to 350 C, the H/C ratio decreased with time from 1.55 (12 hours) to 1.41 (48 hours), and the nitrogen conversion increased with time from 29% (12 hours) to 53% (60 hours).

Figures 11 through 13 present the HYD, HDN, and HDO results for run E4. For run E4, a more severe sulfidation resulted in a higher nitrogen conversion (about 70% for the first 40 hours, as opposed to 53% for run E3). The H/C ratio was also increased (an average of about 1.49 for the first 40 hours, as opposed to an average of 1.47 for the first 48 hours of run E3). As expected, when the space-time for run E4 was halved, the H/C ratio (down to 1.36) and nitrogen conversion (down to 18%) were severely decreased. When the temperature was dropped to 325 C, the product H/C ratio (1.33) became less than that of the feed (1.39), and the nitrogen content became more (0.85 weight percent, apparently greater than the feed's 0.83 weight percent). Complete HDS was achieved (except for the first 12 hours) during all three runs. The data from runs E2 through E4 indicated that a temperature of 350 C (662 F) and a space-time of 0.44 hours were sufficient operating conditions to allow testing of the effect of titanocene dichloride upon the hydrotreatment of the SRC-II Middle Distillate.

Figures 7 through 10 compare the HYD, HDN, HDS, and HDO results for runs E7 and E8. Run E7 was performed as an 'on/off' run where the oil feedstock was periodically doctored with titanocene dichloride. The sulfidation for this run was very severe (see Table II) compared to the sulfidation for runs E2-E4. Comparing sample E7-24 with samples E4-24 and E3-24, the nitrogen conversion for E7-24 (72%) is much higher than that for E4-24 (55%) and for E3-24 (45%). The H/C ratio is also higher for E7-24 (1.57) than for E4-24 (1.45) and for E3-24 (1.47). Thus, a more severe pre-sulfiding results in a higher nitrogen conversion, and a greater H/C ratio.

The usual catalyst deactivation curve appears for run E7, and the addition of titanocene dichloride (from 24-36 hours and 48-60 hours) had no effect on the catalyst deactivation.

Run E8 was an "on/off" non-catalytic run in which the feedstock was periodically doped with 25 and 50 ppm Ti as titanocene dichloride. Titanocene dichloride showed no effect upon the HYD, HDN, or HDO of the Middle Distillate; however, some HDS was achieved during the last 18 hours of the run. Comparing runs E7 and E8 (Figures 7 through 10), the presence of catalyst greatly enhances the HYD, HDS, HDN, and HDO reactions.

The catalytic run E9 was performed to determine the effects of adding titanocene dichloride to the SRC-II Middle Distillate feedstock, and then hydrotreating the feedstock

using a weakly-sulfided catalyst. Operating conditions for the run were identical to those of Run E4, except that 50 ppm of titanium as titanocene dichloride were added to the feed before hydrotreatment. Figures 11 through 13 compare runs E4 and E9, and show the effects of titanocene dichloride upon the HYD, HDN, and HDO reactions. Comparing samples E4-24 and E9-24, significant improvements in H/C ratio (1.59 for E9-24 over 1.45 for E4-24), nitrogen conversion (94% for E9-24 over 55% for E4-24), and oxygen conversion (100% for E9-24 over 45% for E4-24) were noted; complete HDS was achieved in both runs. While decreasing the space-time and reactor temperature decreased the HYD, HDN, and HDO reactions for run E9, the H/C ratio, nitrogen conversion, and oxygen conversion were still much better than those for run E4. Because these improvements were not noted in a run using a strongly-sulfided catalyst (run E7), apparently titanocene dichloride improves catalyst activity only when the catalyst has been weakly sulfided.

Kinetic values for the HDN reaction were extracted from catalytic runs E2 and E4 (no titanocene dichloride added) and E9 (50 ppm Ti as titanocene dichloride added). Assuming a first order reaction dependent only upon nitrogen concentration, the following values were obtained: between 350 C and 375 C the undoped HDN reaction had an activation energy of 8.54 kcal/mol and an Arrhenius pre-exponential constant of 2600/hr; between 325 C and 350 C the doped HDN reaction had an activation energy of 8.88 kcal/mol and an

Arrhenius pre-exponential constant of 9132/hr. A summary of the kinetic values obtained for doped and undoped HDN is presented in Table VII.

Elemental analysis of the non-catalytic runs E10 through E18 are listed in Table VIII and presented in Figures 14 through 17 (no titanocene dichloride added), 18 through 21 (50 ppm titanium as titanocene dichloride added), and 22 through 25 (hydrogen gas, variable titanium doping). Runs E14 through E18 duplicate runs E10 through E13, and thus can be used to check the reproducibility of the first four non-catalytic runs. No effect of titanocene dichloride upon the elemental composition of the liquid product was noted; nor was there any significant difference when hydrogen gas flowed through the reactor rather than nitrogen gas. Reactor temperature also had no effect on product elemental composition.

Simulated Distillations

Samples from all runs were analyzed by g.c.-simulated distillation. A typical chromatogram of the SRC-II Middle Distillate feed is given in Figure 26. The results of the simulated distillations are tabulated in Tables IX and X, and graphed in Figures 27-30.

Table IX presents the boiling point distributions of selected samples from runs E2, E3, E4, E7, E8, and E9. The SRC-II Middle Distillate used during this study was stored in two different 5-gallon cans. The same feed was used in

TABLE VII

KINETICS OF DOPED AND UNDOPED HYDRODENITROGENATION

FEED DOPING	TEMP (C)	SPACE-TIME	CONVERSION	K (1/HR)
50 PPM TI	325	0.22 HR	55%	3.6
50 PPM TI	350	0.22 HR	77%	6.7
0 PPM TI	375	0.44 HR	77%	3.3
0 PPM TI	350	0.44 HR	67%	2.6

FOR DOPED HYDRODENITROGENATION:

$K_{\square}$=9132/HR.

ACTIVATION ENERGY=8.88 KCAL/MOL.

FOR UNDOPED HYDRODENITROGENATION:

$K_{\square}$=2600/HR.

ACTIVATION ENERGY=8.54 KCAL/MOL.

TABLE VIII

ELEMENTAL ANALYSIS OF RUNS E10 TO E18

SAMPLE	%N	%C	%H	%S	%O	H/C	TEMP(C)
FEED	0.88	83.53	9.51	0.15	5.9	1.33	25
E10-1	0.90	85.87	9.75	0.05	3.4	1.36	295
-2	0.84	87.73	9.53	0.05	1.9	1.30	320
-3	0.81	86.36	9.65	0.06	3.1	1.34	350
-4	0.80	87.60	9.03	0.13	2.4	1.24	373
-5	0.86	86.43	9.38	0.08	3.3	1.30	393
E11-1	1.05	87.83	9.84	0.10	1.2	1.35	298
-2	0.91	86.63	9.58	0.11	2.8	1.33	324
-3	0.84	86.66	9.12	0.13	3.3	1.26	348
-4	0.86	86.30	9.39	0.11	3.3	1.31	374
-5	0.81	87.23	9.43	0.15	2.4	1.30	399
E12-1	0.94	85.93	9.36	0.14	3.6	1.31	304
-2	0.87	87.60	9.37	0.15	2.0	1.28	329
-2*	0.86	86.36	9.46	0.15	3.2	1.31	329
-3	0.82	**	9.34	0.14	**	**	348
-4	0.83	87.00	9.57	0.00	2.6	1.32	370
-4*	0.87	87.20	9.71	0.00	2.2	1.34	370
-5	0.91	86.30	9.38	0.10	3.3	1.30	380
E13-1	0.91	85.90	9.22	0.12	3.9	1.29	301
-2	0.88	86.63	9.40	0.11	3.0	1.30	333
-3	0.86	86.40	9.42	0.11	3.2	1.31	355
-4	0.89	86.03	9.36	0.12	3.6	1.31	374
-5	0.86	86.37	9.53	**	**	1.32	395
E14-1	**	**	**	0.17	**	**	62
-2	0.84	87.33	9.36	0.13	2.3	1.29	99
-3	0.84	85.36	9.05	0.11	4.6	1.27	162
-4	0.83	85.80	9.18	0.12	4.1	1.28	200
-5	0.74	87.00	9.36	0.10	2.8	1.29	254
-6	0.86	85.93	9.35	0.12	3.7	1.31	306
-7	0.85	86.40	9.29	0.12	3.3	1.29	363
-8	0.87	86.80	9.27	0.19	2.8	1.28	387
E15-1	0.86	86.43	9.34	0.15	3.2	1.30	53
-2	0.76	86.80	9.47	0.15	2.8	1.31	98
-3	0.85	86.43	9.41	0.12	3.2	1.31	149
-4	0.85	86.40	9.45	0.12	3.2	1.31	209
-5	0.80	85.60	9.13	0.12	4.4	1.28	263
-6	0.79	85.66	8.79	0.11	4.7	1.23	297
-7	0.69	86.74	9.60	0.11	2.9	1.33	350
E16-1	0.85	85.80	8.99	0.14	4.2	1.26	58
-2	0.81	86.23	9.10	0.13	3.7	1.27	100
-3	0.81	85.70	9.17	0.13	4.2	1.28	150
-4	0.85	84.90	8.96	0.18	5.1	1.27	195
-5	0.78	85.76	9.32	0.10	4.0	1.30	247
-6	0.77	85.70	9.21	0.12	4.2	1.29	298

TABLE VIII (CONTINUED)

SAMPLE	%N	%C	%H	%S	%O	H/C	TEMP(C)
E16-7	0.85	85.36	9.20	0.13	4.5	1.29	346
E17-1	0.69	85.97	9.76	0.17	3.4	1.36	59
-2	0.69	83.66	9.40	0.08	6.2	1.35	99
-3	0.71	85.73	9.57	0.13	3.9	1.34	148
-4	0.77	85.66	9.18	0.11	4.3	1.29	193
-5	0.90	87.46	9.42	0.11	2.1	1.29	250
-6	0.81	85.80	9.21	0.11	4.1	1.29	300
-7	0.86	86.06	8.97	0.11	4.0	1.25	350
-8	0.79	85.13	9.22	0.12	4.7	1.30	390
E18-1	0.91	86.60	9.28	0.12	3.1	1.29	60
-2	0.87	85.76	9.45	0.12	3.8	1.32	103
-3	0.76	86.06	9.50	0.10	3.6	1.32	152
-4	0.77	85.60	9.40	0.11	4.1	1.32	204
-5	0.81	86.26	8.95	0.09	3.9	1.25	253
-6	0.83	86.90	9.38	0.14	2.8	1.30	310
-7-1	0.77	86.77	9.30	0.10	3.1	1.29	354
-7-3	0.91	85.90	8.97	0.13	4.1	1.25	352
-7-4	1.09	86.90	9.13	0.15	2.7	1.26	350
-8	0.87	87.10	9.72	0.15	2.2	1.34	395

*Indicates repeat analysis.
**Indicates sample not available for complete analysis.

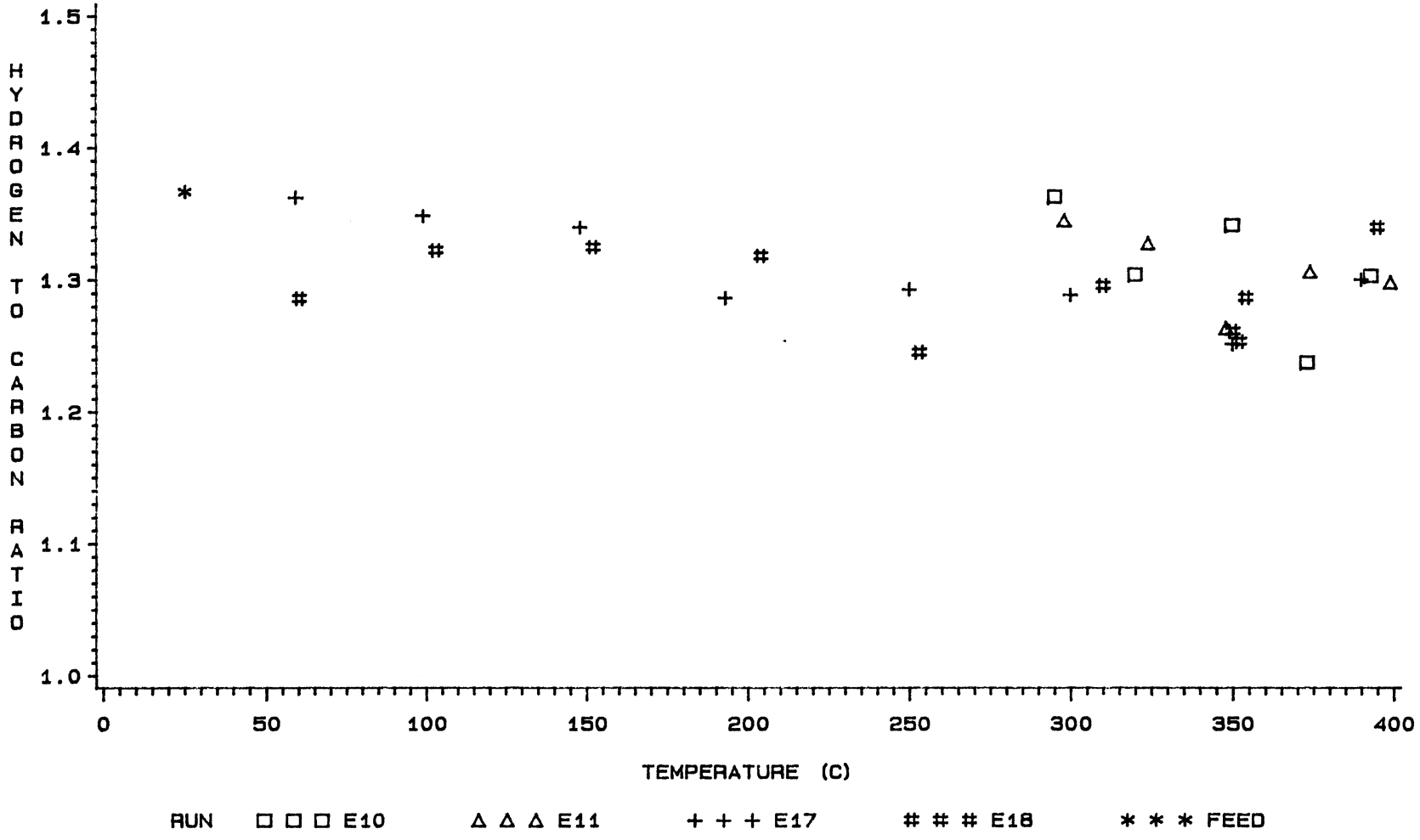

KEY: E10, E18 (NITROGEN) E11, E17 (HYDROGEN)

FIGURE 14. EFFECT OF GAS TYPE ON H/C RATIO FOR UNDOPED NON-CATALYTIC RUNS

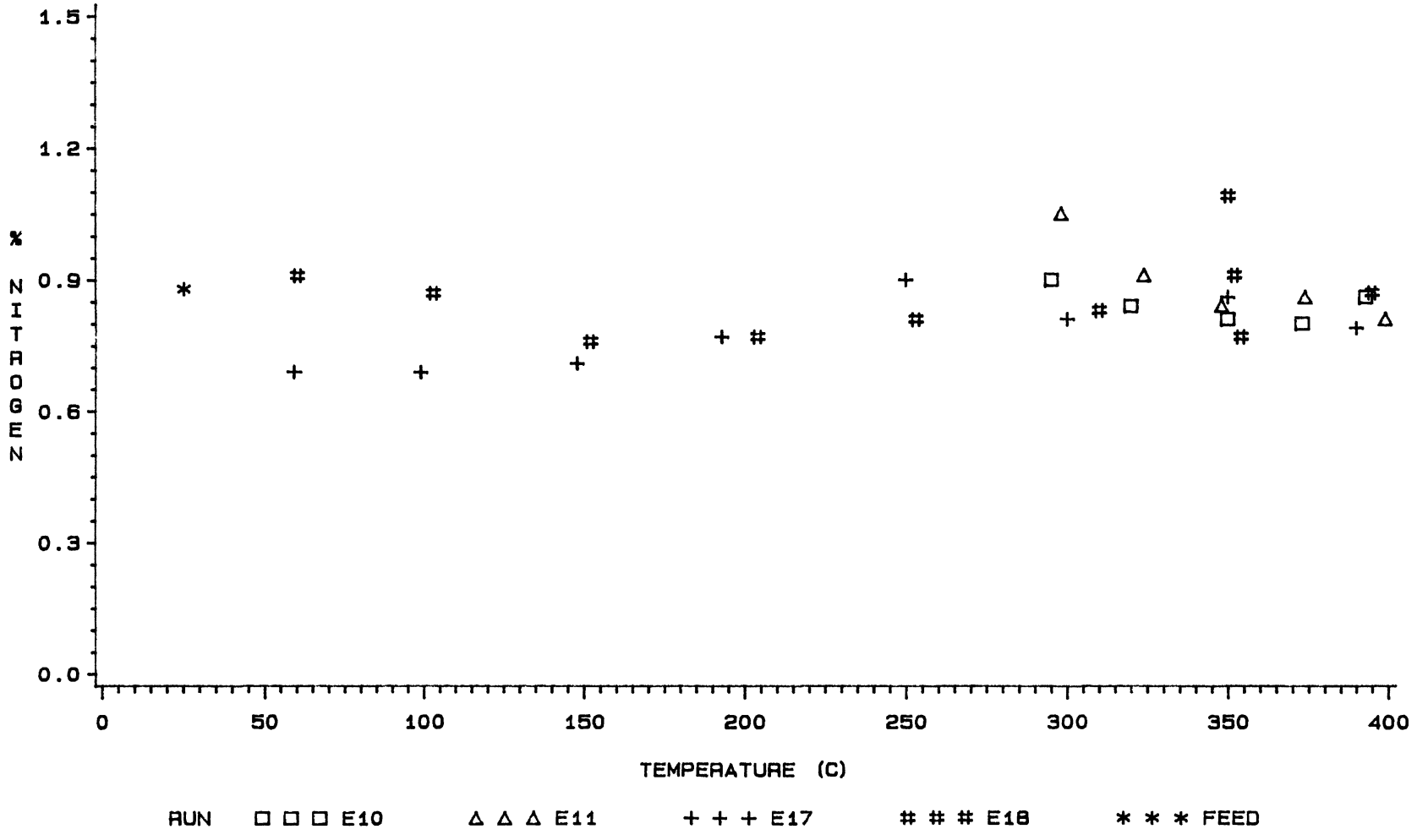

KEY: E10, E18 (NITROGEN) E11, E17 (HYDROGEN)

FIGURE 15. EFFECT OF GAS TYPE ON NITROGEN CONCENTRATION FOR UNDOPED NON-CATALYTIC RUNS

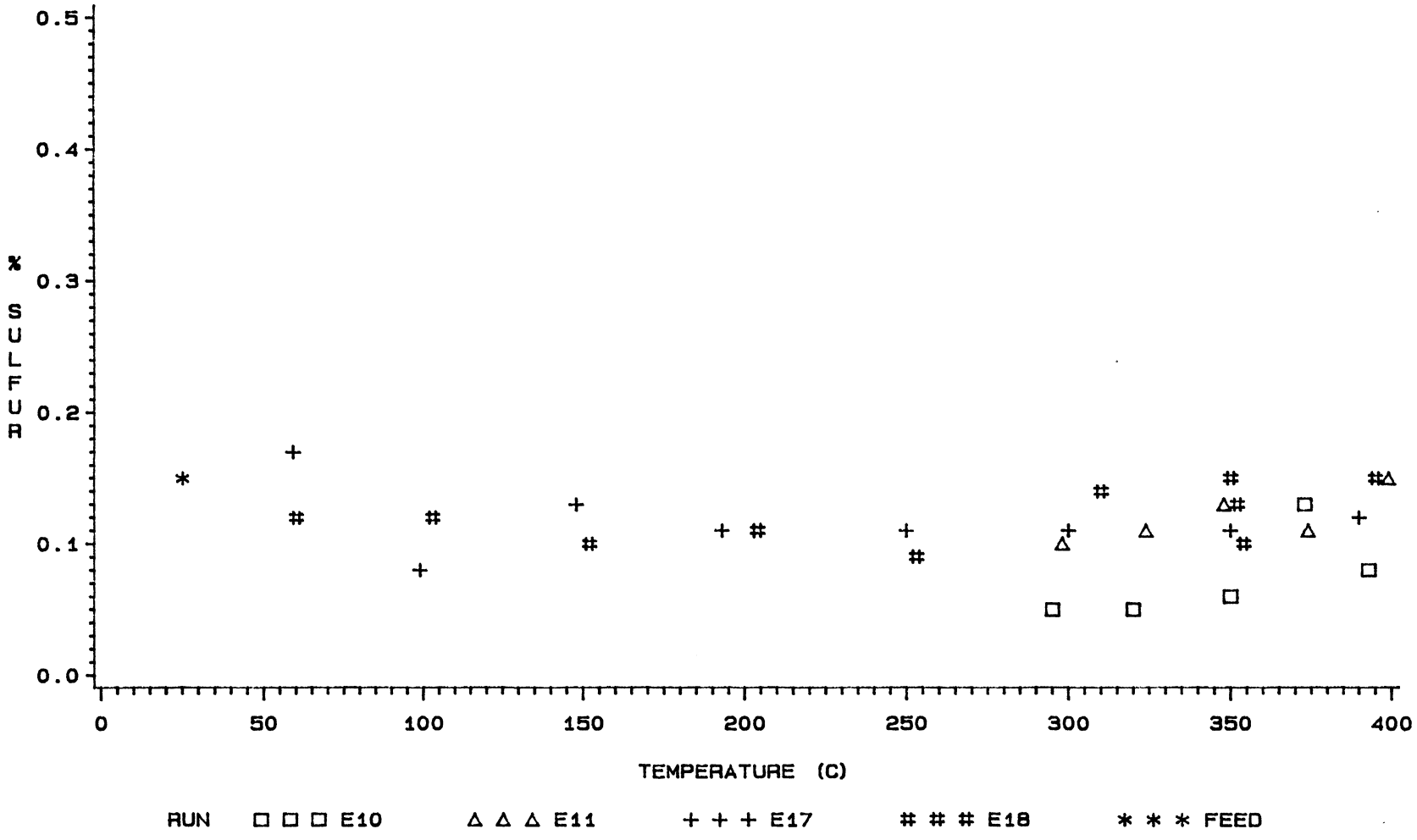

KEY: E10, E18 (NITROGEN) E11, E17 (HYDROGEN)

FIGURE 16. EFFECT OF GAS TYPE ON SULFUR CONCENTRATION FOR UNDOPED NON-CATALYTIC RUNS

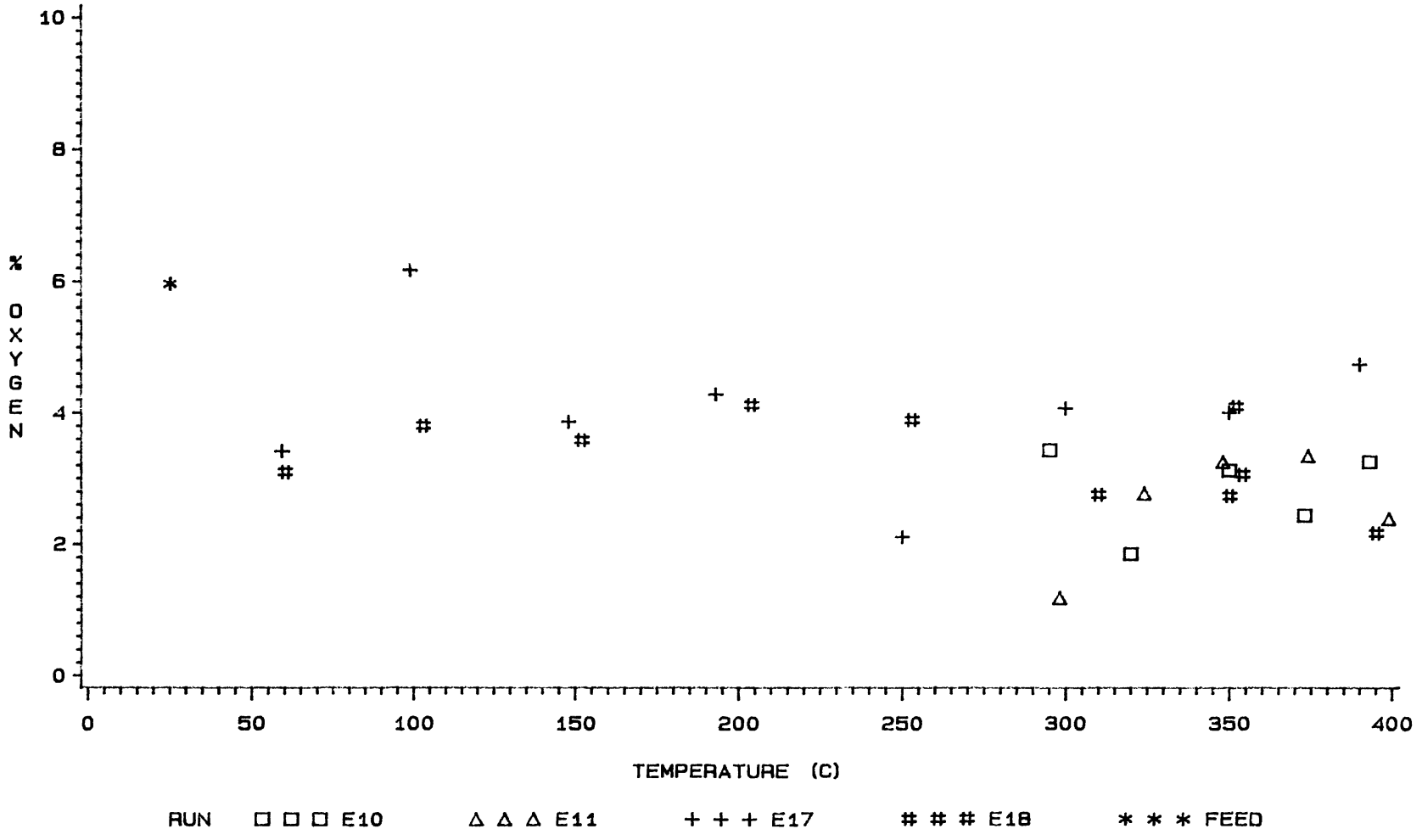

FIGURE 17. EFFECT OF GAS TYPE ON OXYGEN CONCENTRATION FOR UNDOPED NON-CATALYTIC RUNS

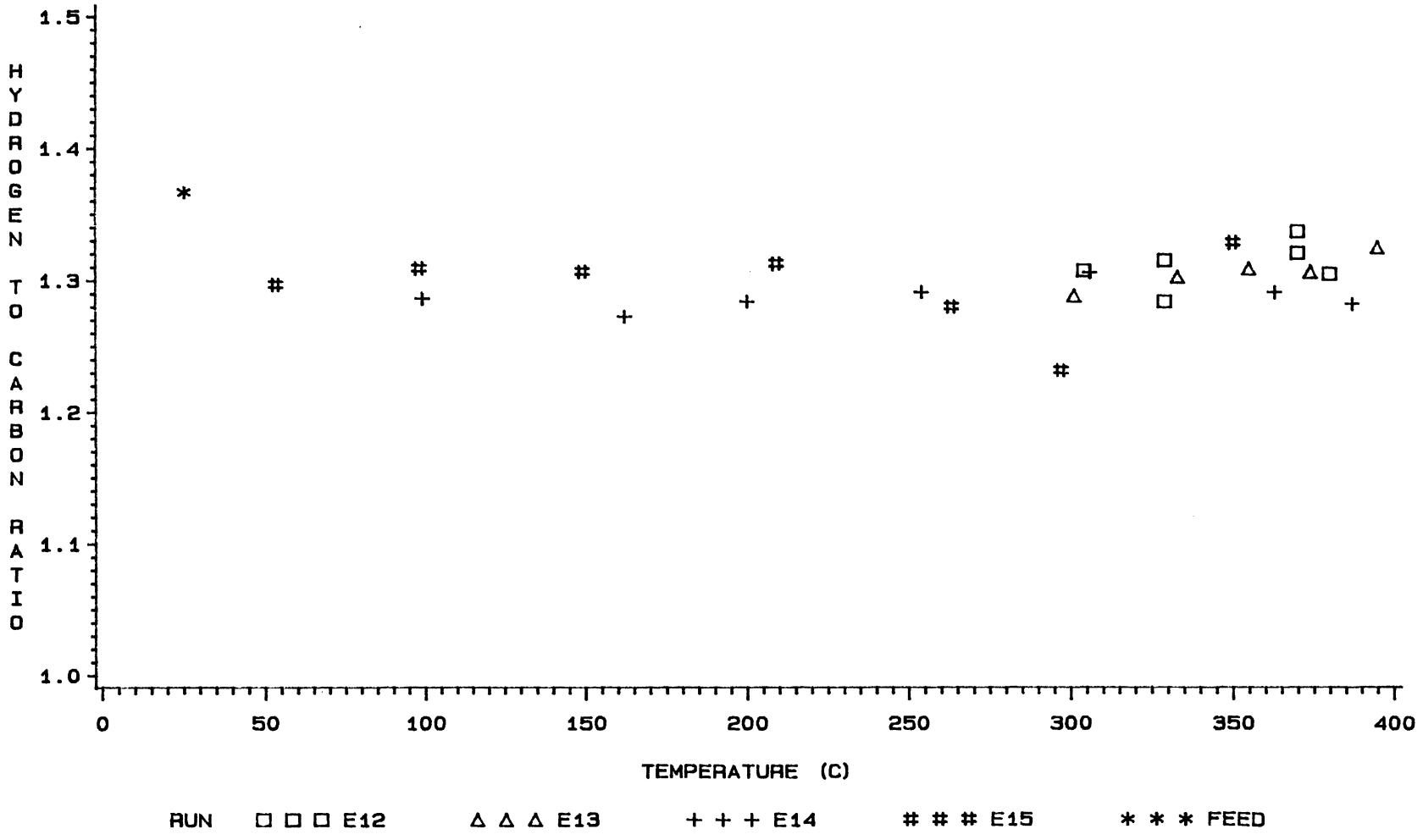

FIGURE 18. EFFECT OF GAS TYPE ON H/C RATIO FOR NON-CATALYTIC RUNS DOPED WITH 50 PPM TI

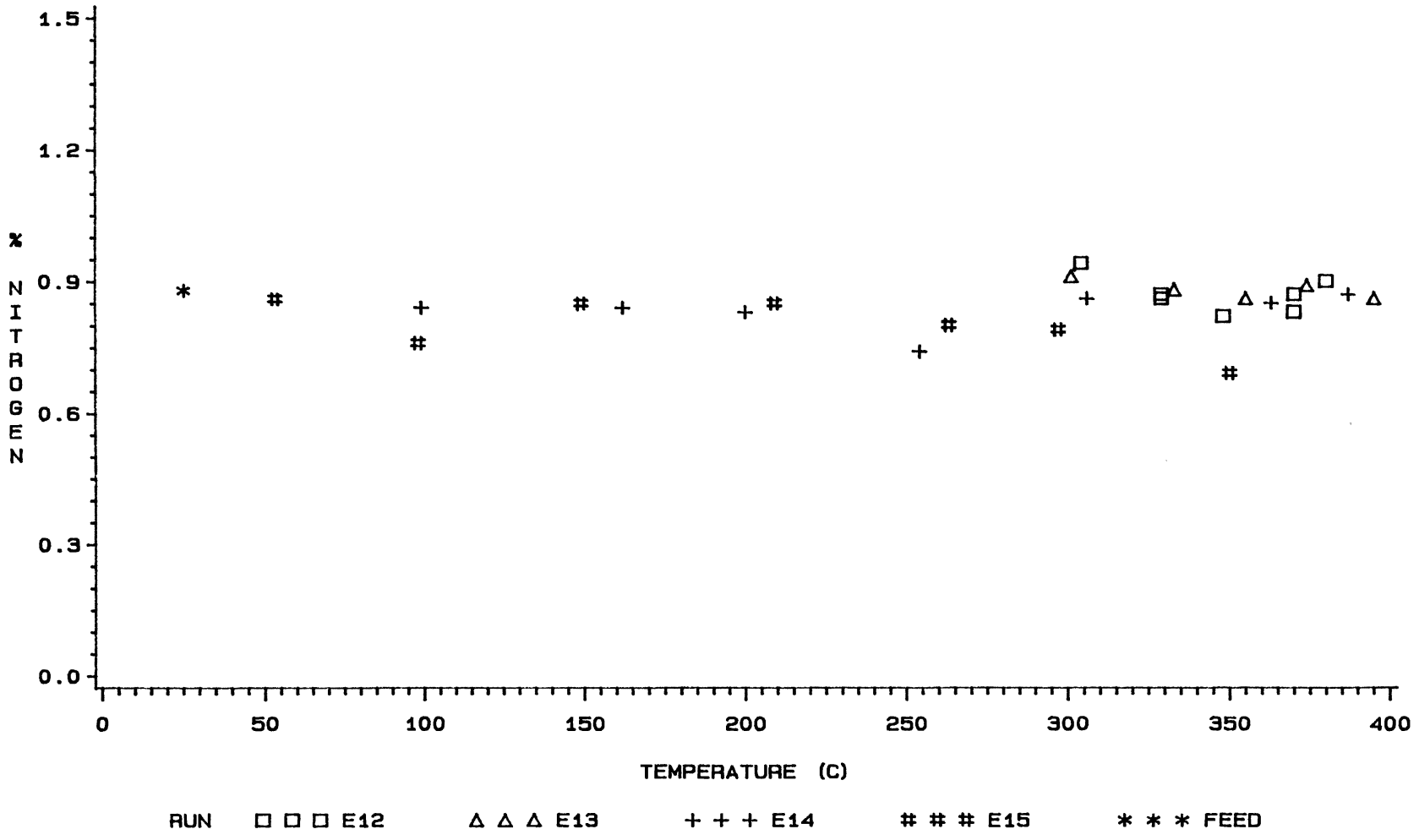

FIGURE 19. EFFECT OF GAS TYPE ON NITROGEN CONCENTRATION FOR NON-CATALYTIC RUNS DOPED WITH 50 PPM TI

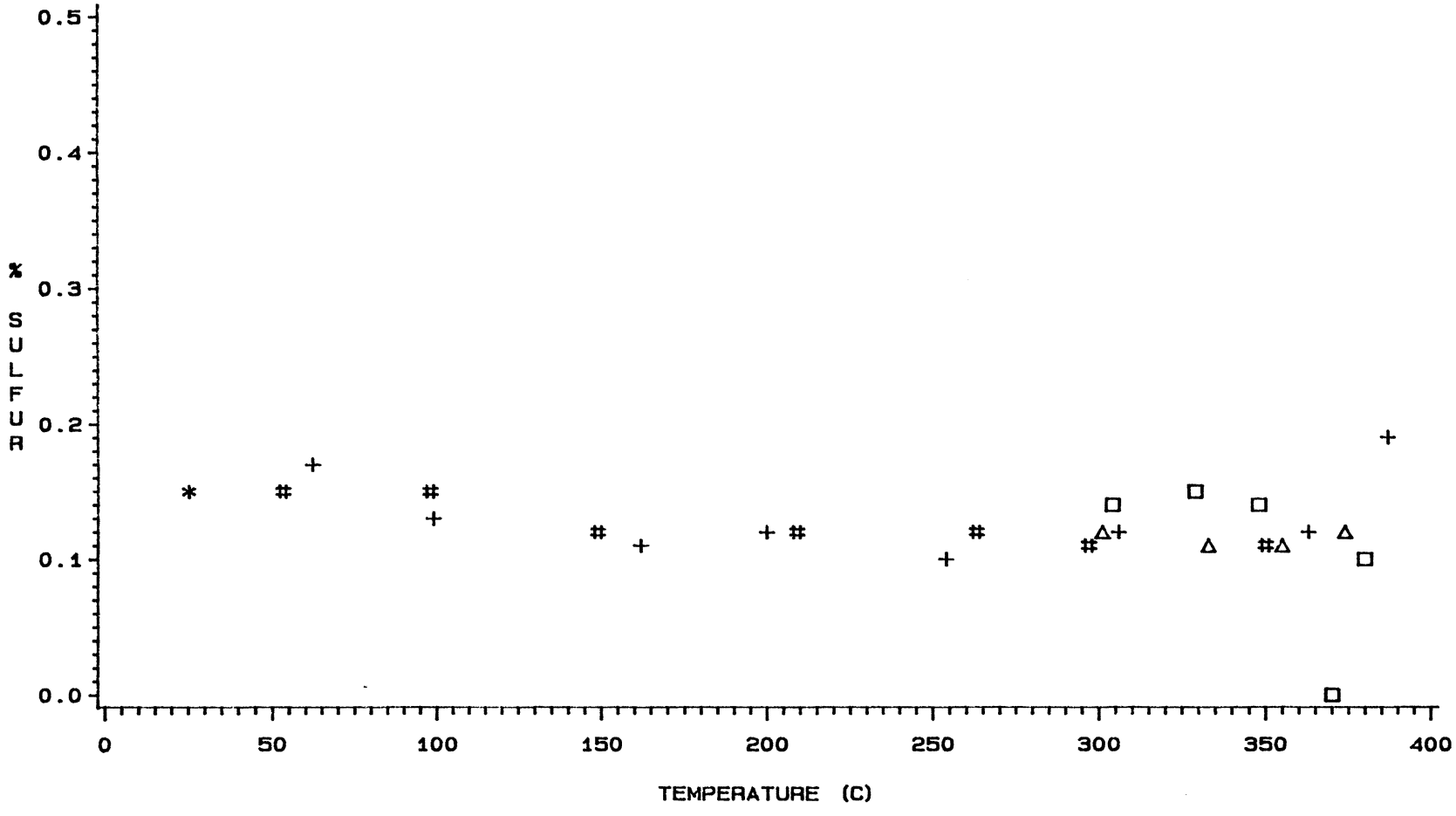

FIGURE 20. EFFECT OF GAS TYPE ON SULFUR CONCENTRATION FOR NON-CATALYTIC RUNS DOPED WITH 50 PPM TI

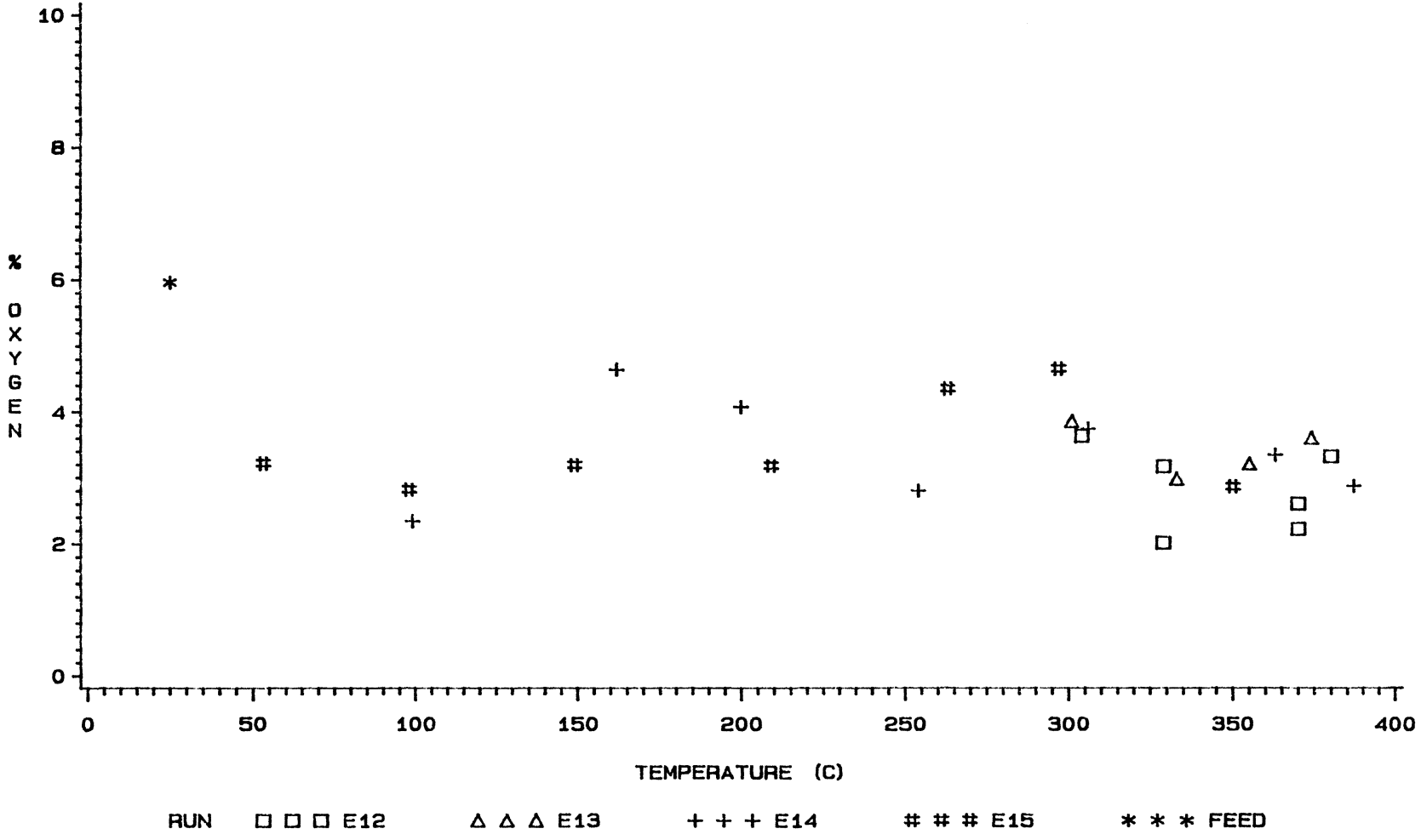

KEY: E12, E14 (NITROGEN) E13, E15 (HYDROGEN)

FIGURE 21. EFFECT OF GAS TYPE ON OXYGEN CONCENTRATION FOR NON-CATALYTIC RUNS DOPED WITH 50 PPM TI

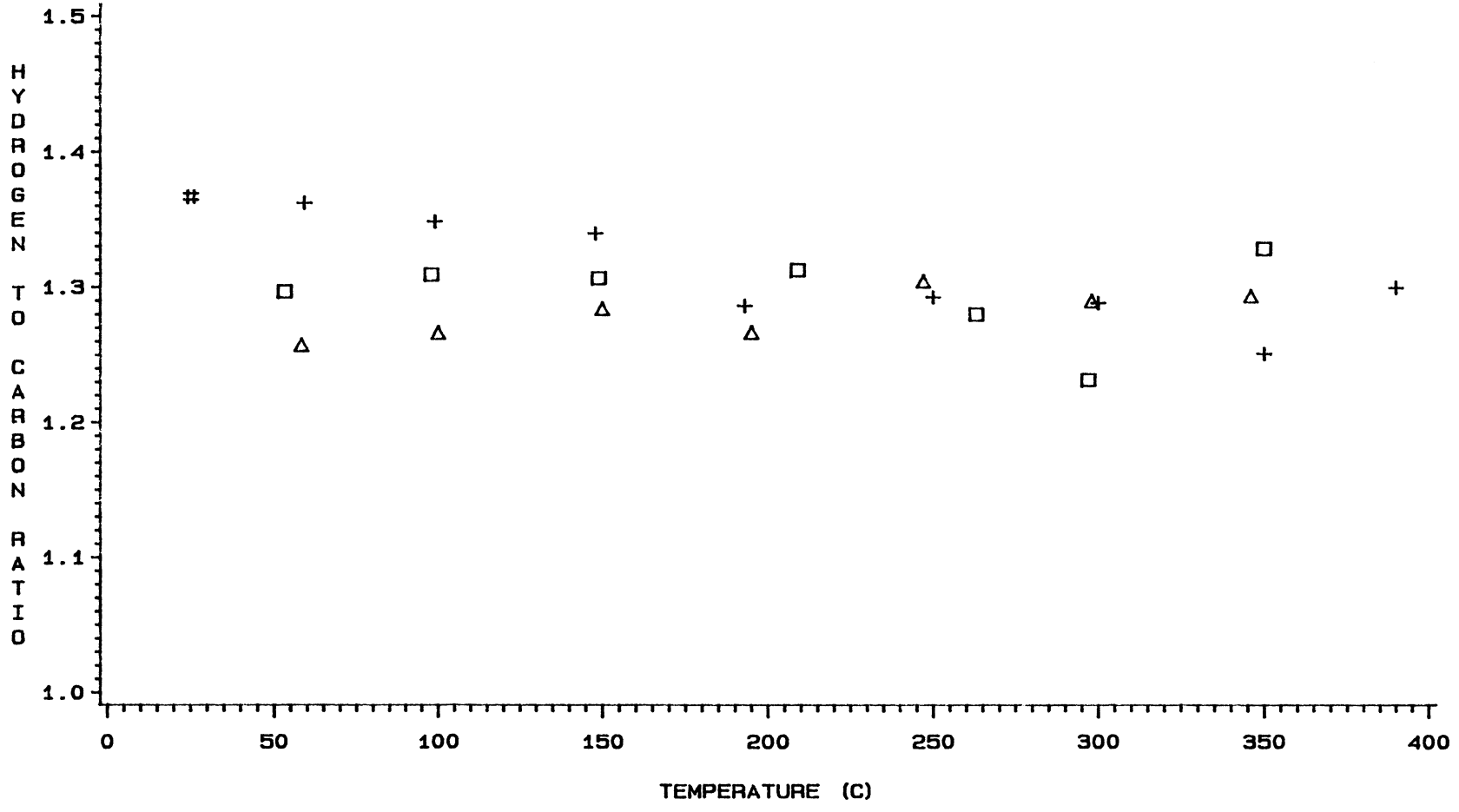

KEY: E15 (50 PPM TI/H2) E16 (200 PPM TI/H2) E17 (NO TI/H2)

FIGURE 22. EFFECT OF TDC-DOPING ON H/C RATIO FOR RUNS E15, E16, AND E17

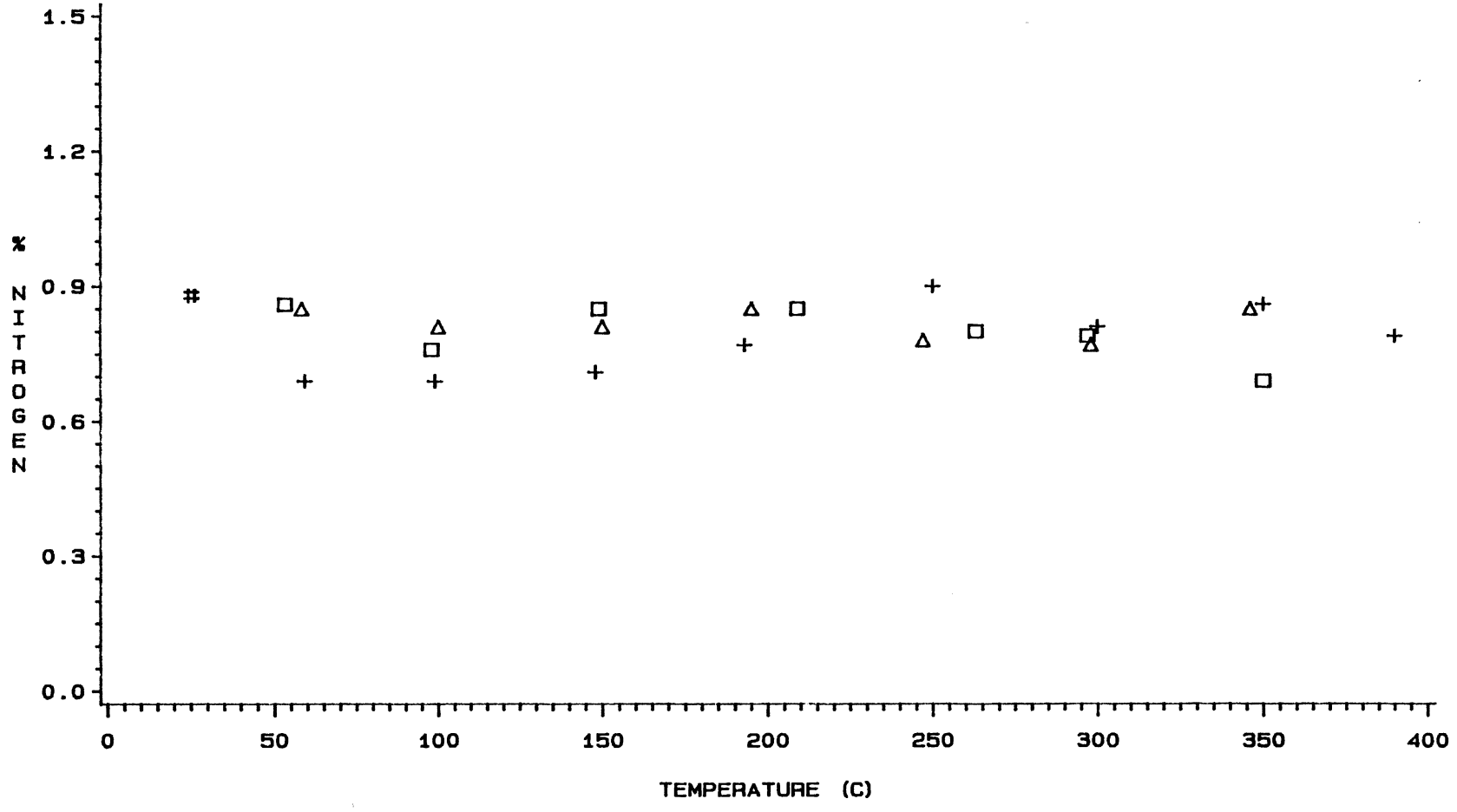

FIGURE 23. EFFECT OF TDC-DOPING ON NITROGEN CONCENTRATION FOR RUNS E15, E16, AND E17

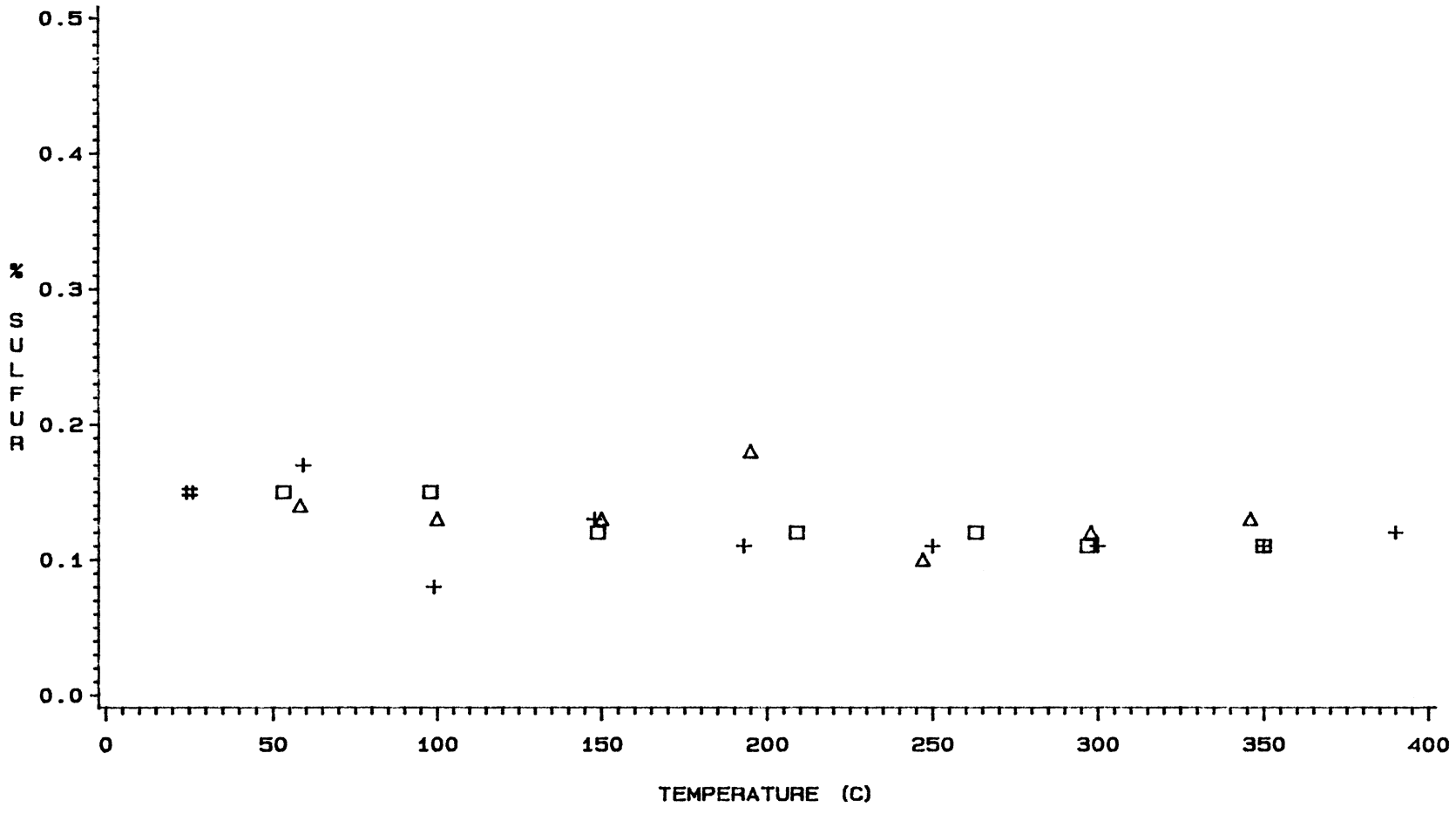

FIGURE 24. EFFECT OF TDC-DOPING ON SULFUR CONCENTRATION FOR RUNS E15, E16, AND E17

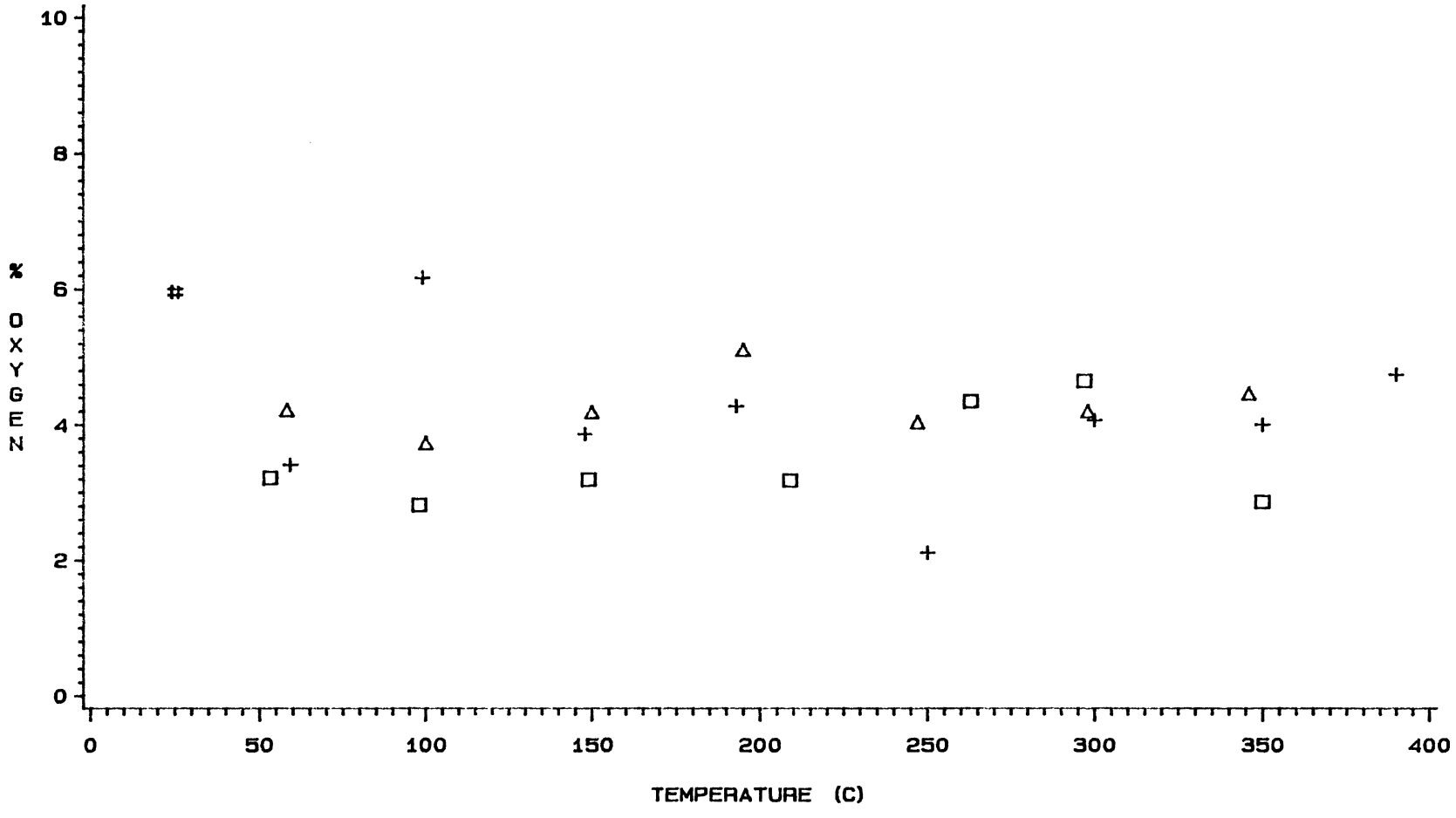

FIGURE 25. EFFECT OF TDC-DOPING ON OXYGEN CONCENTRATION FOR RUNS E15, E16, AND E17

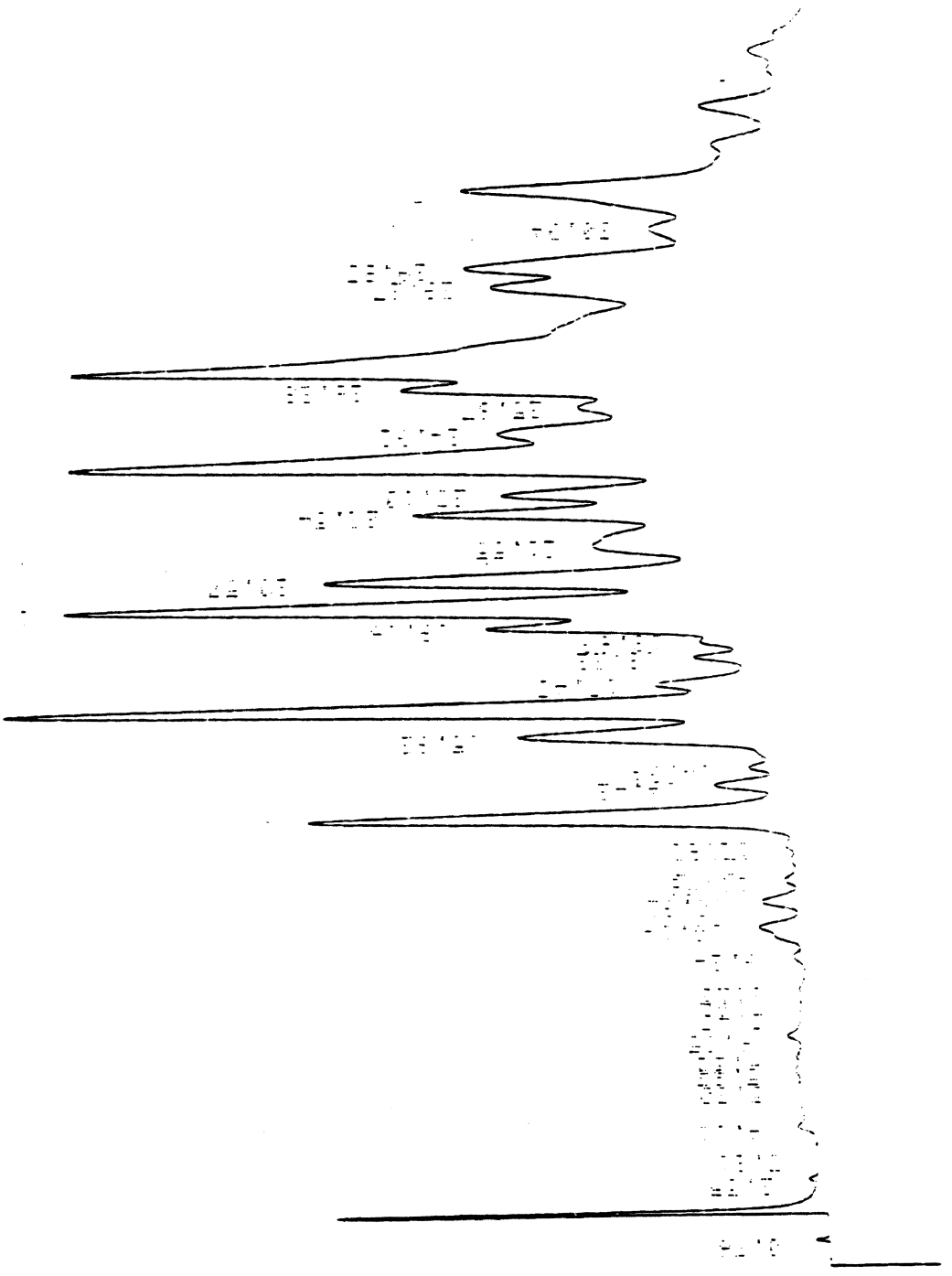

Figure 26. Chromatogram of Feed

TABLE IX

SUMMARY OF BOILING POINT DISTRIBUTIONS
OF PRODUCT OILS FOR
RUNS E2 TO E9

SAMPLE	<100C	100-150C	150-200C	200-250C	250-300C	>300C
FEED*	1.2	1.1	26.6	46.6	20.1	4.3
E2-24	4.5	9.1	29.7	35.0	20.4	1.3
E2-60	8.4	8.3	28.6	34.6	19.3	0.8
E3-24	2.8	4.2	26.6	36.3	23.3	6.8
E3-60	2.2	5.9	28.3	35.2	22.3	6.1
E4-24	2.8	7.5	27.8	34.4	22.0	5.4
E4-50	5.4	3.6	29.0	42.0	18.2	1.7
E4-60	1.1	2.0	25.8	42.8	20.9	7.4
FEED**	7.9	0.8	22.6	40.3	20.0	8.4
TO	8.0	0.8	23.1	40.3	19.7	8.1
E7	9.9	1.0	24.8	44.1	18.3	1.8
AVG.	8.6	0.9	23.5	41.6	19.3	6.1
E7-24	7.4	7.8	29.3	34.1	19.7	1.7
E7-60	3.3	5.0	29.2	39.7	21.2	1.6
E8-24	0.5	9.5	29.7	36.1	21.1	3.1
E8-60	0.3	9.9	30.3	35.4	20.6	3.5
FEED/E9@	1.8	0.8	24.9	42.2	20.1	10.1
E9-24	18.8	5.9	24.6	31.6	17.9	1.0
E9-50	16.8	6.5	24.0	34.6	16.9	1.2
E9-60	7.0	2.7	27.2	42.0	18.1	2.8

*Feed from Tank #1; sample is not available for analysis; analysis of feed from Tank #2 represents Tank #1.
**Feed from Tank #1, with 9.1 wt% MIBK to facilitate dissolving of titanocene dichloride.
@Feed from Tank #2, with 9.1 wt% MIBK to facilitate dissolving of titanocene dichloride.

TABLE X

SUMMARY OF BOILING POINT DISTRIBUTIONS
OF PRODUCT OILS FOR
RUNS E9 TO E18

SAMPLE	<100C	100-150C	150-200C	200-250C	250-300C	>300C
FEED/E9	1.8	0.8	24.9	42.2	20.1	10.1
E9-24	18.8	5.9	24.6	31.6	17.9	1.0
E9-50	16.8	6.5	24.0	34.6	16.9	1.2
E9-60	7.0	2.7	27.2	42.0	18.1	2.8
FEED/	1.3	1.3	27.4	48.3	19.8	2.0
E10 TO	1.4	1.0	27.3	48.4	19.9	2.0
E18	0.9	1.0	25.2	43.2	20.7	8.9
AVG	1.2	1.1	26.6	46.6	20.1	4.3
E10-3	1.7	0.6	24.7	42.8	20.9	9.3
E10-5	1.3	0.9	25.7	42.5	20.3	9.3
E11-3	0.5	0.8	24.7	43.4	21.0	9.5
E11-5	0.2	0.7	25.2	43.8	20.9	9.2
E12-3	0.8	0.8	27.2	47.7	20.0	3.5
E12-5	0	1.3	28.2	48.2	20.1	2.2
E13-3	0.3	1.3	27.9	48.5	20.0	2.1
E13-5	0	0.7	27.0	49.6	20.5	2.2
E14-2	0.7	0.9	27.6	48.9	20.0	1.9
E14-7	1.2	0.7	27.4	48.5	20.0	2.1
E15-2	0.2	0.2	32.8	40.8	23.1	2.9
E15-7	0	0.8	27.5	49.6	20.1	2.0
E16-2	0.4	0.7	25.7	43.7	20.6	8.9
E16-7	0	0.7	28.0	49.0	20.2	2.1
E17-2	16.4	0.4	23.5	41.0	16.7	1.9
E17-7	2.4	0.9	26.8	47.4	20.0	2.5
E18-2	5.5	0.6	24.1	41.6	19.9	8.3
E18-7-4	1.4	0.3	25.5	42.9	20.7	9.2

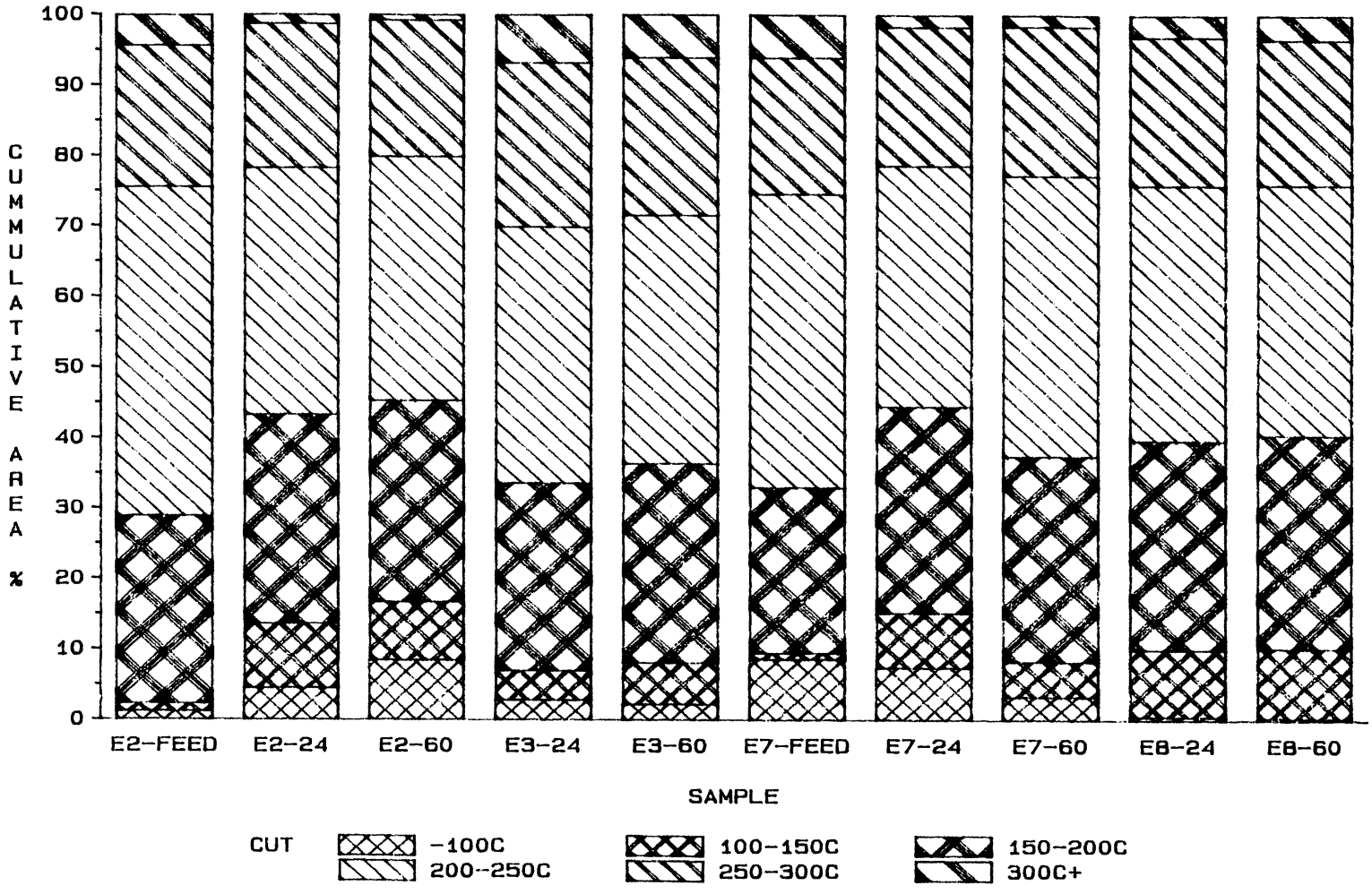

KEY: E2 (375 C) E3 (350 C) E7 (350 C, ON/OFF WITH TI)
E8 (350 C, NON-CATALYTIC, ON/OFF WITH TI)

FIGURE 27. DISTILLATION CUTS FOR RUNS E2, E3, E7, & E8

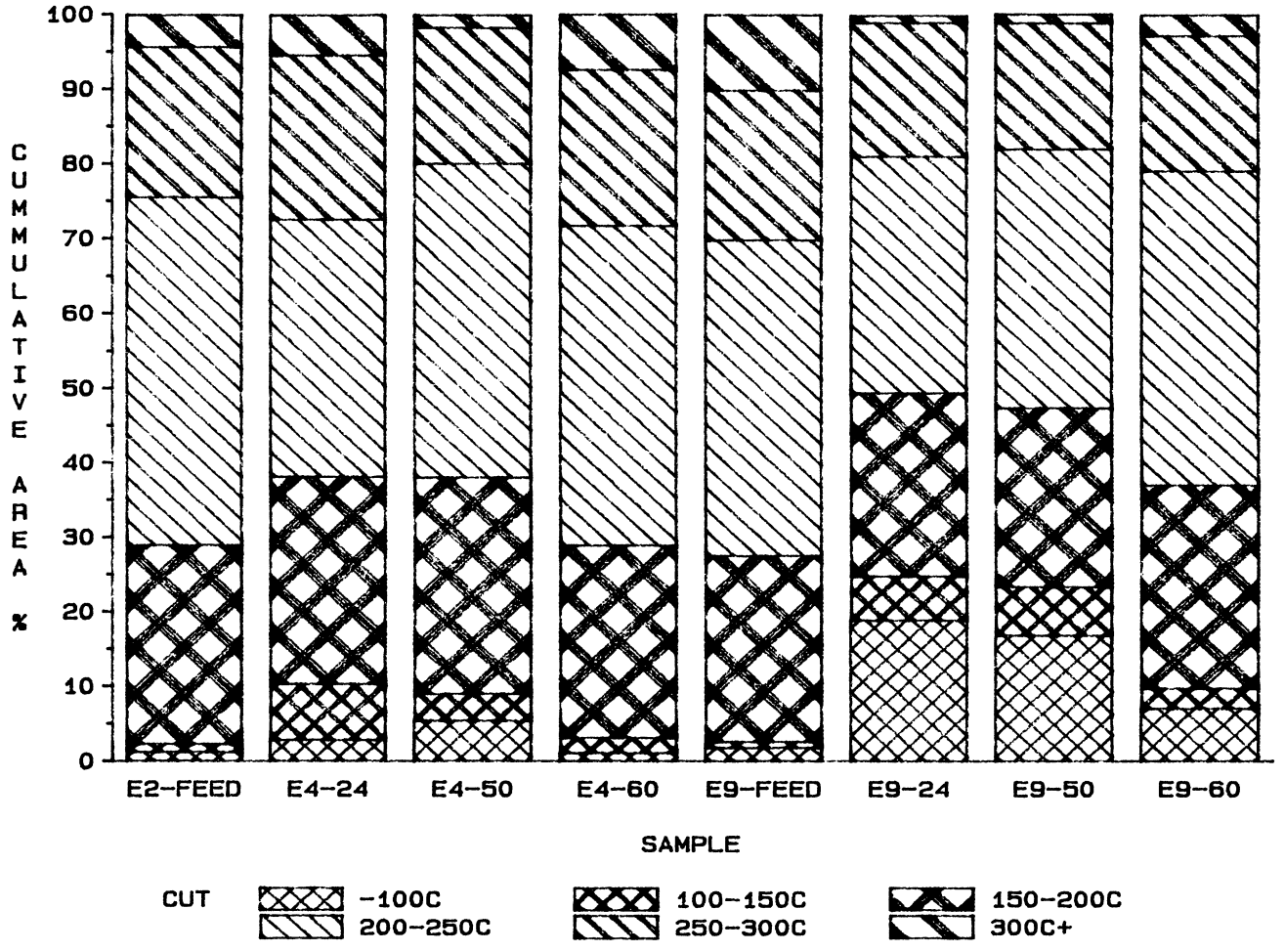

KEY: E4 (0 PPM TI) E9 (50 PPM TI)
0-40 HRS: 350 C/0.44 HR; 40-50 HRS: 350 C/0.22 HR;
50-60 HRS: 325 C/0.22 HR SPACETIME

FIGURE 28. DISTILLATION CUTS FOR RUNS E4 AND E9

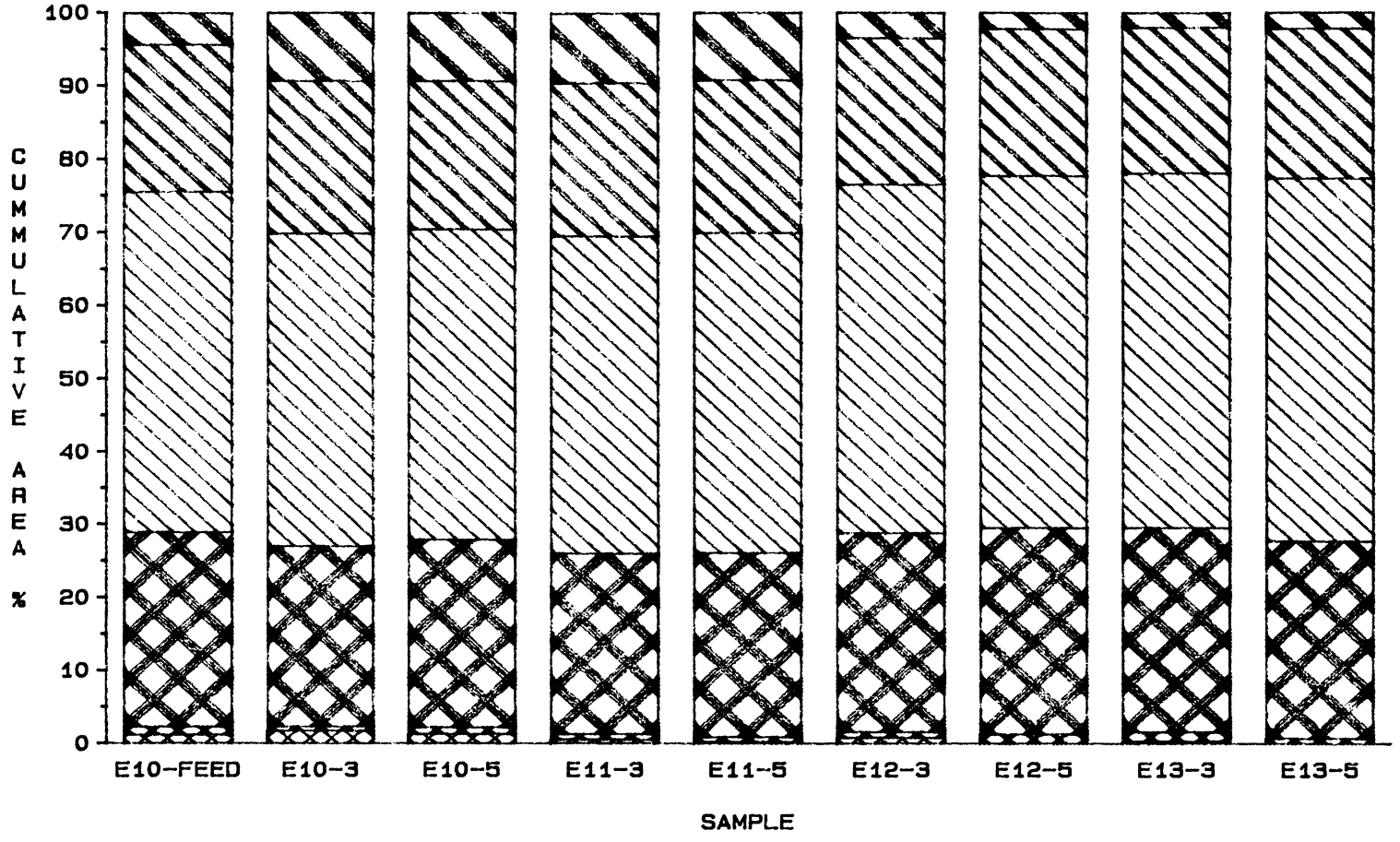

KEY: E10 (NO TI/N2) E11 (NO TI/H2) E12 (50 PPM TI/N2)
E13 (50 PPM TI/H2)

FIGURE 29. DISTILLATION CUTS FOR RUNS E10-E13

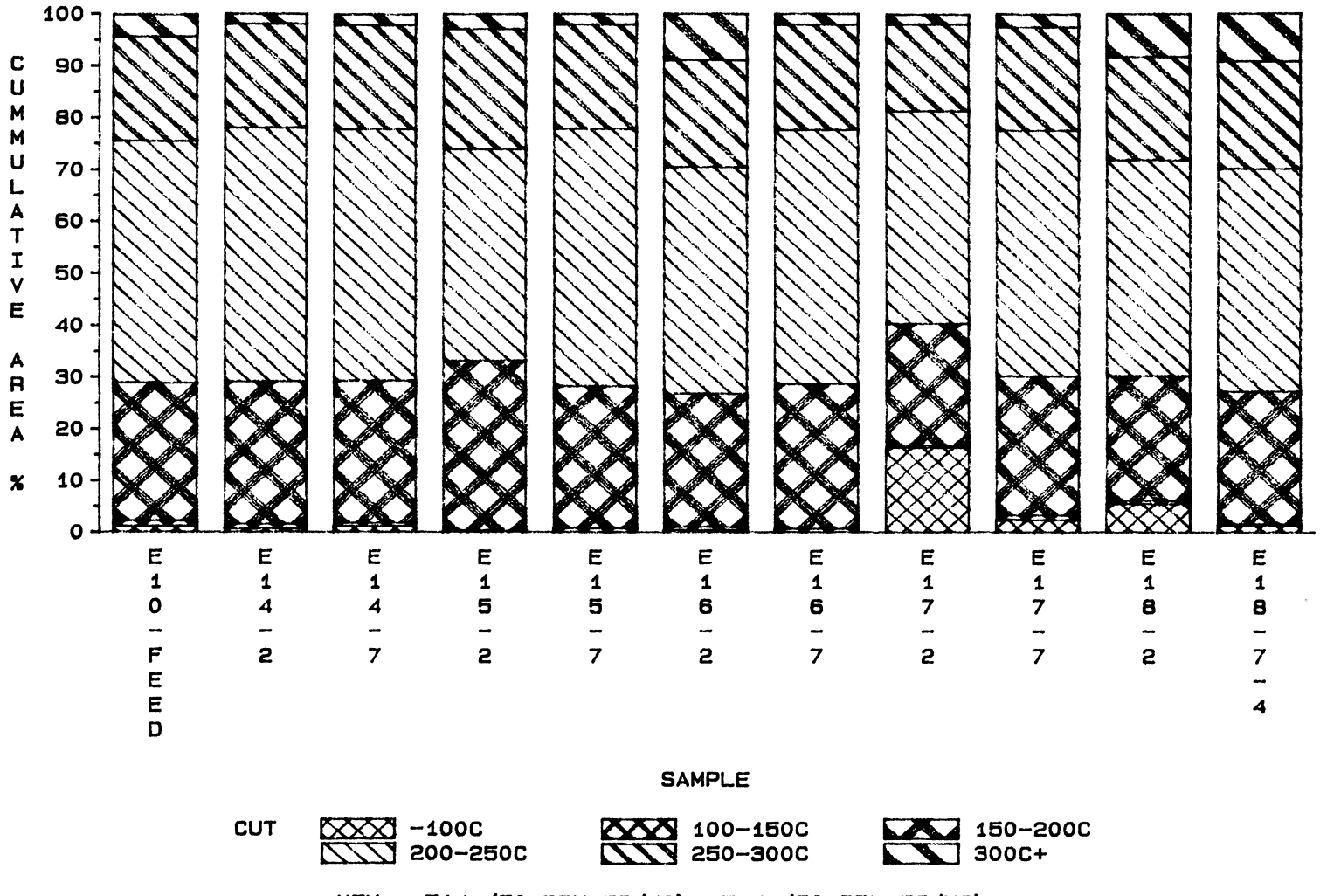

KEY: E14 (50 PPM TI/N2) E15 (50 PPM TI/H2)
E16 (200 PPM TI/H2) E17 (NO TI/H2) E18 (NO TI/N2)

FIGURE 30. DISTILLATION CUTS FOR RUNS E14-E18

all runs, although two different cans were used; the first can for runs E1 to E8; the second can for the subsequent runs. Table X presents the boiling point distributions of selected samples from runs E10 through E18. The same feed was used in runs E10 through E18.

Figure 27 compares the distillation results for runs E2, E3, E7, and E8. When comparing runs E2 and E3, the light fraction decreases and the heavy fraction increases as the reaction temperature is lowered from 375 C (run E2) to 350 C (run E3). Again, when the temperature is lowered from 350 C (E4-50 and E9-50) to 325 C (E4-60 and E9-60), the light fraction decreases, and the heavy fraction increases. Thus, a higher hydrotreatment temperature increases the light fraction and decreases the heavy fraction of the product oil, due to better hydrotreatment and possibly some hydrocracking side reactions.

Samples E4-24 and E7-24 were under identical reaction conditions, except that the pre-sulfiding for run E7 was more severe than that for E4. Comparing samples E7-24 (Figure 27) and E4-24 (Figure 28), shows the increased volatility of sample E7-24 over sample E4-24, because the catalyst sulfidation is more complete.

Figure 28 compares distillaton results for runs E4 and E9. When comparing runs E4 and E9 (identical reactor conditions, except that 50 ppm of Ti as titanocene dichloride is added to the E9 feed), there is a large shift to lighter components, and a corresponding decrease in the

heavier components after hydrotreatment when the titanocene dichloride is added to the feed, even though the feed used for run E9 originally contained a larger amount of heavier components than the feed used for run E4, making the shift to lighter components even more pronounced than if the identical feed was used for each run. Thus, addition of titanocene dichloride to the feed causes a large increase in the light fractions and decrease in the heavy fractions of the hydrotreated feed.

Runs E10 through E18 were non-catalytic runs. Figure 29 presents the distillation results for runs E10-E13, and Figure 30 for runs E14-E18. Runs E10 through E13 showed that the presence of hydrogen had no effect upon the boiling point distribution of the products. However, the presence of titanocene dichloride in the feed for runs E12 and E13 reduced the amount of heavy ends in the product oil. This is confirmed by runs E14, E15, E17, and E18.

Thus, titanocene dichloride does influence the boiling point distribution of the product oil during both catalytic and non-catalytic hydrotreatment.

E.S.R. Analysis

E.S.R. analysis of the instantaneous samples taken from the reactor's interstage sampler are listed in Tables XI, XII, and XIII and presented in Figures 31 through 42. A sample e.s.r. spectrum is given in Figure 43. E.S.R. samples were taken from both the catalytic and non-catalytic

TABLE XI

E.S.R. RESULTS OF RUNS E2 TO E9

SAMPLE	CONDITIONS	GAMMAO	GAMMAM
FEED	25 C	1.	1.
E2-12H	375 C,NO TI	15.0	1.1
E2-36H	375 C,NO TI	1.5	0
E2-60H	375 C,NO TI	0.75	0
E3-24H	350 C,NO TI	6.3	0.24
E3-36H	350 C,NO TI	2.4	0.24
E3-48H	350 C,NO TI	10.0	0.48
E3-60H	350 C,NO TI	2.2	0.24
E4-12H	350 C,NO TI,0.44H	1.4	0
E4-24H	350 C,NO TI,0.44H	3.1	0
E4-36H	350 C,NO TI,0.44H	1.0	0
E4-50H	350 C,NO TI,0.22H	2.5	0.20
E4-60H	325 C,NO TI,0.22H	1.4	0.24
E7-24H	350 C,NO TI	3.2	0.0
E7-36H	350 C,50PPM TI	1.3	0.5
E7-60H	350 C,50PPM TI	3.7	0.0
E8-24H	350 C,NO TI	105	5.6
E8-36H	350 C,50PPM TI	130	8
E8-48H	350 C,NO TI	74	5
E8-60H	350 C,25PPM TI	10	1
E9-12H	350 C,50PPM TI,0.44H	2.5	0.0
E9-24H	350 C,50PPM TI,0.44H	0.42	0.18
E9-36H	350 C,50PPM TI,0.44H	0.63	0.0
E9-60H	350 C,50PPM TI,0.22H	2.6	0.0

TABLE XII

E.S.R. RESULTS OF RUNS E10 TO E13

SAMPLE	GAMMAO	GAMMAM	TEMP (C)
E10-1	10.	1.9	294
E10-2	8.7	1.	318
E10-3	5.6	0.9	49
E10-4	5.9	0.9	369
E10-5	2.6	0.42	389
E11-1	15.	2.5	298
E11-2	4.8	0.6	324
E11-3	1.7	0.1	348
E11-4	4.6	0.3	373
E11-5	1.3	0.3	399
E12-1	14.	1.	304
E12-2	50.0	3.5	329
E12-3	3.44	0.35	348
E12-4	1.9	0.3	370
E12-5	9.7	0.7	380
E13-1	19.	1.	301
E13-2	2.0	0.67	332
E13-3	1.8	0.52	355
E13-4	2.4	0.52	374
E13-5	1.6	0.42	395

TABLE XIII

E.S.R. RESULTS OF RUNS E14 TO E18

SAMPLE NUMBER	GAMMAO	GAMMAM	TEMP (C)
E14-1	5.6	1.1	62
E14-2	4.8	0.6	99
E14-3	5.4	0.7	162
E14-4	6.9	0.7	200
E14-5	4.6	0.6	254
E14-6	2.6	0.6	306
E14-7	0.64	0.1	363
E14-8	0.82	0.1	387
E15-1	4.1	0.7	53
E15-2	4.6	0.6	98
E15-3	3.3	0.6	149
E15-4	7.1	0.7	209
E15-5	10.2	1.1	263
E15-6	38	2.	297
E15-7	59	2.	350
E16-1	5.9	0.6	58
E16-2	6.9	0.7	100
E16-3	4.3	0.6	150
E16-4	3.1	0.6	195
E16-5	10.7	1.3	247
E16-6	4.6	1.2	298
E16-7	14.	1.	346
E17-1	3.3	1.1	59
E17-2	5.6	1.1	99
E17-3	5.1	0.7	148
E17-4	4.6	0.7	193
E17-5	6.6	0.7	250
E17-6	13.	0.9	300
E17-7	15.	1.	350
E17-8	7.1	0.7	390
E18-1	4.6	1.1	60
E18-2	4.6	0.9	103
E18-3	3.8	0.7	152
E18-4	4.6	0.7	204
E18-5	5.2	0.7	253
E18-6	13.	1.	310
E18-7(1)	0.50	0.22	354
E18-7(2)	1.0	0.2	354
E18-7(3)	0.56	0.1	353
E18-7(4)	1.3	0.09	350
E18-8	1.9	0.2	394

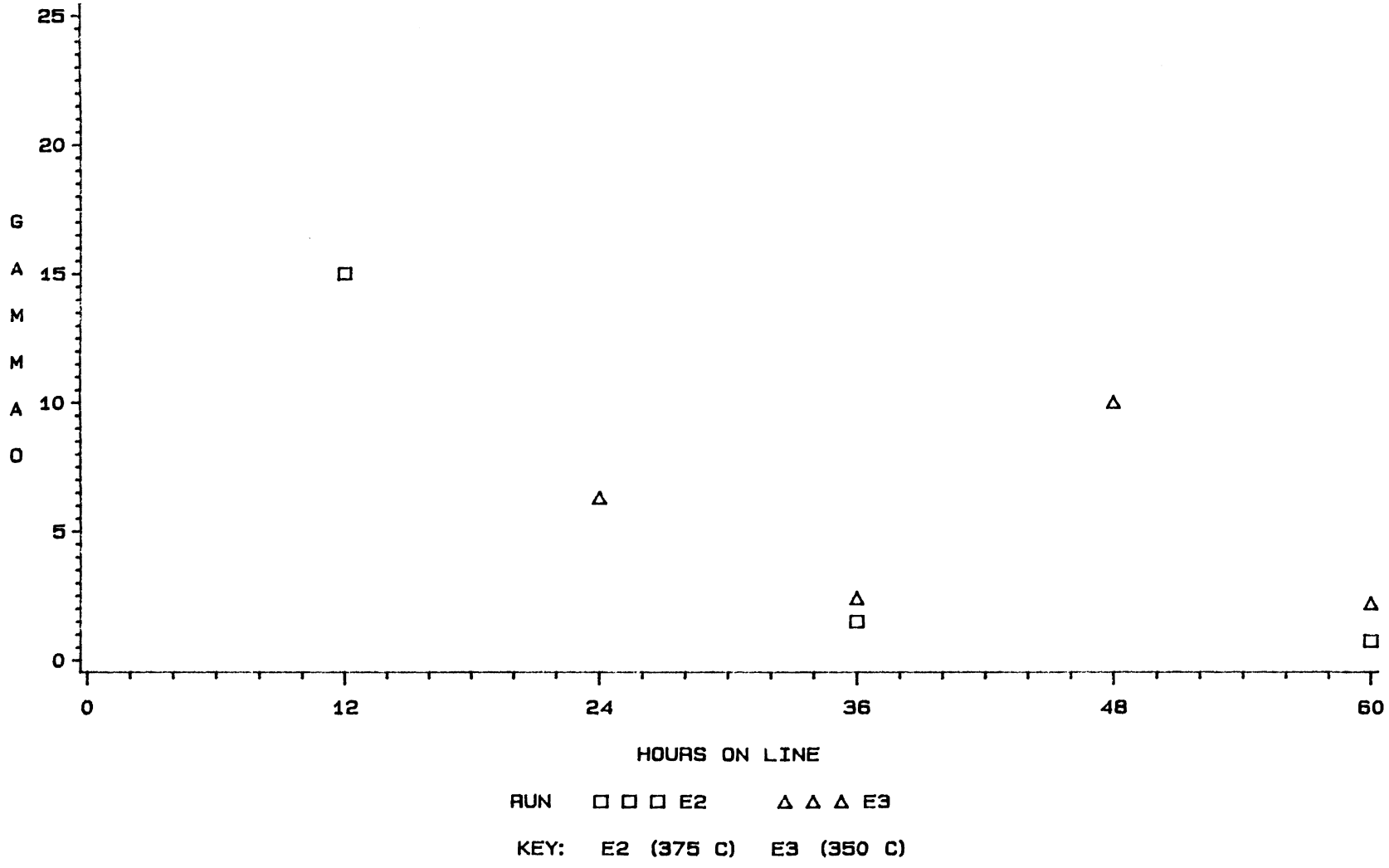

FIGURE 31. EFFECT OF TEMPERATURE ON RELATIVE FREE RADICAL CONCENTRATIONS FOR RUNS E2 AND E3

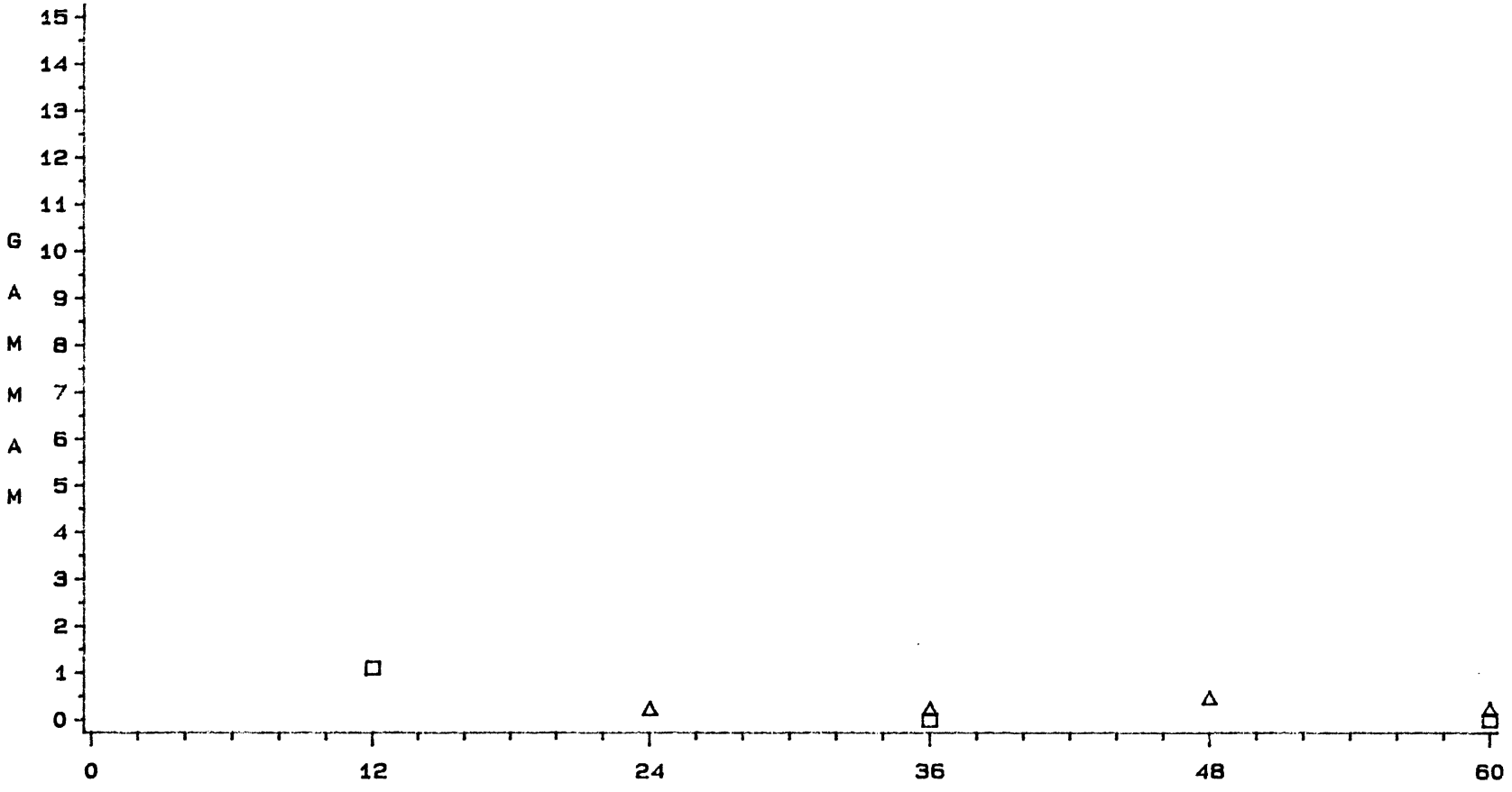

FIGURE 32. EFFECT OF TEMPERATURE ON RELATIVE FE(III) CONCENTRATIONS FOR RUNS E2 AND E3

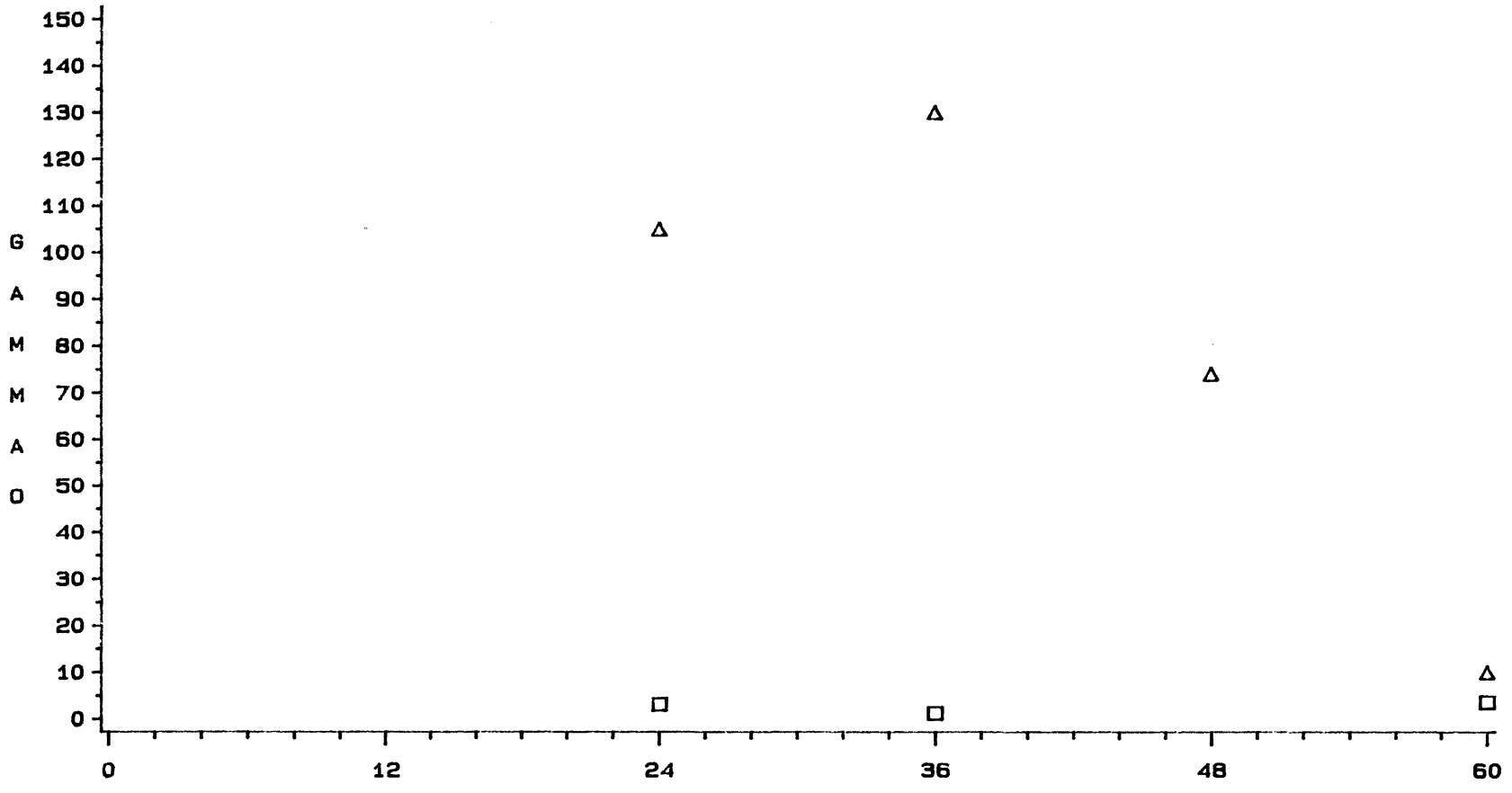

KEY: E7 (CATALYTIC) E8 (NON-CATALYTIC)

FIGURE 33. EFFECT OF CATALYST ON RELATIVE FREE RADICAL CONCENTRATIONS FOR RUNS E7 AND E8

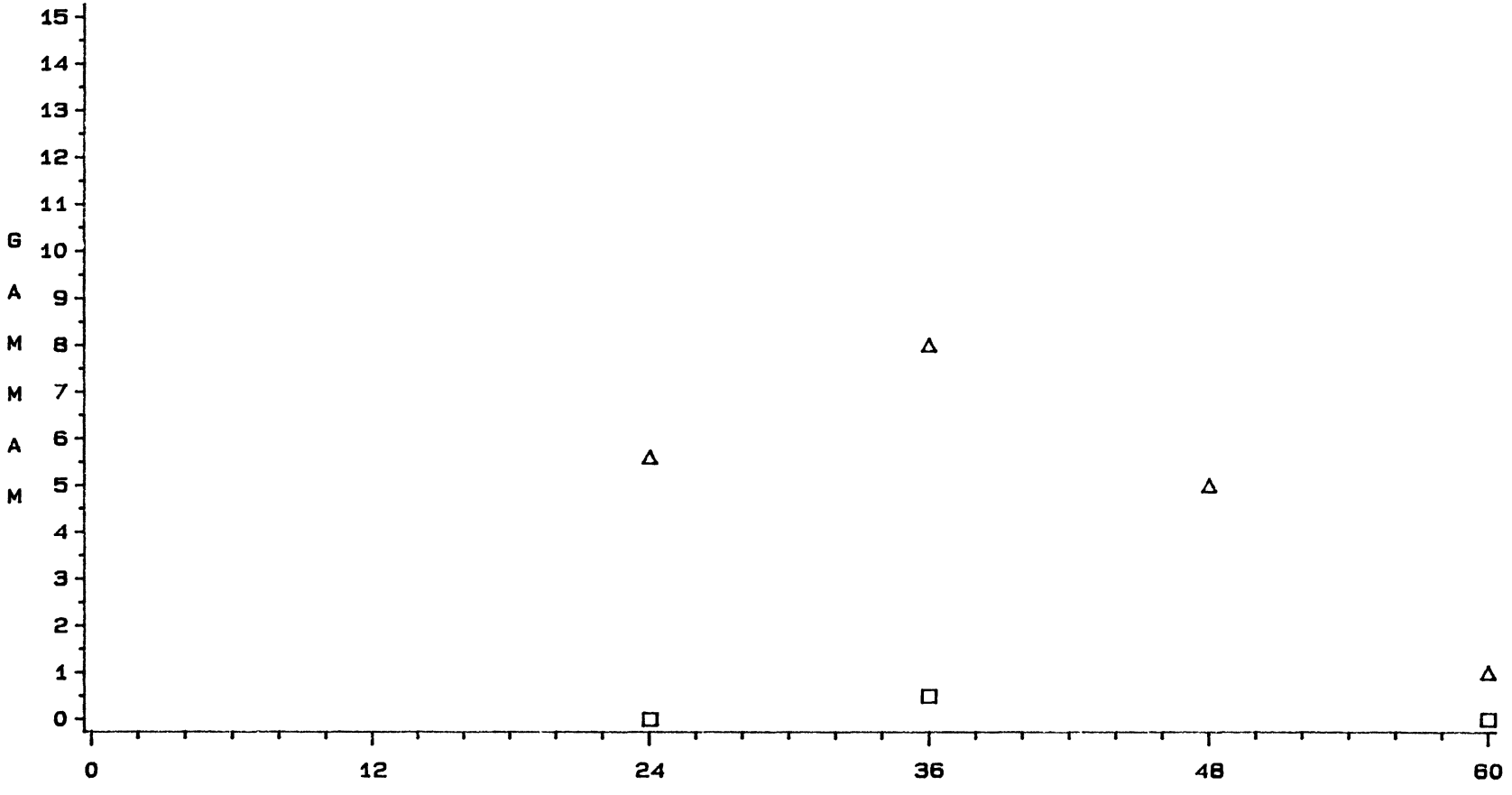

KEY: E7 (CATALYTIC) E8 (NON-CATALYTIC)

FIGURE 34. EFFECT OF CATALYST ON RELATIVE FE(III) CONCENTRATIONS FOR RUNS E7 AND E8

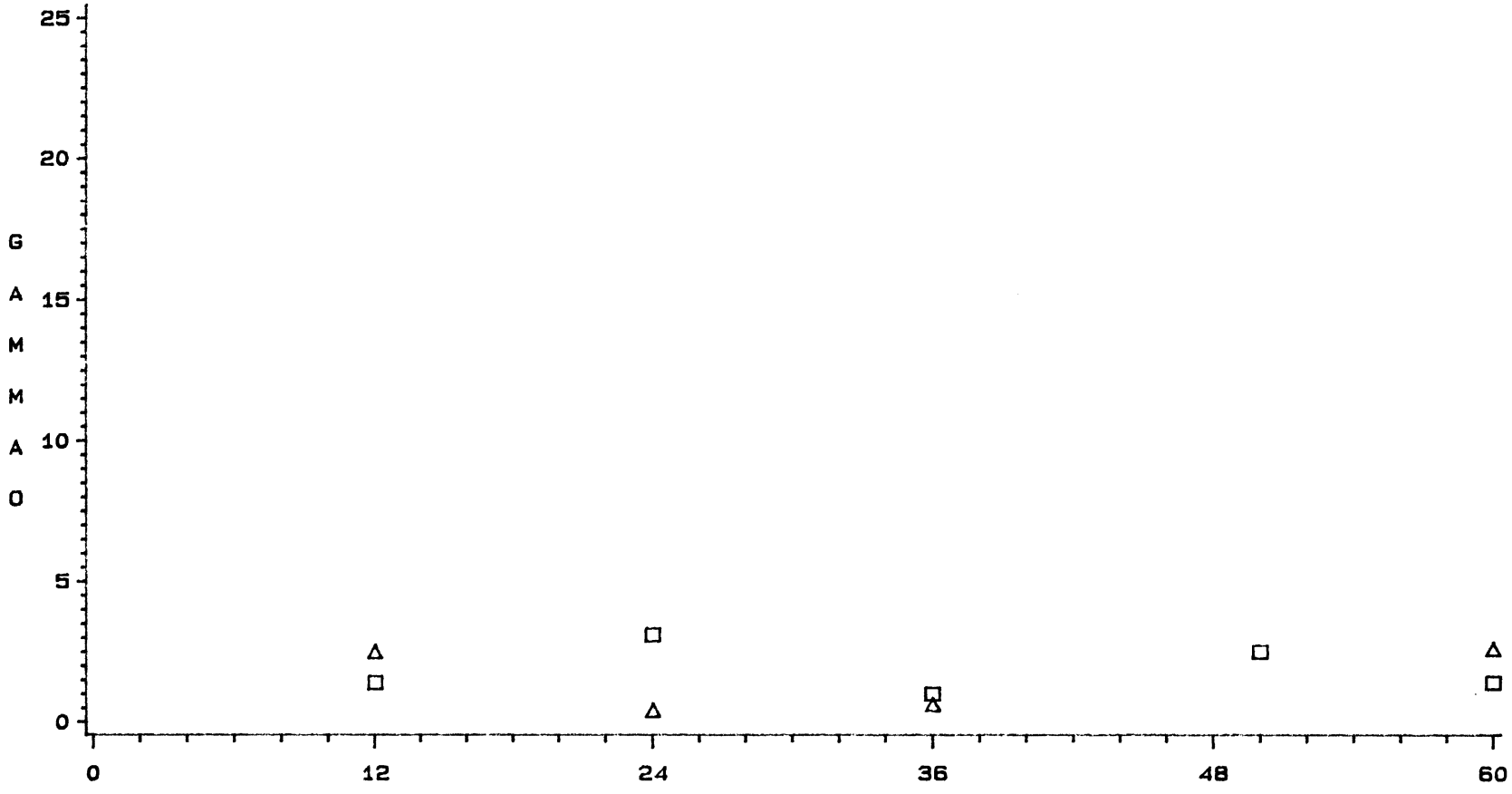

FIGURE 35. EFFECT OF TDC-DOPING ON RELATIVE FREE RADICAL CONCENTRATIONS FOR RUNS E4 AND E9

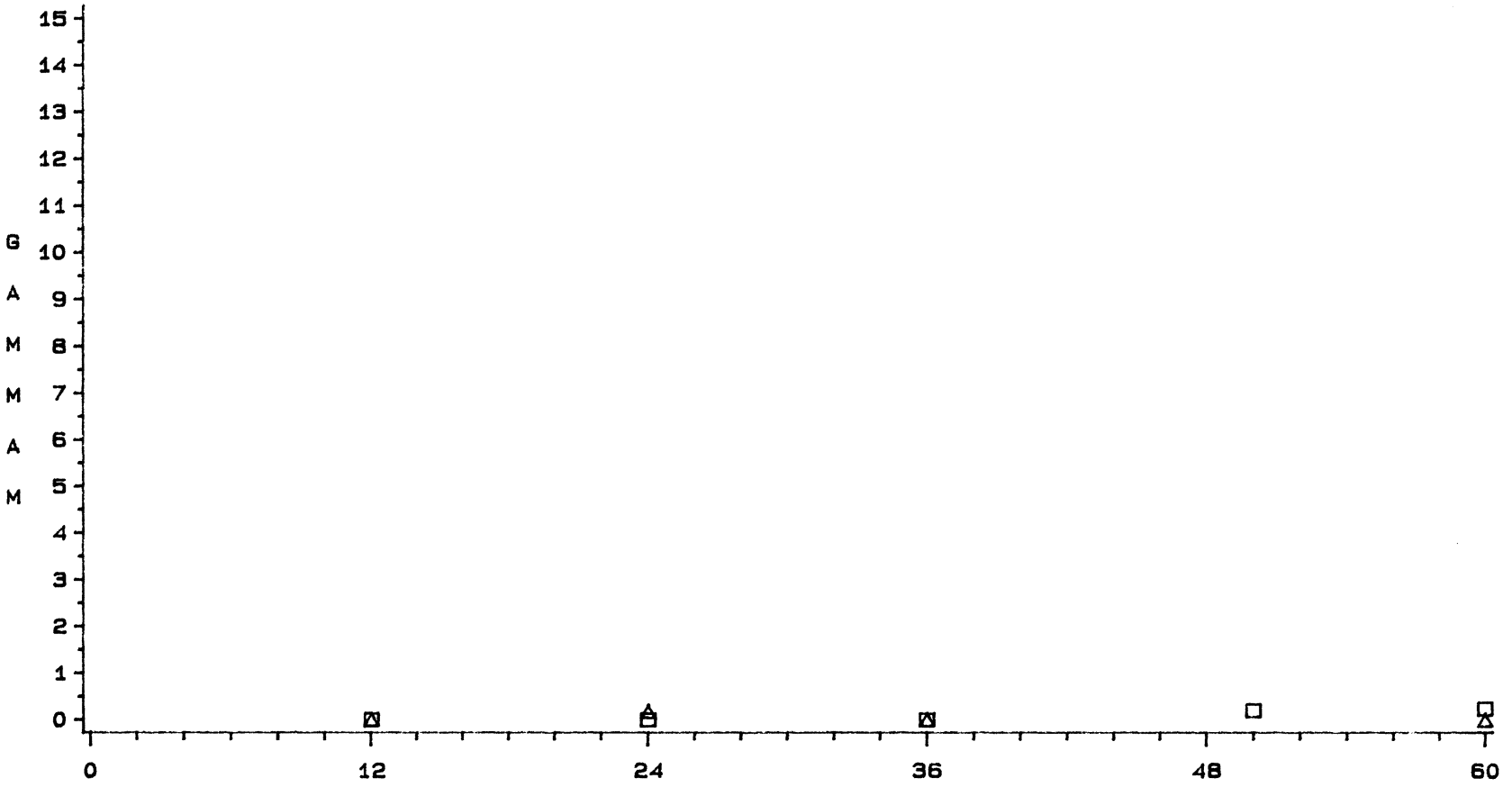

FIGURE 36. EFFECT OF TDC-DOPING ON RELATIVE FE(III) CONCENTRATIONS FOR RUNS E4 AND E9

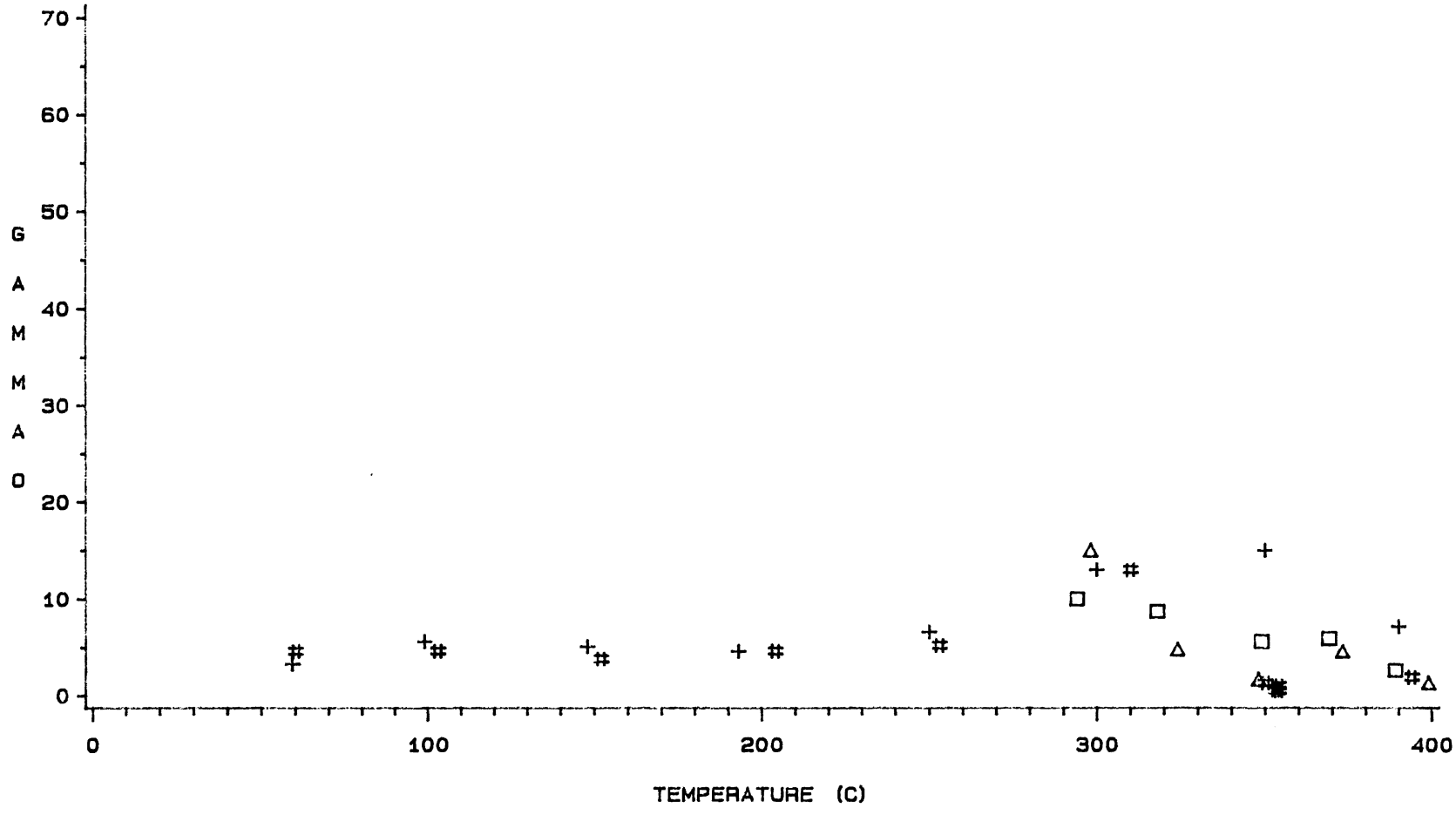

FIGURE 37. EFFECT OF GAS TYPE ON RELATIVE FREE RADICAL CONCENTRATION FOR UNDOPED NON-CATALYTIC RUNS

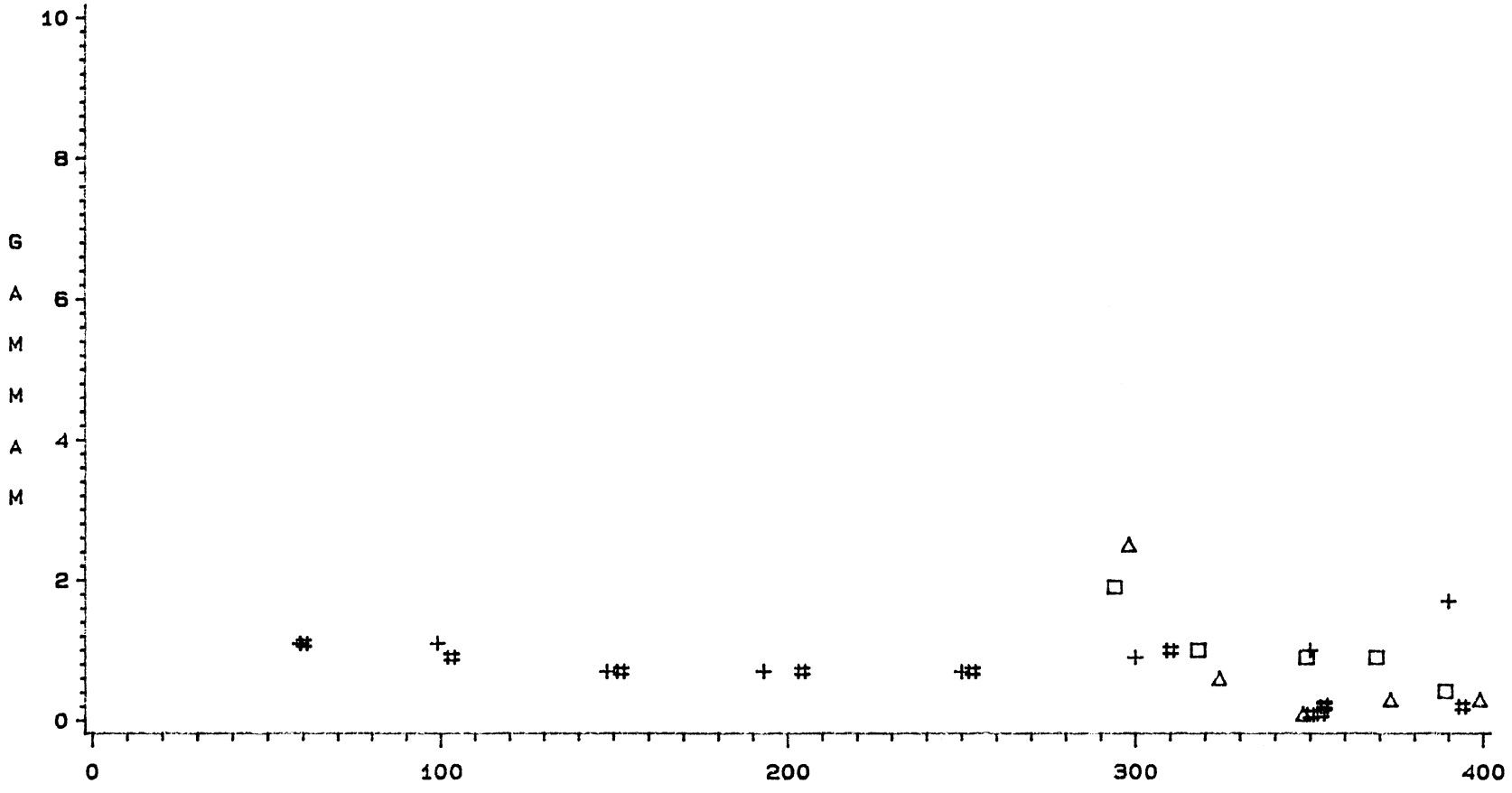

KEY: E10, E18 (NITROGEN) E11, E17 (HYDROGEN)

FIGURE 38. EFFECT OF GAS TYPE ON RELATIVE FE(III) CONCENTRATION FOR UNDOPED NON-CATALYTIC RUNS

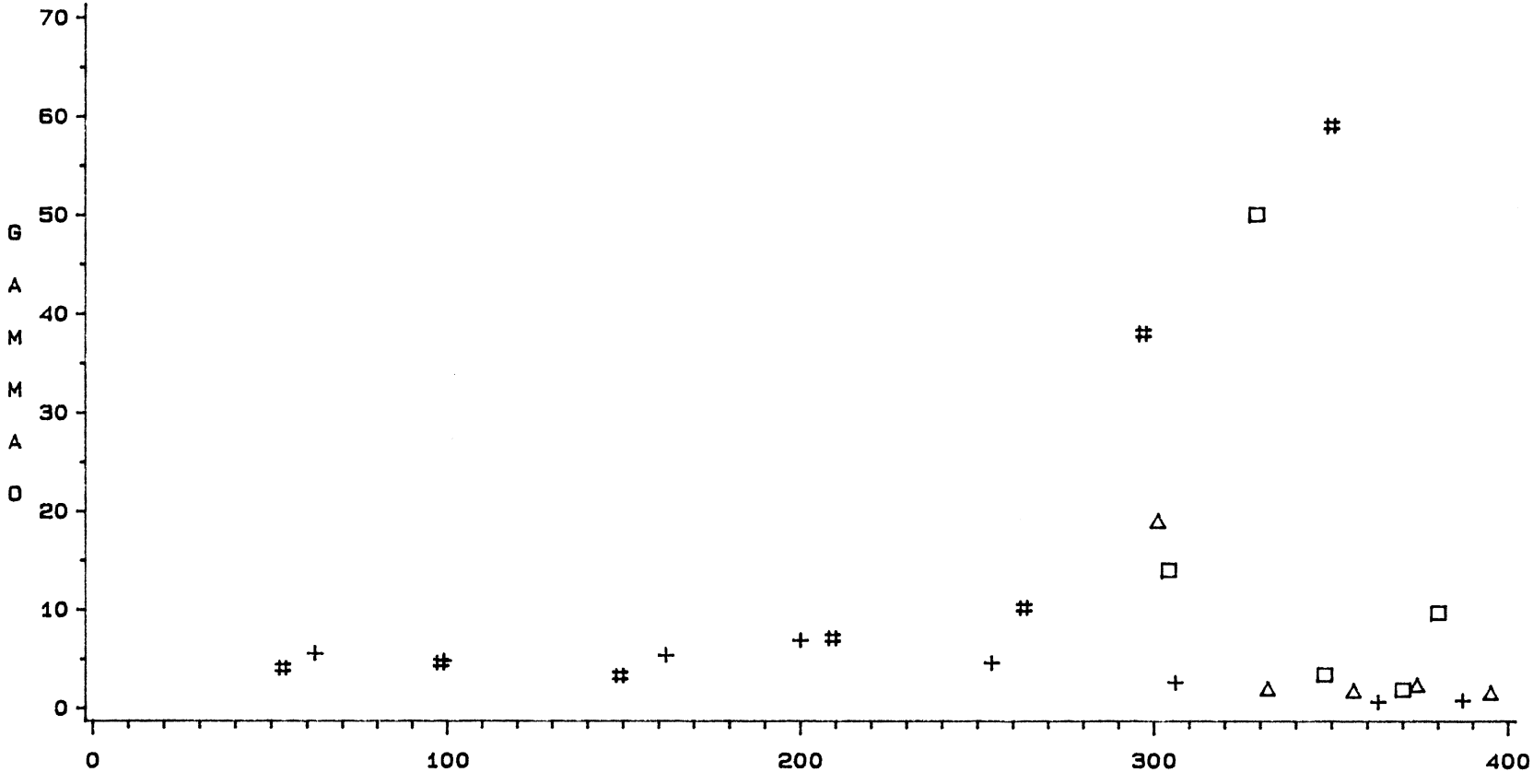

FIGURE 39. EFFECT OF GAS TYPE ON RELATIVE FREE RADICAL CONCENTRATION FOR NON-CATALYTIC RUNS DOPED WITH 50 PPM TI

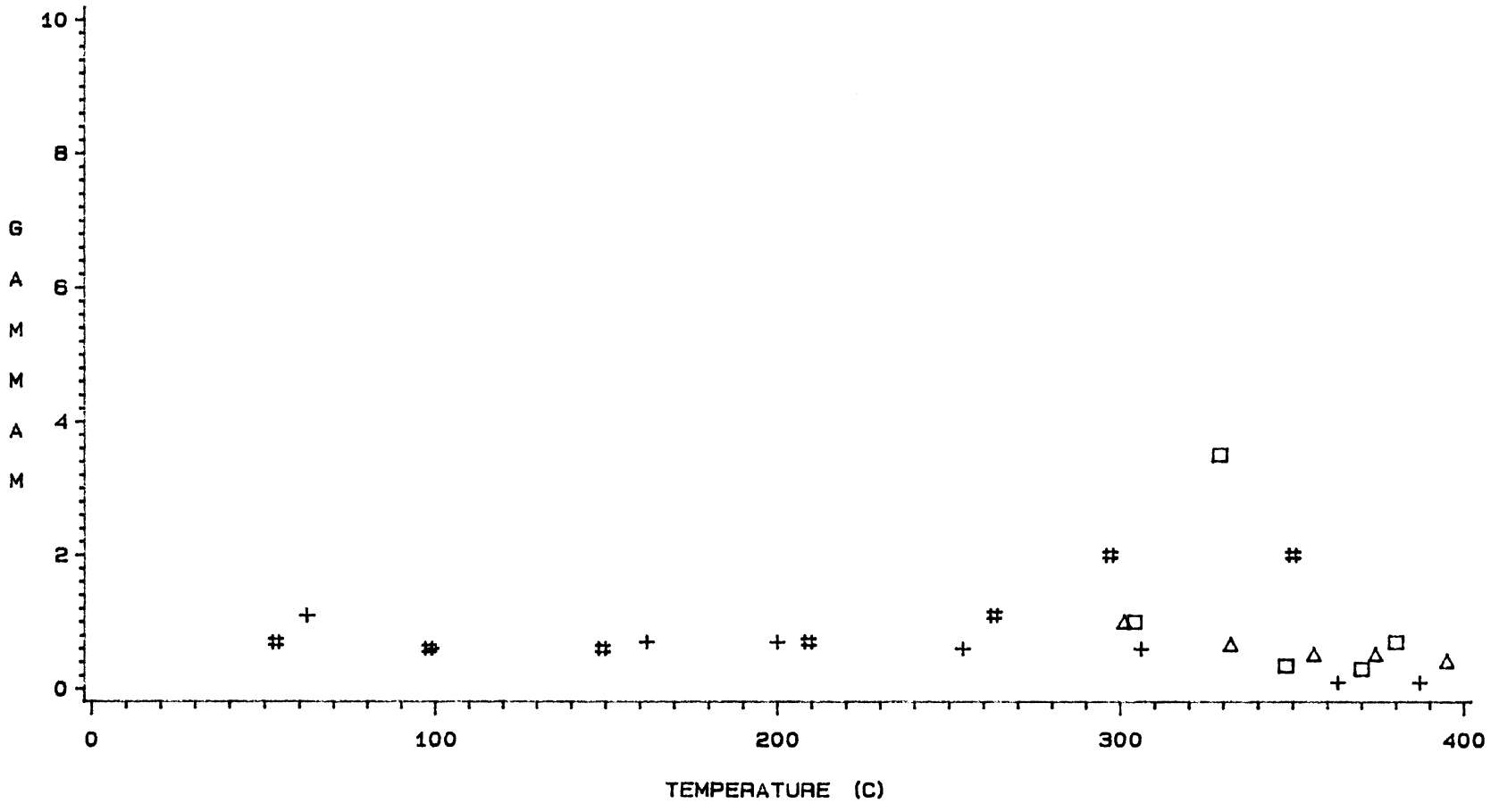

FIGURE 40. EFFECT OF GAS TYPE ON RELATIVE FE(III) CONCENTRATION FOR NON-CATALYTIC RUNS DOPED WITH 50 PPM TI

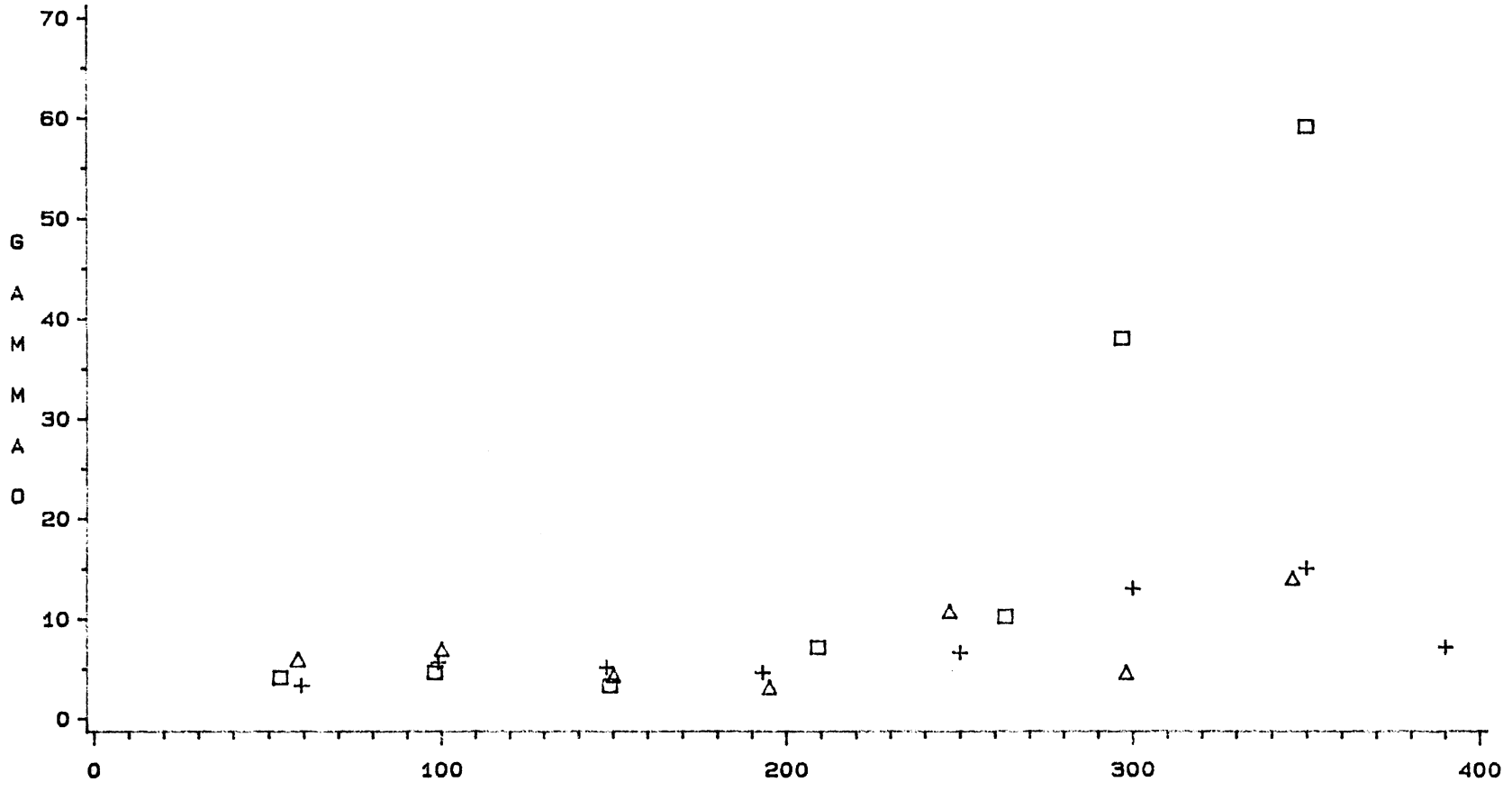

KEY: E15 (50 PPM TI/H2) E16 (200 PPM TI/H2) E17 (NO TI/H2)

FIGURE 41. EFFECT OF TDC-DOPING ON RELATIVE FREE RADICAL CONCENTRATION FOR RUNS E15, E16, AND E17

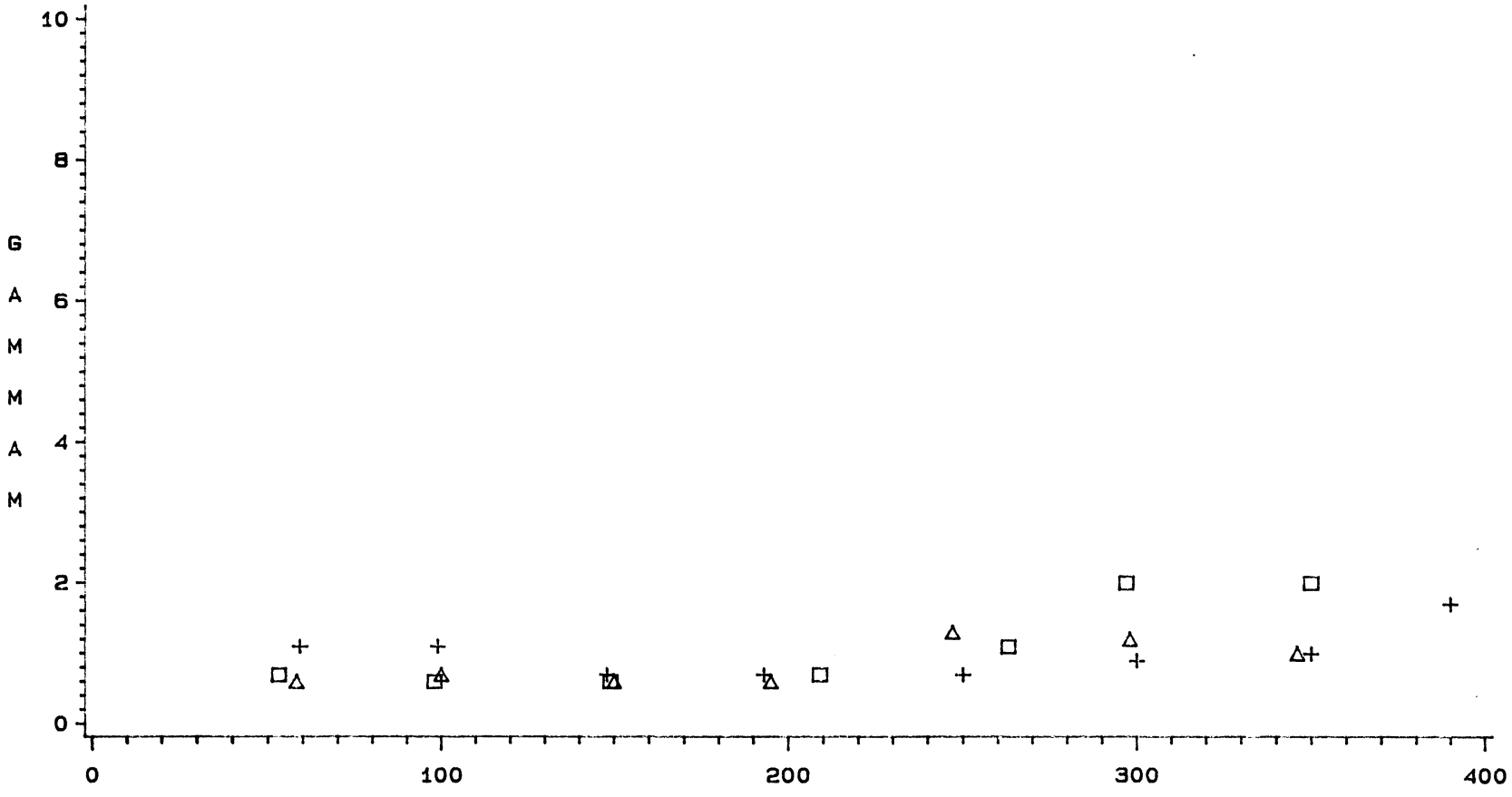

KEY: E15 (50 PPM TI/H2) E16 (200 PPM TI/H2) E17 (NO TI/H2)

FIGURE 42. EFFECT OF TDC-DOPING ON RELATIVE FE(III) CONCENTRATION FOR RUNS E15, E16, AND E17

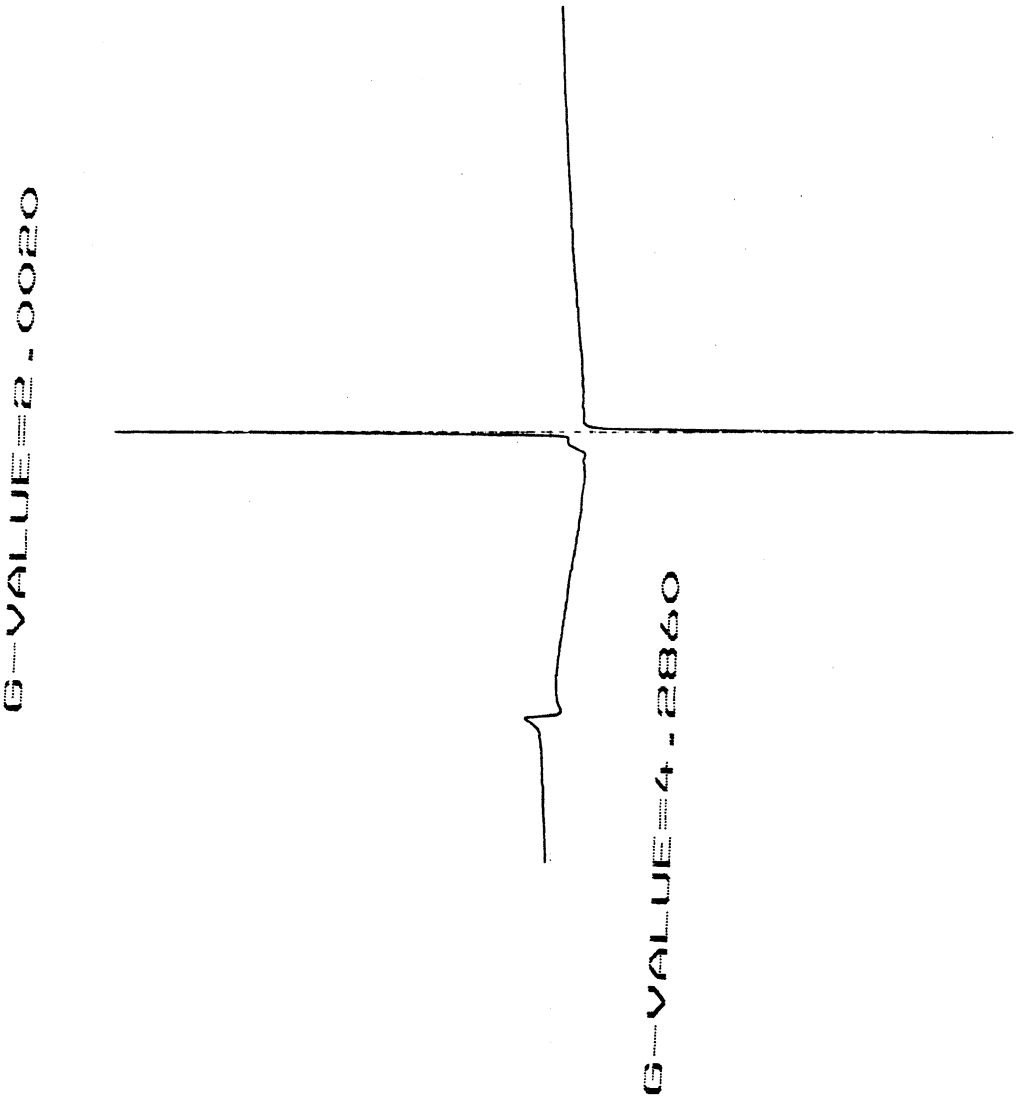

Figure 43. E.S.R. Spectrum of Feed

runs. During e.s.r. analysis, two peaks were noted for each sample. The first peak, with a g-value of about 4.2860, was attributed to the presence of Fe(III) ions in the samples. The second peak, with a g-value of about 2.0020, was attributed to the presence of organic free radicals in the samples. These numbers are consistent with Dack et al. (1985).

To relate relative concentrations of both the Fe(III) ions and the organic free radicals, the variables GAMMAM (for the iron) and GAMMAO (for the organic free radicals) were introduced, where GAMMA is simply the height of the sample peak divided by the height of the feed peak (at 25 C).

Based on these two relative concentrations, several observations can be made. Figures 31 and 32 present the GAMMA values for runs E2 and E3. For runs E2 and E3, the free radical concentration jumps to a high level at the start of the run, and then decreases as run time increases. Very little or no Fe(III) is noted once the run begins, possibly due to the HDM reaction, or perhaps conversion of the Fe(III) ion to the Fe(II) state.

Figures 33 and 34 present the GAMMA values for runs E7 and E8. The data from run E7 (on/off run with catalyst) indicates that there is apparently no effect of titanocene dichloride on free radical concentration. This is confirmed by Figure 35 for runs E4 (no titanocene dichloride, with catalyst) and E9 (50 ppm Ti as titanocene dichloride, with

catalyst), in which there is basically no difference in free radical concentration for the two runs. Once again, GAMMAM was significantly reduced during the run (see Figures 34 and 36).

For the catalytic runs, the free radical concentration is unrelated to the Fe(III) concentration; however, for the non-catalytic runs, when comparing the relative free radical concentration of each run with its respective Fe(III) relative concentration, there appears to be a definite correlation between the two. Where the free radical concentration increases, there also appears a jump in the Fe(III) concentration, and when the free radical concentration decreases, there is a corresponding drop in the Fe(III) concentration. Figure 44 presents the free radical concentration versus the Fe(III) concentration for all samples from runs E10 through E18. There appears to be a definite correlation beween the two.

When comparing runs E10 through E18, the product relative free radical concentration remains stable up to a temperature of 250 C; increases dramatically between 250 C and 350 C; and then falls again from 350-400 C (see Figures 37, 39, and 41). This phenomenon occurs regardless of gas type or titanocene doping of the feed, and is similar to the findings of Rudnick and Sinclair (1984). The free radical initiation reaction becomes dominant from 250 C to 350 C (thus, a higher free radical concentration results), and the free radical termination reactions become dominant above 350

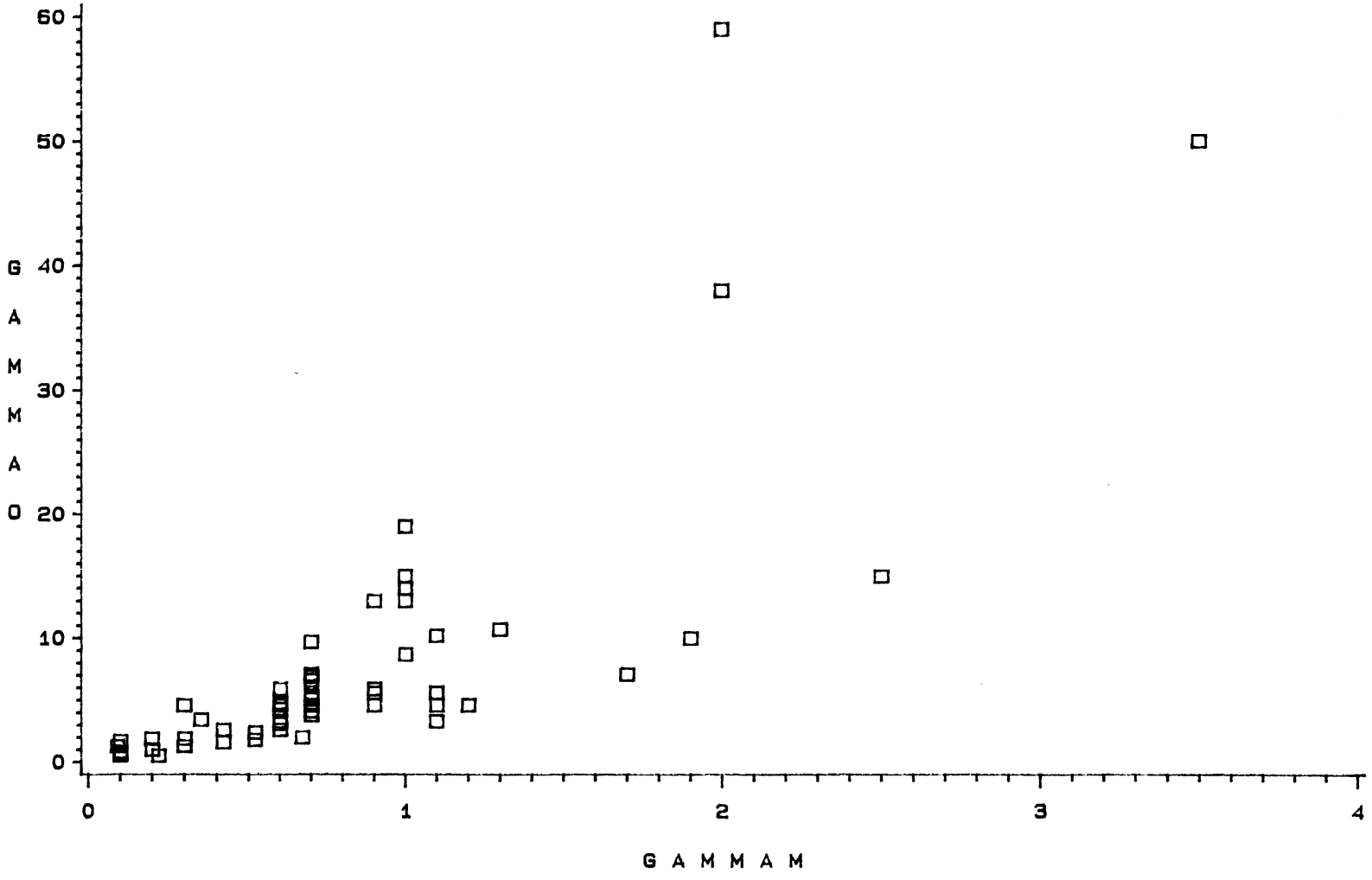

FIGURE 44. RELATIONSHIP BETWEEN GAMMAO AND GAMMAM FOR RUNS E10-18

C, resulting in a relatively lower free radical concentration.

When comparing runs E10 through E13 (Figures 37 and 39), there is relatively no effect of hydrogen gas flowing through the reactor or the addition of titanocene dichloride to the oil feedstock upon the relative free radical concentrations of samples treated between the temperatures of 300 and 400 C. When comparing runs E17 and E18 (Figure 37), there is no effect of hydrogen gas flowing through the reactor when the samples are treated from room temperature all the way up to 400 C. However, in comparing runs E15 and E16 (Figure 41), the addition of titanocene dichloride increases the free radical concentration of the samples at around 350 C when hydrogen gas flows through the system. This phenomenon did not appear in runs E10 through E13, and thus, results are not conclusive.

When comparing the relative free radical concentrations from samples at around 350 C for runs E10 through E18 (Figures 37, 39, and 41), there is a wide variance in free radical concentrations from those samples. This is confirmed from the e.s.r. results obtained from run E8 (Figure 33), in which the values for GAMMAO and GAMMAM vary widely, although reactor conditions were constant. Thus, there is an area of instability in free radical concentrations at a temperature of around 350 C. Some of the samples that were high in free radical concentration were re-analyzed several months after their first analysis

and they still had consistently highly values of GAMMAO, indicating that their relatively high free radical concentrations were stable.

Iron Analysis of Accumulated Samples

Iron content of the accumulated oil samples from both the catalytic and non-catalytic runs are listed in Table XIV. Several of the oil samples were analyzed twice in order to check the reliability and reproducibility of the atomic absorption unit that was used to analyze the samples. The results of these multiple analyses are listed in Table XV. Reproducibility seems to be fairly good, as most of the duplicated samples are within 10% of each other. The samples E18-7-1&2, E18-7-3, and E18-7-4 were taken under identical conditions, and the iron results are within 5% of each other, indicating that the machine reliability is very good. There are some discrepancies between various samples (the iron concentration of the feed is reported as 45.4 micrograms/liter for sample E7-FD, 24.2 micrograms/liter for sample E10-FD, 20.7 micrograms/liter for sample E12-FD, and 44.6 micrograms/liter for sample E15-FD), but these discrepancies are probably due to particulate matter (containing higher concentrations of iron) rather than the oil itself being detected by the AA unit.

The SRC-II Middle Distillate was tested for metals content before and after hydrotreatment. Table XVI presents the results of the test. All the metals in the oil

TABLE XIV

IRON CONCENTRATION IN ACCUMULATED SAMPLES
(in micrograms/liter)

SAMPLE	CONCENTRATION	SAMPLE	CONCENTRATION
E2-12	8.7	E10-0	24.2
-24	10.5	-1	41.4
-36	30.1	-2	41.3
-48	7.8	-3	22.4
-60	29.1	-4	23.7
E3-12	37.2	-5	20.4
-24	28.6	E11-1	23.8
-36	36.7	-2	22.4
-48	41.6	-3	20.9
-60	36.2	-4	18.4
E4-12	30.6	-5	17.3
-24	34.7	E12-0	20.7
-36	32.1	-1	37.7
-40	38.8	-2	30.5
-50	37.8	-3	15.8
-60	41.3	-4	15.8
E7-0	45.4	-5	19.9
-6	30.6	E13-1	10.1
-12	23.5	-2	11.7
-24	28.6	-3	15.8
-36	28.6	-4	18.9
-48	31.1	-5	45.9
-60	31.6	E14-1	52.1
E8-6	37.2	-2	10.7
-12	40.3	-3	13.1
-18	39.3	-4	14.1
-24	40.3	-5	15.6
-30	39.8	-6	73.4
-36	62.7	-7	48.5
-42	37.7	-8	3.6
-48	40.3	E15-0	44.6
-54	37.7	-1	38.8
-60	37.2	-2	48.2
E9-6	33.7	-3	44.6
-12	37.2	-4	45.4
-18	36.2	-5	42.3
-24	29.1	-6	36.7
-30	32.1	-7	49.7
-36	31.1	E16-1	32.8
-40	29.1	-2	46.4
-50	34.2	-3	50.5
-55	51.0	-4	47.9
-60	46.4	-5	61.2

TABLE XIV (CONTINUED)

SAMPLE	CONCENTRATION	SAMPLE	CONCENTRATION
E16-6	21.9	E18-1	71.9
-7	19.4	-2	43.9
E17-1	23.1	-3	44.4
-2	60.2	-4	48.5
-3	47.2	-5	51.5
-4	47.0	-6	47.9
-5	50.0	-7-1&2	47.9
-6	45.9	-7-3	44.4
-7	46.4	-7-4	48.7
-8	45.4	-8	65.3

TABLE XV

REPEATABILITY OF IRON ANALYSIS
BY MULTIPLE ANALYSIS
(in micrograms/liter)

SAMPLE	#1	#2	#3
E3-48	33.2	50.0	
E4-50	35.7	39.8	
E4-60	42.3	40.3	
E9-50	31.1	37.2	
E12-2	29.1	32.3	30.1
E14-1	49.0	55.1	
E14-7	47.9	49.0	
E15-2	46.4	50.0	
E15-7	46.4	53.0	
E17-1	8.7	37.7	
E18-7-4	47.4	50.0	

TABLE XVI

METALS ANALYSIS OF FEEDSTOCK AND HYDROGENATED SRC-II MIDDLE DISTILLATE (ppm)

Metal	Feed	Product
Ca	0.44	0.31
Fe	9.3	0.19
Mn	0.13	0.050
Ni	0.37	1.5
Ti	0.69	0.33
Na	3.7	2.0

decreased after hydrotreatment except nickel, which increased in content. This may be attributed to transfer of the nickel from the Ni/Mo catalyst into the oil. None of the metals tested for were present in the feed in significant amount.

Titanocene Dichloride

Samples from all runs doctored with titanocene dichloride were analyzed by atomic absorption for titanium concentration. All samples from the catalytic runs that employed titanocene dichloride were found to have no titanium in them, indicating complete removal of titanium from the oils by the catalytic hydrotreatment process.

Table XVII presents the titanium analysis for non-catalytic runs E12 through E16. These results are plotted in Figure 45. It should be noted that run E16 was doctored with 200 ppm of Ti as titanocene dichloride rather than the usual 50 ppm, resulting in higher concentrations of Ti in the oil samples. Titanium concentration in the product oil samples stays fairly constant as the reactor temperature is increased from 50 C to 300 C, and then declines rapidly as the reaction temperature is increased from 300 C to 400 C. This phenomenon occurs both when hydrogen and nitrogen gas is flowing through the reactor, indicating that the titanocene dichloride decomposes above 250 C.

TABLE XVII

TITANIUM AND IRON CONCENTRATIONS FOR
RUNS E12-E16 (in micrograms/liter)

SAMPLE	Fe CONC.	Ti CONC.	TEMPERATURE (C)
E12-1	37.7	4	304
E12-2	30.5	4	329
E12-3	15.8	2	348
E12-4	15.8	2	370
E12-5	19.9	3	380
E13-1	10.1	7	301
E13-2	11.7	6	332
E13-3	15.8	8	356
E13-4	18.9	6	374
E13-5	45.9		395
E14-1	52.1	23	62
E14-2	10.7	37	99
E14-3	13.1	39	162
E14-4	14.1	38	200
E14-5	15.6	38	254
E14-6	73.4	35	306
E14-7	48.5	11	363
E14-8	3.6	6	387
E15-1	38.8	21	53
E15-2	48.2	20	98
E15-3	44.6	23	149
E15-4	45.4	22	209
E15-5	42.3	24	263
E15-6	36.7	15	297
E15-7	49.7	10	350
E16-1	32.8	49	58
E16-2	46.4	76	100
E16-3	50.5	67	150
E16-4	47.9	78	195
E16-5	61.2	77	247
E16-6	21.9	51	298
E16-7	19.4	28	346

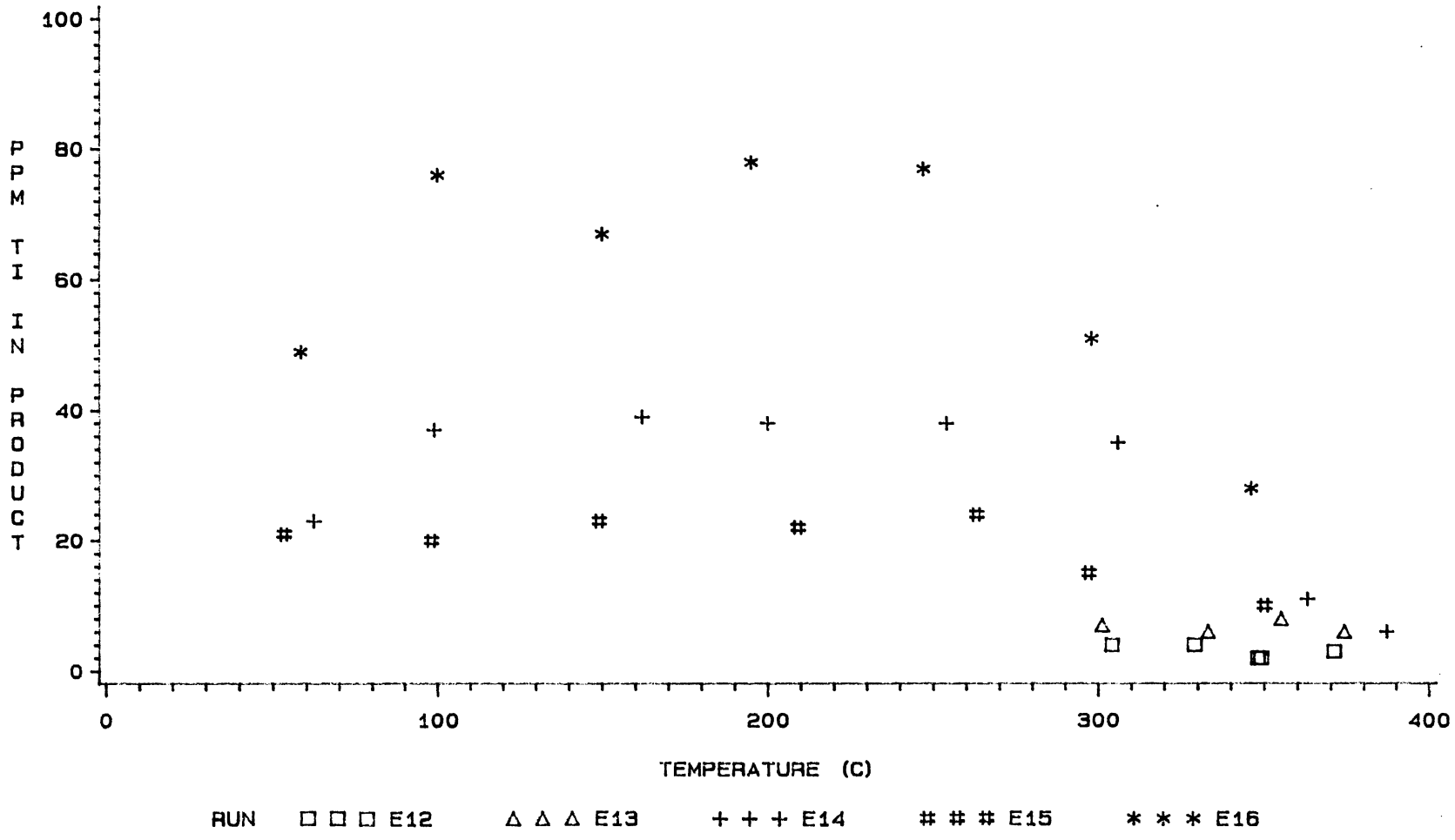

KEY: E12 (50 PPM TI/N2) E13 (50 PPM TI/H2)
E14 (50 PPM TI/N2) E15 (50 PPM TI/H2) E16 (200 PPM TI/H2)

FIGURE 45. EFFECT OF TEMPERATURE ON TITANIUM CONCENTRATIONS FOR RUNS E12-E16

Catalyst Characteriztion

The surface area, pore volume, and coke content of the spent catalyst for each run is tabulated in Tables XVIII and XIX, and plotted in Figures 46 through 54. The amount of surface area and pore volume of the catalyst indicates just how much of the catalyst is blocked by coke. However, the catalyst coke content is a direct measure of coke on the catalyst, which is related to how much the catalyst has been deactivated. During catalyst coke determination, three pellets were randomly selected from each sample, weighed, decoked, weighed again, and an average taken from the three pellets.

The coked catalyst had basically one-third less surface area and pore volume than the fresh catalyst. Runs E2 and E3 were similar except that run E3 was at 25 C lower than E2. As a result, the catalyst surface area and pore volume for run E3 are lower than that for E2 (Figures 46 and 47), while the weight percent coke on the catalyst is correspondingly higher (Figure 52), indicating that a higher reactor temperature (375 C over 350 C) results in lower coking of the catalyst. This was also observed by Tscheikuna (1984).

Conditions for runs E4 and E9 were similar except that in run E4, the feedstock was doctored with 50 ppm of titanocene dichloride. When the spent catalysts were compared, the remaining surface area and pore volume for run E4 was moderately higher than those for run E9 (Figures 50

TABLE XVIII

SURFACE AREA AND PORE VOLUME OF SPENT CATALYSTS
FOR NON-CATALYTIC RUNS

RUN #	ZONE	SURFACE AREA (M**2/GM)	PORE VOLUME (M**3/GM)
FRESH		150	0.47
E2	1	157	0.30
E2	2	174	0.34
E2	3	133	0.29
E2	4	151	0.32
E2	5	158	0.32
E2	5	127	0.28
E3	1	120	0.26
E3	2	133	0.28
E3	2	129	0.28
E3	3	135	0.31
E3	4	126	0.27
E3	5	130	0.30
E4	1	161	0.32
E4	2	153	0.33
E4	3	165	0.40
E4	4	152	0.33
E4	5	165	0.34
E7	1	171	0.33
E7	2	113	0.27
E7	3	134	0.30
E7	4	128	0.29
E7	5	115	0.26
E9	1	148	0.28
E9	2	144	0.29
E9	3	151	0.32
E9	4	146	0.30
E9	5	140	0.31

*Catalyst zone 1=Top, 3=Middle, 5=Bottom

TABLE XIX

CATALYST COKING FOR CATALYTIC RUNS

RUN	ZONE	SAMPLE #1	SAMPLE #2	SAMPLE #3	AVERAGE
E2	1	23.1	24.1	24.5	23.9
E2	2	15.7	15.0	14.9	15.2
E2	3	24.1	21.9	22.9	23.0
E2	4	18.2	17.5	17.0	17.6
E2	5	18.7	20.8	21.2	20.2
E3	1	29.4	30.4	28.9	29.6
E3	2	29.2	26.3	24.2	26.6
E3	3	29.2	30.1	27.5	29.0
E3	4	27.9	20.8	30.8	26.5
E3	5	27.0	24.0	28.5	26.5
E4	1	20.2	20.6	31.5	24.1
E4	1	17.0	20.8	22.2	20.0
E4	2	24.9	24.0	22.1	23.7
E4	3	27.6	27.9	26.6	27.4
E4	4	23.4	22.8	22.0	22.7
E4	5	24.0	25.0	23.5	24.2
E7	1	9.2	25.0	22.6	18.9
E7	2	27.9	28.9	30.0	28.9
E7	3	29.4	28.4	28.2	28.7
E7	4	29.6	28.8	31.0	29.8
E7	5	26.6	28.5	27.3	27.5
E9	1	26.9	15.3	26.6	22.9
E9	2	23.9	27.9	25.2	25.7
E9	2	27.7	29.6	27.2	28.2
E9	3	19.4	16.2	14.5	16.7
E9	4	28.3	24.2	27.0	26.5
E9	5	18.3	18.2	18.7	18.4

*Reactor zone 1=Top, 3=Middle, 5=Bottom

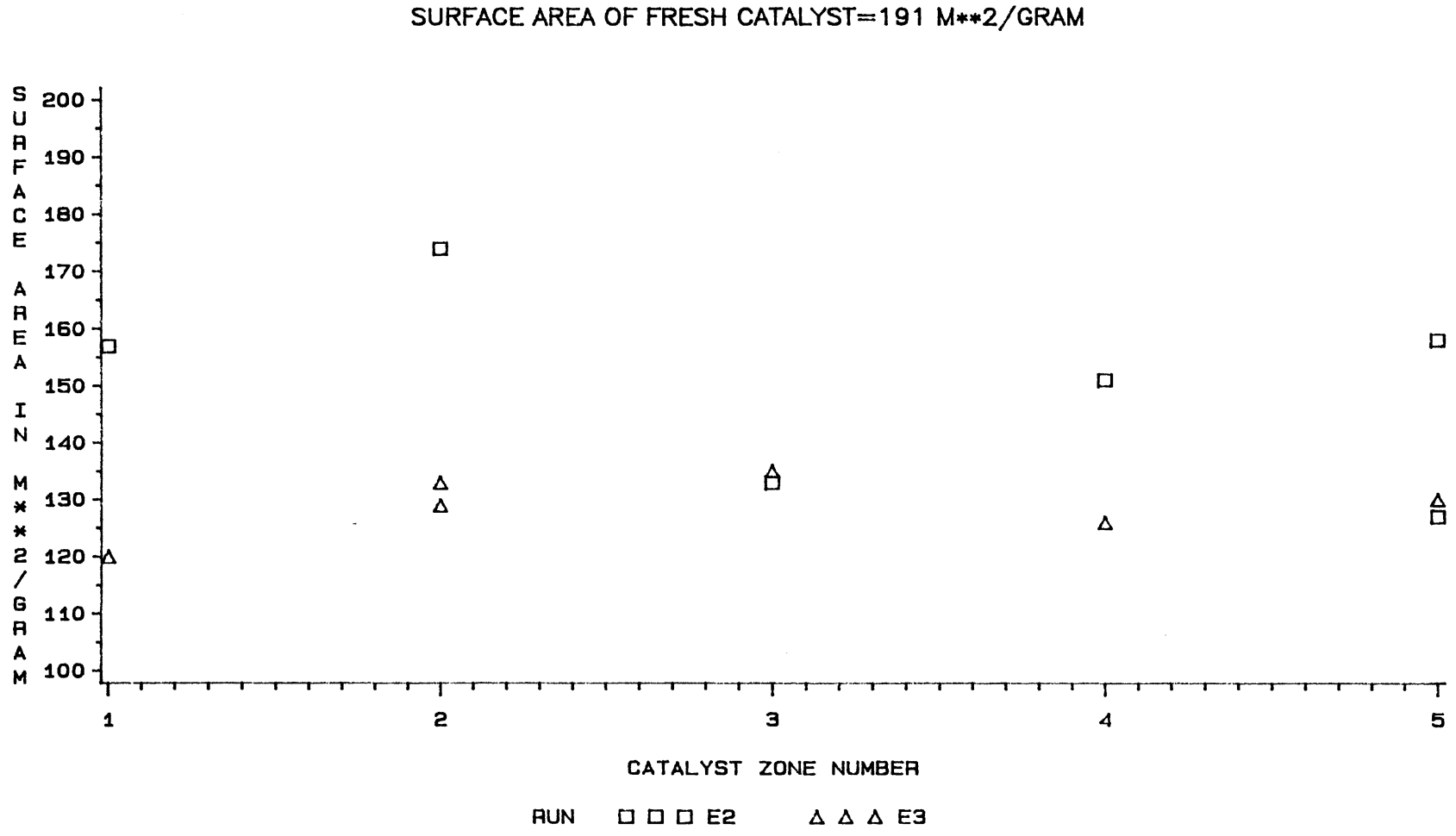

FIGURE 46. EFFECT OF TEMPERATURE ON SURFACE AREA OF SPENT CATALYST FOR RUNS E2 AND E3

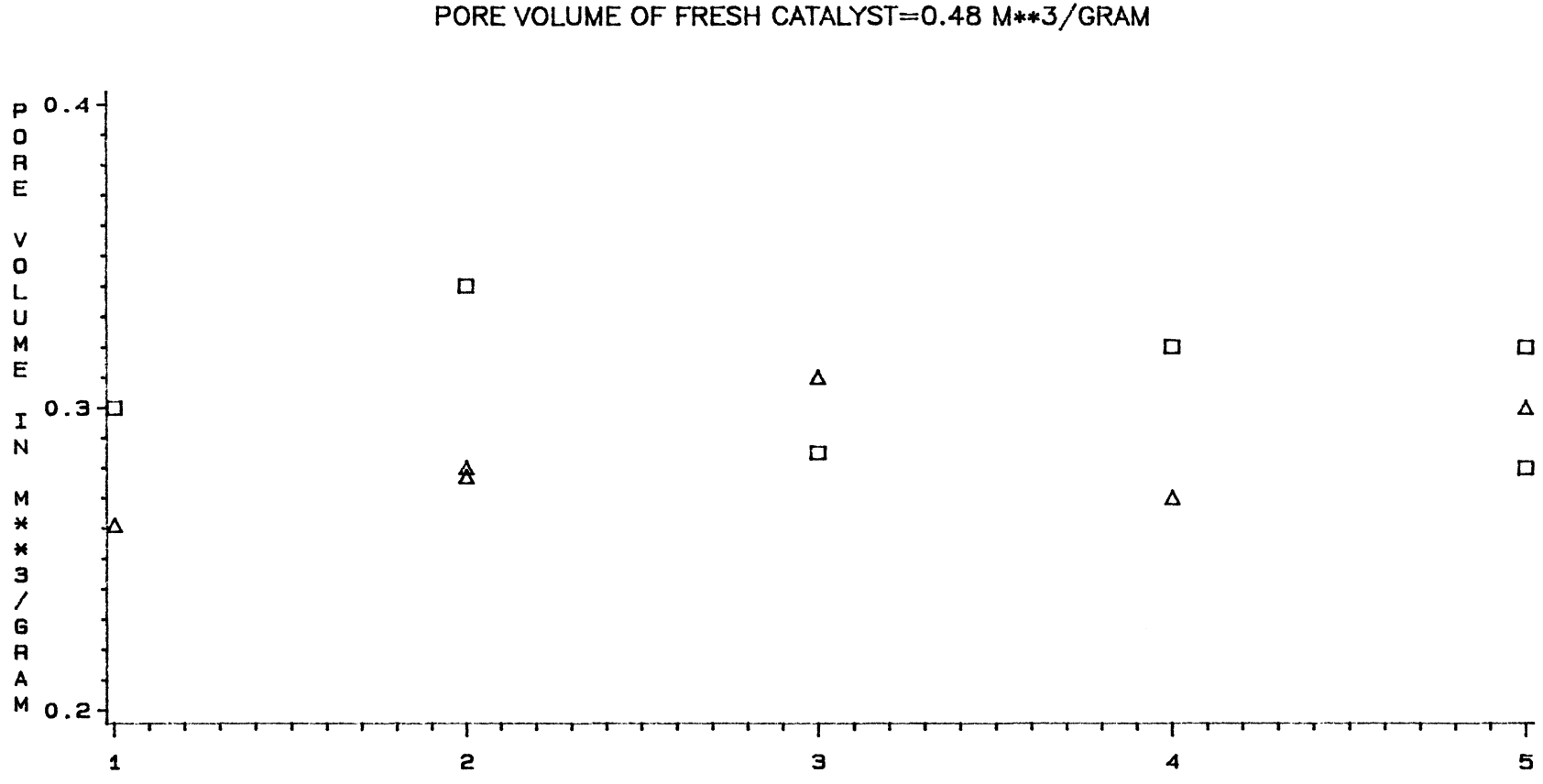

FIGURE 47. EFFECT OF TEMPERATURE ON PORE VOLUME OF SPENT CATALYST FOR RUNS E2 AND E3

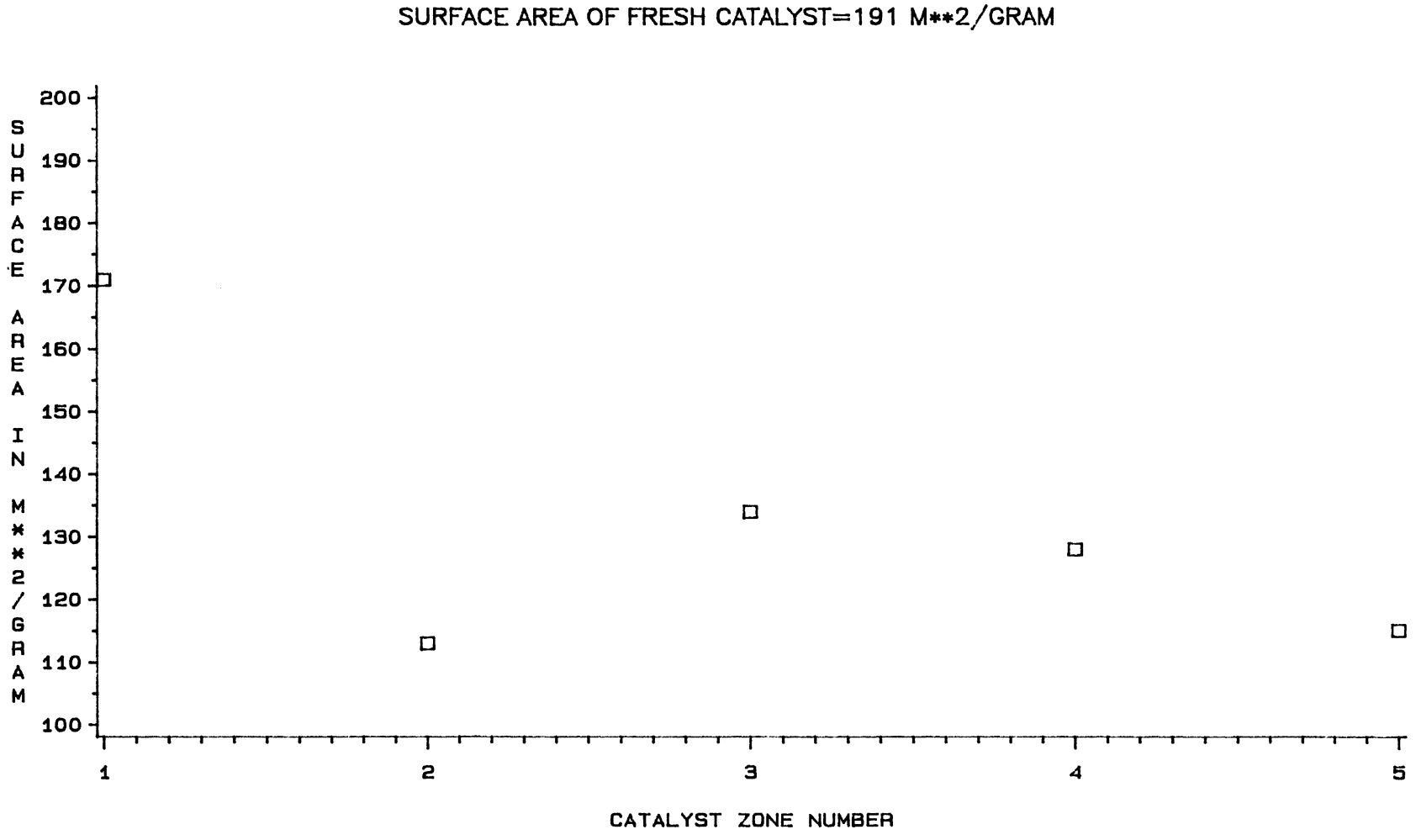

KEY: 1=REACTOR TOP 3=REACTOR MIDDLE 5=REACTOR BOTTOM

FIGURE 48. SURFACE AREA OF SPENT CATALYST FOR RUN E7

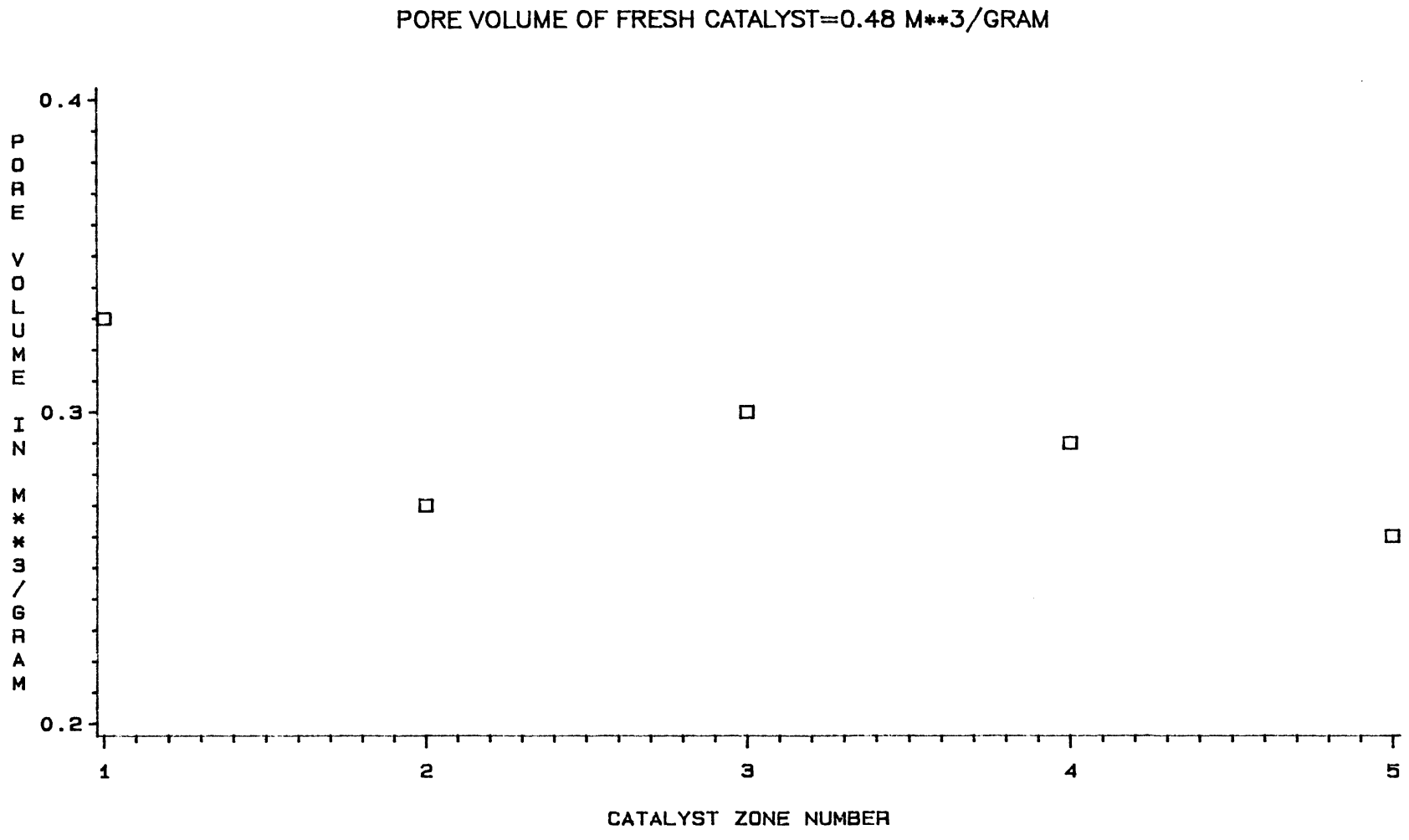

KEY: 1=REACTOR TOP 3=REACTOR MIDDLE 5=REACTOR BOTTOM

FIGURE 49. PORE VOLUME OF SPENT CATALYST FOR RUN E7

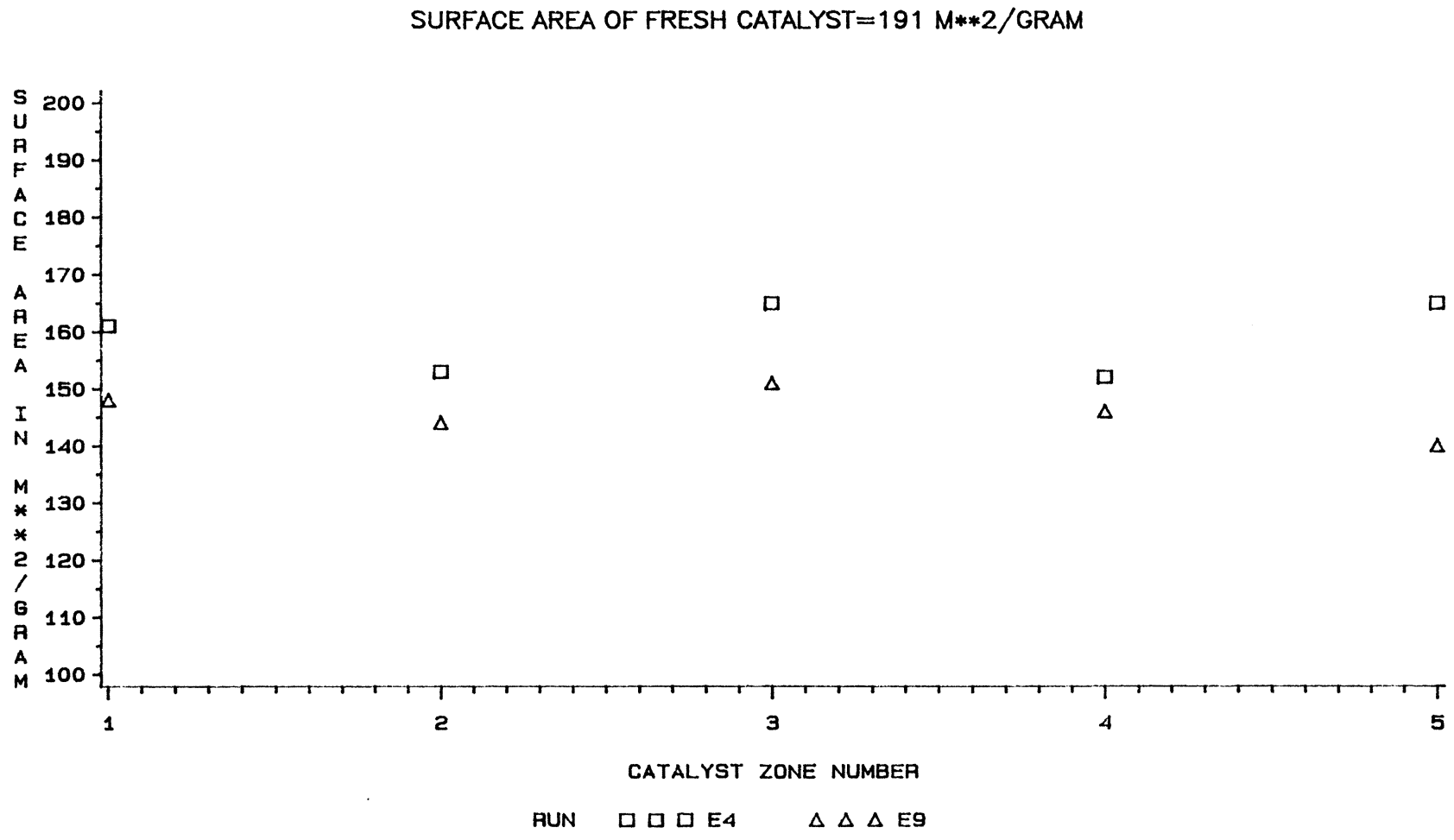

KEY: 1=REACTOR TOP 3=REACTOR MIDDLE 5=REACTOR BOTTOM
E4 (NO TI) E9 (50 PPM TI)

FIGURE 50. EFFECT OF TDC-DOPING ON SURFACE AREA OF SPENT CATALYST FOR RUNS E4 AND E9

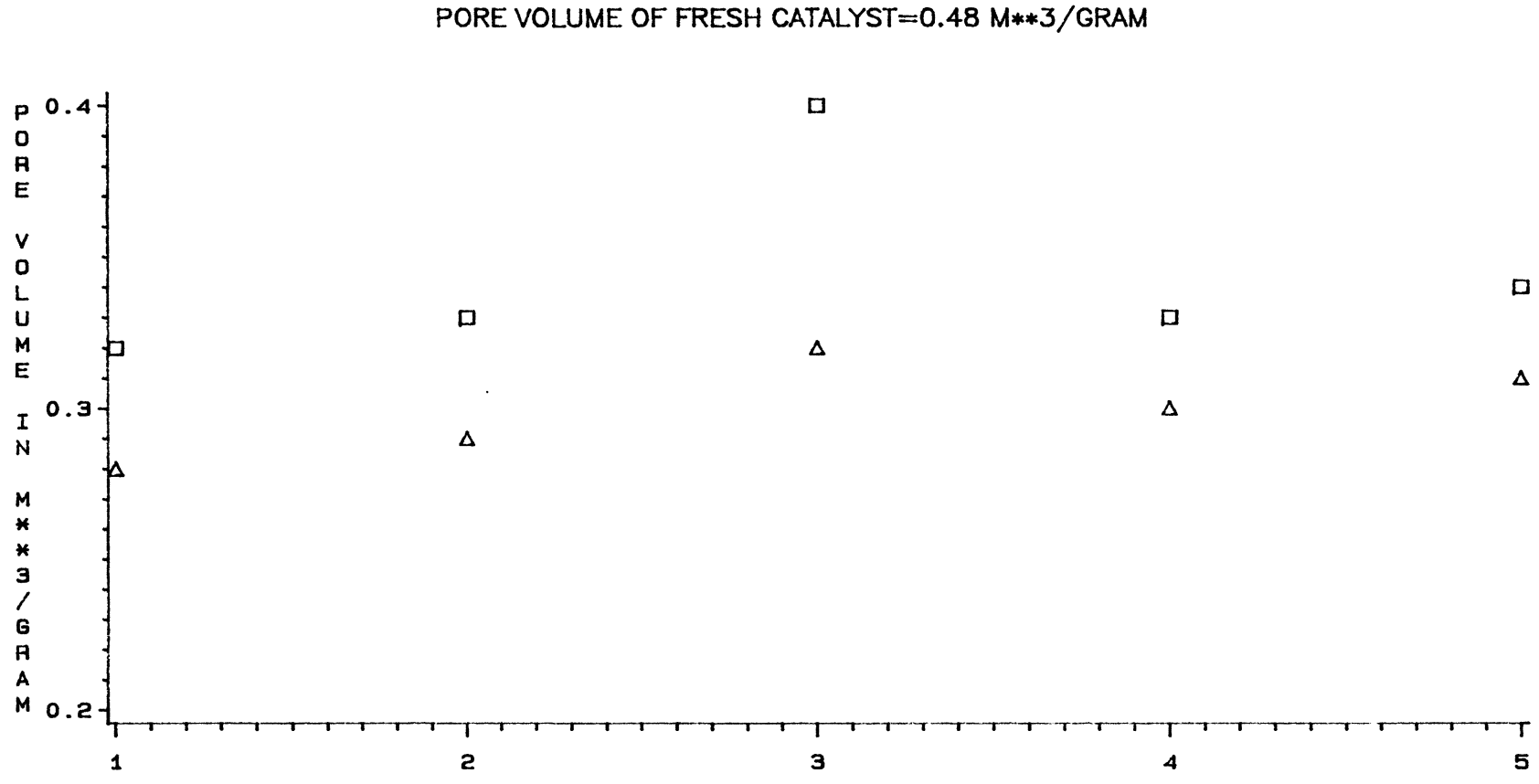

FIGURE 51. EFFECT OF TDC-DOPING ON PORE VOLUME OF SPENT CATALYST FOR RUNS E4 AND E9

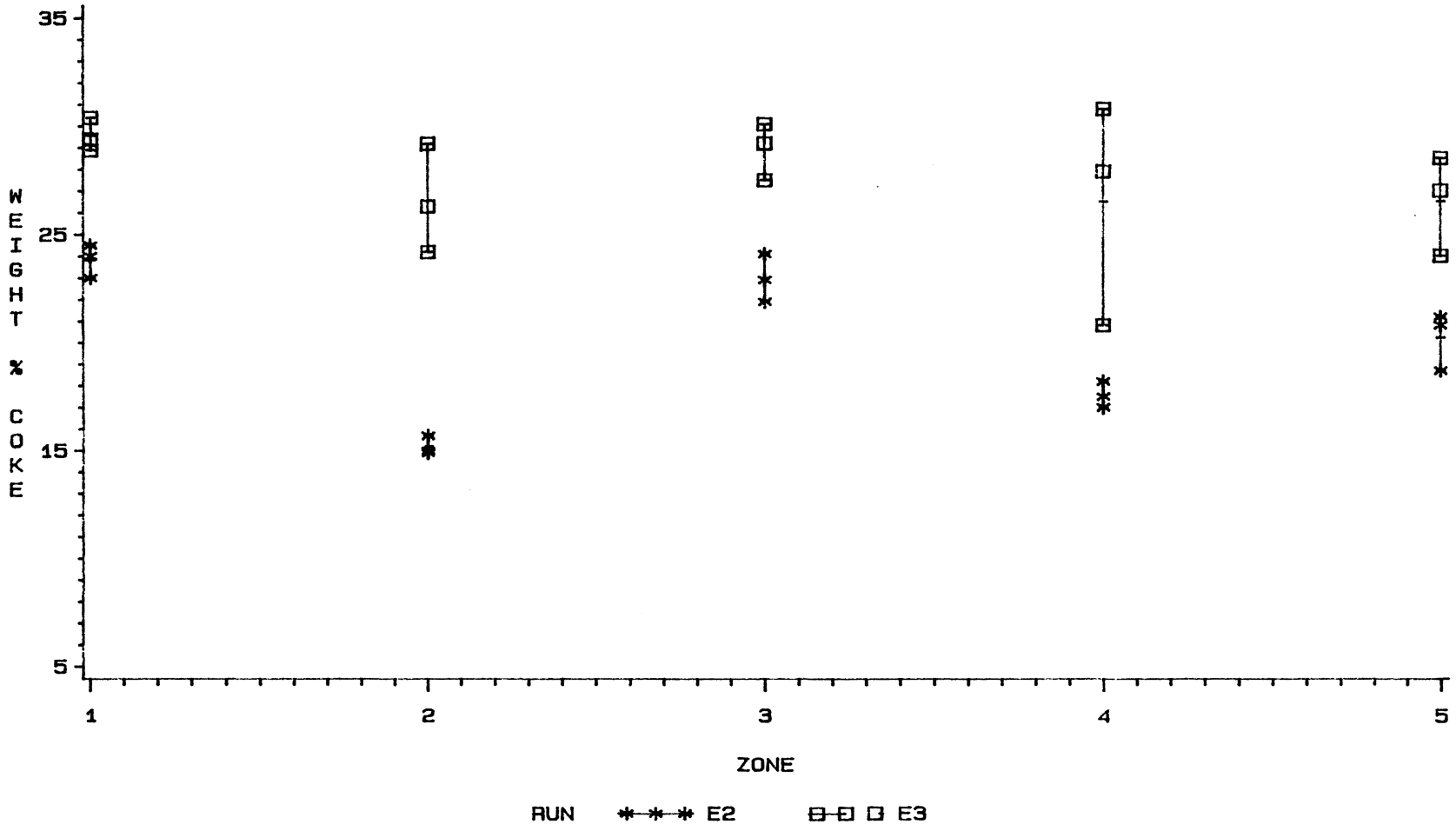

KEY: ZONE 1=REACTOR TOP 3=REACTOR MIDDLE 5=REACTOR BOTTOM
E2 (375 C) E3 (350 C)

FIGURE 52. EFFECT OF TEMPERATURE ON COKING PROFILE FOR RUNS E2 AND E3

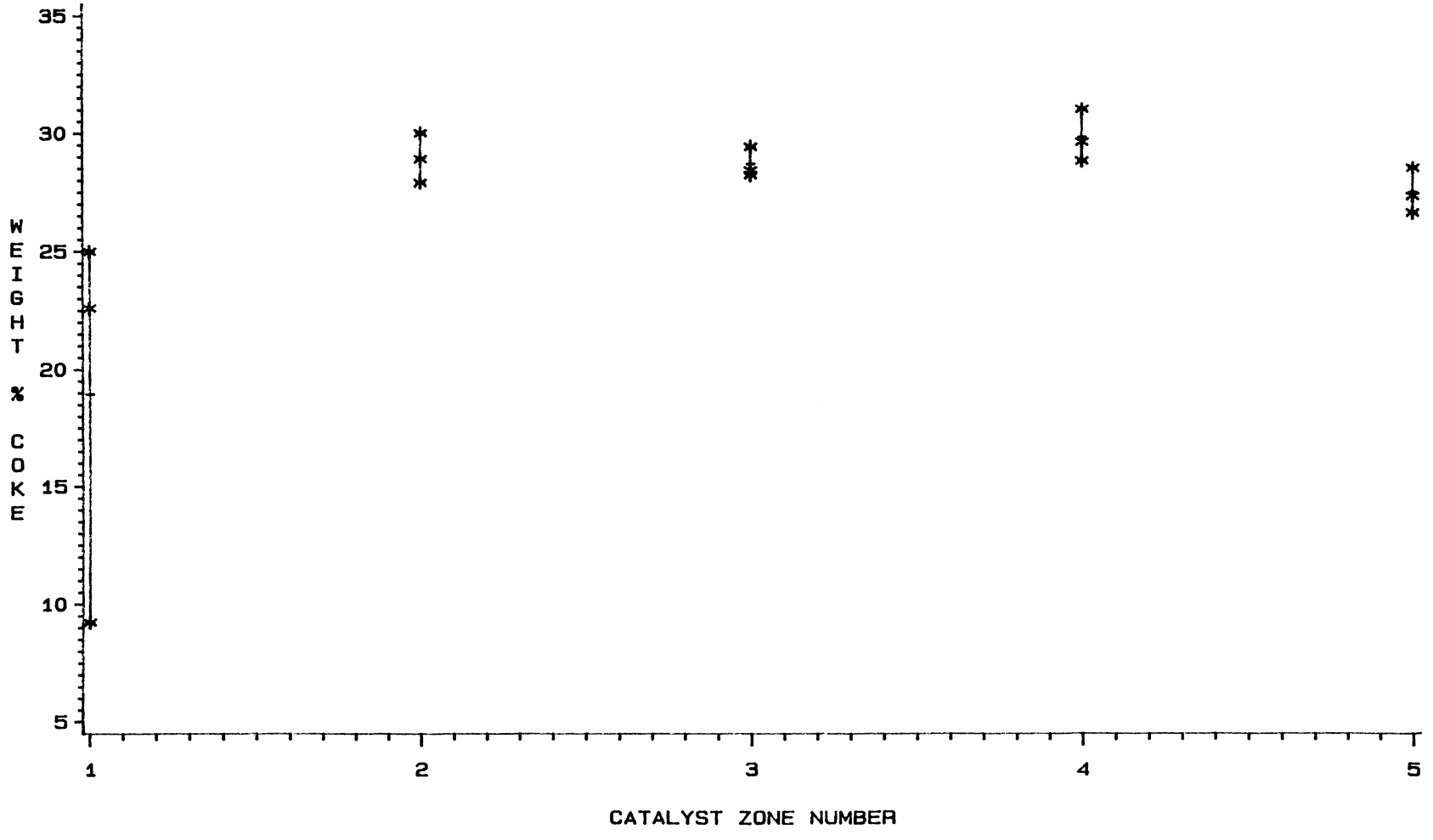

KEY: ZONE 1=REACTOR TOP 3=REACTOR MIDDLE 5=REACTOR BOTTOM

FIGURE 53. COKING PROFILE FOR RUN E7

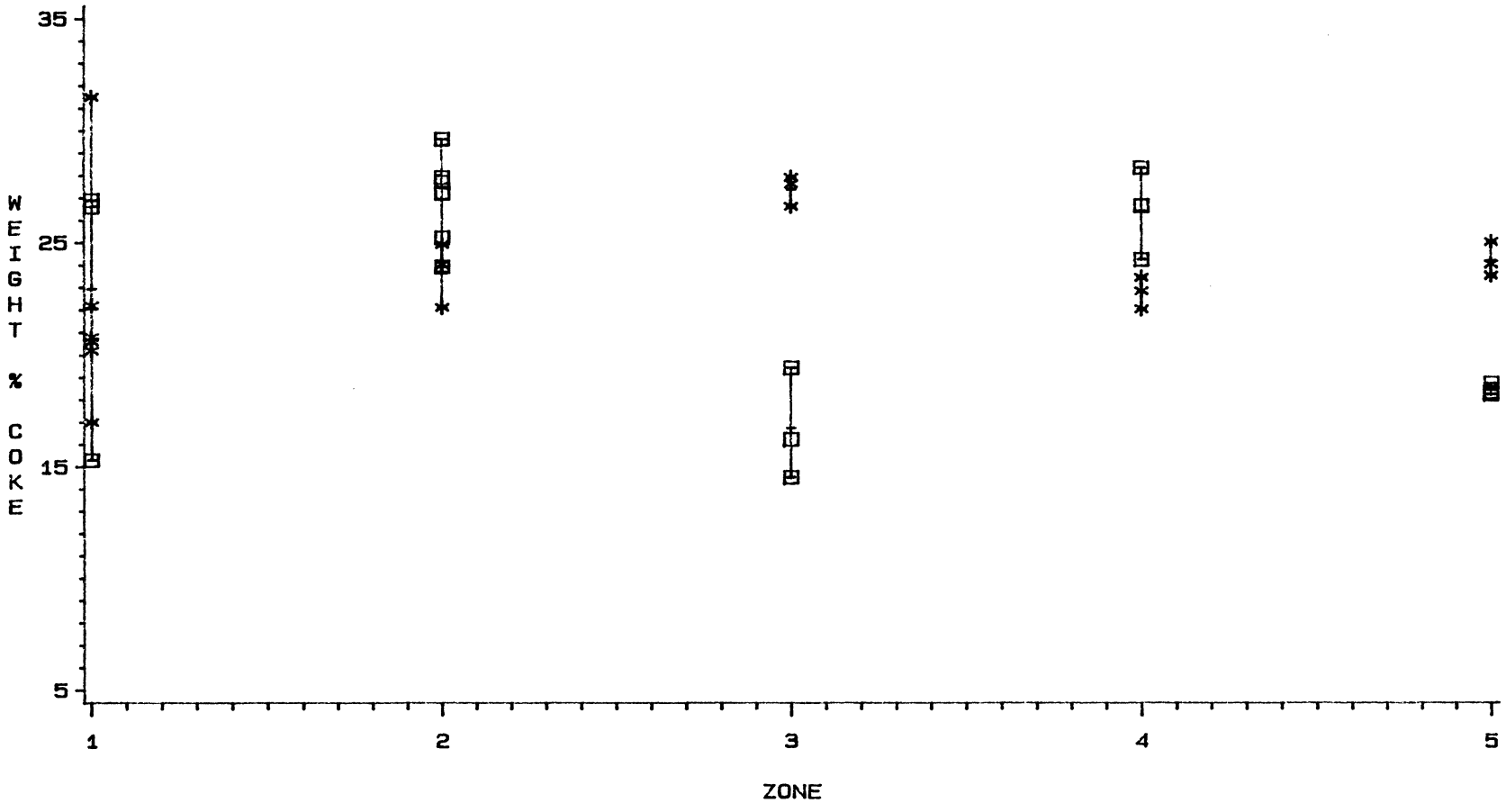

KEY: ZONE 1=REACTOR TOP 3=REACTOR MIDDLE 5=REACTOR BOTTOM
E4 (NO TI) E9 (50 PPM TI)

FIGURE 54. EFFECT OF TDC-DOPING ON COKING PROFILE
FOR RUNS E4 AND E9

and 51); however, there was virtually no difference in the coking profile for the two runs (Figure 54), indicating that there was no effect of titanocene dichloride upon catalyst coking.

S.E.M./EDAX of Run E9

Spent catalyst from run E9 was analyzed by S.E.M. and EDAX to determine if titanium was penetrating the catalyst pores. Figure 55 is a micrograph of the center of a pellet. The pore structure is evident in the photograph, and there appear to be small particles deposited on the catalyst. Figure 56 is an EDAX spectra at the center of the same pellet; the concentration of titanium is quite high in the center, and remains consistently high all the way out to the edge of the catalyst surface. However, when the same pellet was analyzed on the outer surface, no titanium was seen (see Figure 57). At no time was there seen any trace of chlorine. Thus, it appears that titanium deposits mainly in the catalyst pores, and not on the external surface of the catalyst.

Non-Catalytic Coking Results

Although the reactors for runs E10-E18 contained no catalyst, they did contain cut 1/8-inch and 1/4-inch O.D. stainless steel tubing. After each run, the reactor was cut into three sections (top, middle, and bottom), and two pellets from each section were analyzed for weight percent

Figure 55. S.E.M. of Catalyst Center

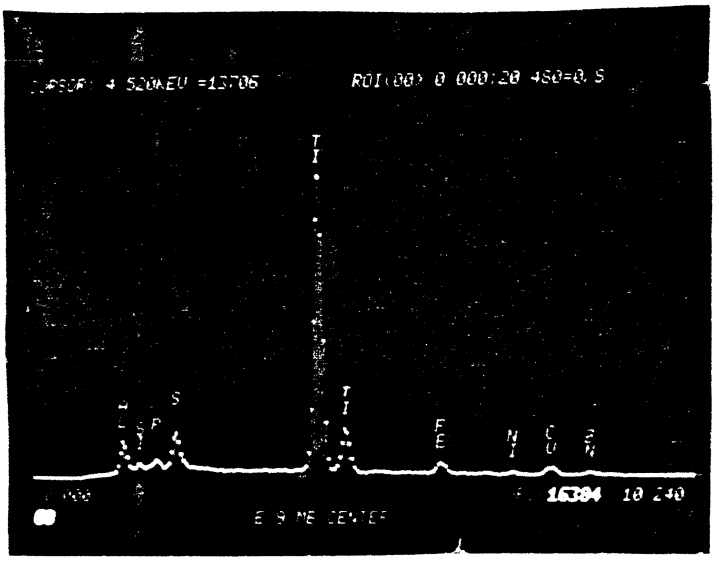

Figure 56. EDAX of Catalyst Center

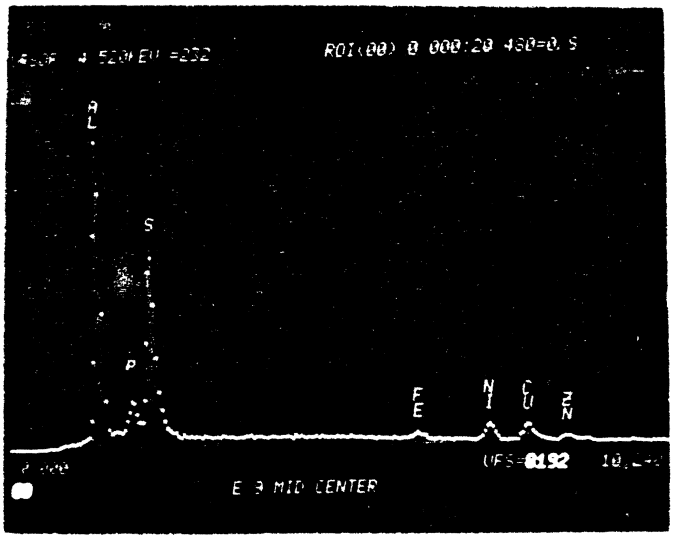

Figure 57. EDAX of Catalyst Surface

coke on the pellets. The results are listed in Table XX, and plotted in Figure 58.

In all cases, the presence of molecular hydrogen seems to significantly reduce the amount of coke on the pellets. In runs E10-E13, the presence of titanocene appears to increase the amount of coke on the pellets, while in runs E14-E18, the presence of titanocene dichloride seems to significantly reduce the amount of pellet coking. Thus, results are not conclusive as to whether or not titanocene dichloride has any effect on non-catalytic coking; this is not suprising, since there was no apparent effect of titanocene dichloride upon catalytic coking.

Error Analysis

Data from elemental analysis, e.s.r. analysis, atomic absorption analysis for iron, and coking analysis were subjected to error analysis. Table XXI presents the results of the error analysis. The table gives the average value, standard deviation, and number of times analyzed for each different analysis method.

The values obtained from elemental analysis for nitrogen (standard deviation 5% of average value), for H/C ratio (standard deviation 4% of average value) and for sulfur (standard deviation 7% of average value) all indicate that these analysis methods are fairly precise. However, the elemental analysis for oxygen (standard deviation 17% of average value) is much poorer, probably because the oxygen

TABLE XX

COKING RESULTS FOR NON-CATALYTIC RUNS

SAMPLE	GRAMS COKE/GRAM METAL
E10-TOP	0.0016
E10-MID	0.0017
E10-BOTTOM	0.0022
E11-TOP	0.0005
E11-MID	0.0000
E11-BOTTOM	0.0011
E12-TOP	0.0027
E12-MID	0.0018
E12-BOTTOM	0.0044
E13-TOP	0.00098
E13-MID	0.00013
E13-BOTTOM	0.0018
E14-TOP	0.0017
E14-MID	0.00065
E14-BOTTOM	0.00060
E15-TOP	0.00050
E15-MID	0.00042
E15-BOTTOM	0.00048
E17-TOP	0.0014
E17-MID	0.00074
E17-BOTTOM	0.0010
E18-TOP	0.0026
E18-MID	0.0021
E18-BOTTOM	0.00091

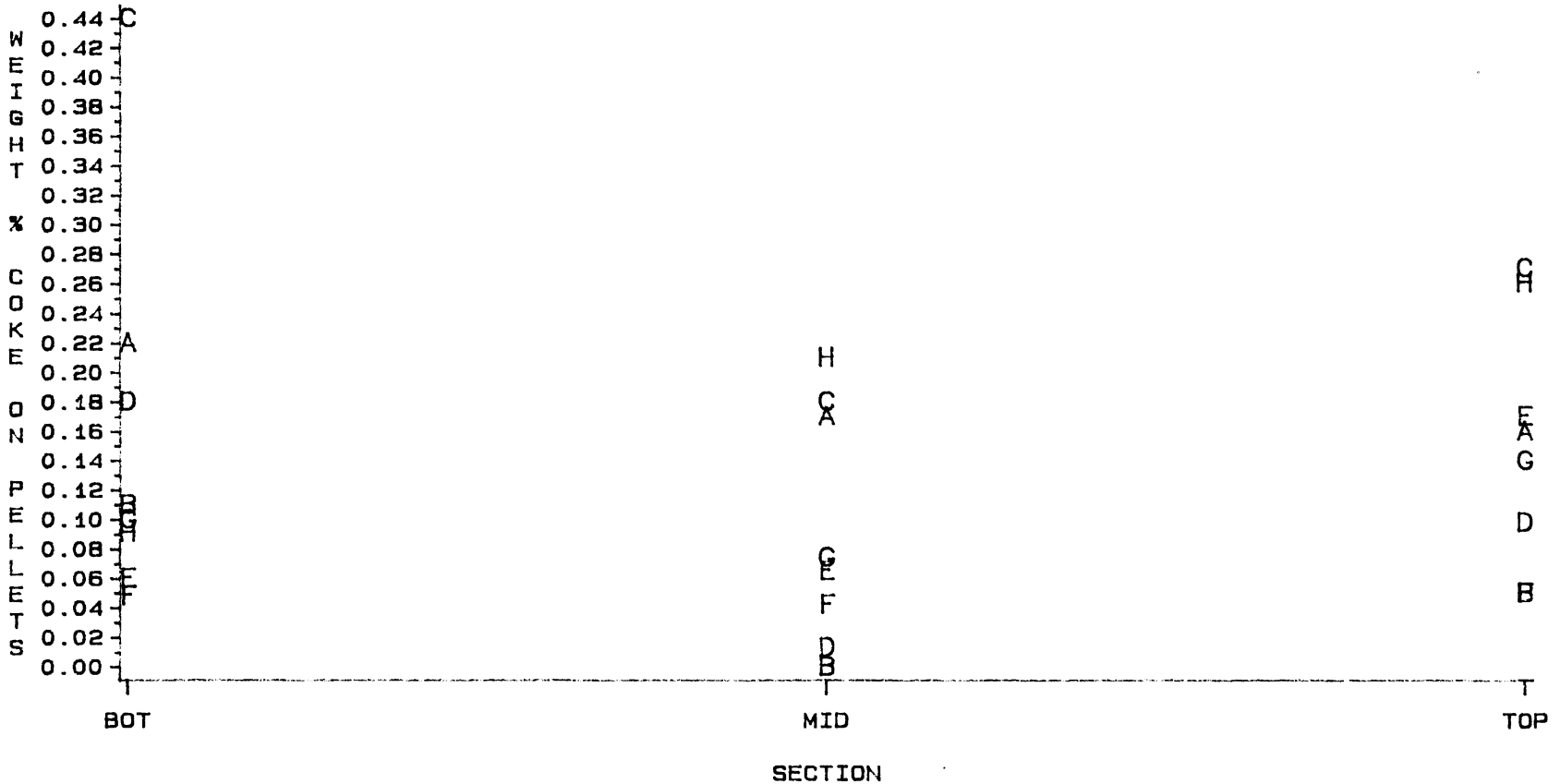

RUN A A A E10 B B B E11 C C C E12 D D D E13
E E E E14 F F F E15 G G G E17 H H H E18

KEY: E10 (NO TI/N2) E11 (NO TI/H2) E12 (50 PPM TI/N2)
E13 (50 PPM TI/H2) E14 (50 PPM TI/N2) E15 (50 PPM TI/H2)
E17 (NO TI/H2) E18 (NO TI/N2)

FIGURE 58. COKING PROFILES FOR NON-CATALYTIC RUNS E10-E18

TABLE XXI

ERROR ANALYSIS OF DATA

TYPE ANALYSIS	SAMPLE ANALYZED	TIMES ANALYZED	AVERAGE VALUE	STANDARD DEVIATION
NITROGEN WT. %	E7-FEED	5	0.73	0.04
H/C RATIO	E7-FEED	5	1.27	0.05
SULFUR WT. %	E7-FEED	5	0.15	0.01
OXYGEN WT. %	E7-FEED	5	6.9	1.2
GAMMAO*	E17-8	3	7.1	0.2
GAMMAM*	E17-8	3	0.7	0.0
GAMMAO**	E18-7	4	0.84	0.38
GAMMAM**	E18-7	4	0.15	0.07
IRON CONCEN.	FEED@	4	33.7 PPM	11.3 PPM
WT.% COKE	E4 (ZONE 1)	6	22.0	4.5
WT.% COKE	E9 (ZONE 2)	6	26.9	2.0

*MACHINE PRECISION
**SAMPLING PRECISION
@FEEDS USED WERE FROM RUNS E7, E10, E12, AND E15.

content is an indirectly calculated value rather than a directly analyzed value.

Sample E17-8 was analyzed three times at the same setting by e.s.r.. The values obtained for GAMMA0 (standard deviation 3% of average value) and GAMMAM (standard deviation equals 0.0) indicate that the machine precision is very good. Samples E18-7-1, E18-7-2, E18-7-3, and E18-7-4 were all obtained under the exact same conditions; the values obtained for GAMMA0 (standard deviation 45% of average value) and GAMMAM (standard deviation 18% of average value) indicate that sampling precision is very poor, probably due to the crude method of obtaining the E.S.R. samples.

Feeds from runs E7, E10, E12, and E15 were all analyzed by atomic absorption for iron content. The value obtained for feed iron concentration (standard deviation 34% of average value) indicates that the sampling precision is very poor, probably due to particulate matter containing large amounts of iron being drawn from the samples.

Spent catalyst pellets were analyzed for coke for runs E4 (zone 1) and E9 (zone 2). The values obtained for run E4 (standard deviation 20% of average value) and E9 (standard deviation 7% of average value) indicate that the catalyst coke content within each catalyst zone is somewhat scattered.

CHAPTER V

CONCLUSIONS AND RECOMMENDATIONS

The following conclusions can be drawn from this study:

1) Titanocene dichloride had no effect on catalyst performance when the catalyst has been severely sulfided; however, when a weaker sulfidation procedure was used on the catalyst, titanocene dichloride significantly increased the hydrogenation, hydrodenitrogenation, and hydrodeoxygenation of the SRC-II Middle Distillate feed. Complete hydrodesulfurization was achieved with and without the addition of titanocene dichloride to the feedstock. Catalyst coking was in no case affected by the presence of titanocene dichloride in the feedstock.

2) Titanocene dichloride had no effect on the non-catalytic hydrogenation, hydrodenitrogenation, hydrodesulfurization, or hydrodeoxygenation of the SRC-II Middle Distillate feedstock.

3) In both catalytic and non-catalytic runs, the presence of titanocene dichloride in the feedstock was responsible for a significant lightening of the product in terms of boiling point behavior as determined by g.c. simulated distillation.

4) During non-catalytic hydrotreatment, a dramatic

increase in free radical concentration in the liquid product from the reactor was noted as the reactor temperature was increased from 250 to 350 C, followed by a decrease in free radical concentration as the reactor temperature was increased from 350 C to 400 C; this behavior occurred regardless of whether nitrogen or hydrogen gas was flowing through the reactor. The presence of titanocene dichloride in the feedstock and molecular hydrogen significantly increased the free radical concentration of the feed from 250 to 350 C.

5) During the non-catalytic runs, the concentration of titanium in the liquid product remained at a steady level up to about 300 C; above this temperature, the concentration of titanium dramatically decreased, which is attributed to the decomposition of titanocene dichloride at the high reaction temperatures. During catalytic runs in which titanocene dichloride doping was used, no titanium survived the hydrotreatment process.

The following recommendations are made based on the results of this study:

1) A study utilizing coal liquids of different ranks should be carried out to determine the effects of titanocene dichloride upon catalytic hydrotreatment reactions in more detail. E.S.R. spectroscopy should be used in this study to determine whether or not there are any effects of titanocene dichloride on the free radical concentrations of the reactants during hydrotreatment.

2) A study utilizing e.s.r. spectroscopy should be carried out to determine the effects of reaction temperature upon reactant free radical concentrations during both catalytic and non-catalytic hydrotreatment.

3) A study utilizing e.s.r. spectroscopy should be carried out to determine the effects of catalyst aging upon reactant free radical concentrations during catalytic hydrotreatment.

4) A study of the effect of catalyst pre-sulfiding on catalytic hydrotreatment should be carried out. The coked catalyst should be examined for its sulfidation level by elemental sulfur analysis and for coke type by elemental hydrogen/carbon/nitrogen analysis.

BIBLIOGRAPHY

Adkins, B.D., and Davis, B.H., "Coking and Porosity in a Two-Stage Coal Liquefaction Catalyst", PREPRINTS, ACS, Div. Petroleum Chemistry, 30(3), 479-487 (1985).

Atkins, P.W., Physical Chemistry, W.H. Freeman and Co., 613-622 (1978).

Asaoka, S., Nakata, S., Shiroto, Y., and Takeuchi, C., "The Characteristics of Metal Complexes Before and After Hydrotreating", PREPRINTS, ACS, Div. Petroleum Chemistry, 31(2), 597-605 (1986).

Bartholemew, C.H., "Catalyst Deactivation", Chemical Engineering, 11/12/84, 96-112 (1984).

Bearden, Jr., et. al., U.S. Patent 4,134,825, Jan. 16, 1979.

Beazer, J.R., "The Effect of Catalyst Temperature Zoning on Upgrading a Coal-Derived Liquid", M.Sc. Thesis, Oklahoma State University (1984).

Benesi, H.A., and Winquist, B.H.C., "Surface Acidity of Solid Catalysts", Advances in Catalysis, 27, 97-182 (1978).

Bhan, O.K., "An Investigation of the Activity of Composite Catalyst Beds for Hydrotreatment of a Coal-Derived Liquid", Ph.D. Thesis, Oklahoma State University (1983).

Boduszynski, M.M., "Characterization of 'Heavy' Crude Components", PREPRINTS, ACS, Div. Petroleum Chemistry, 30(4), 626-635 (1985).

Bonds, Jr., W.D., Brubaker, Jr., C.H., Chandrasekaran, E.S., Gibbons, C., Grubbs, R.H., and Kroll, L.C., "Polystyrene Attached Titanocene Species, Preparation and Reactions", Journal American Chemical Society, 97(8), 2128-2132 (1975).

Bunger, J.W., "Inhibition of Coke Formation in Hydropyrolysis of Residual Oils", PREPRINTS, ACS, Div. Petroleum Chem. 30(3), 549-554 (1985).

Chan, W.S., "Effects of Titanocene Dichloride on the Hydrotreatment of Coal Liquids", M.Sc. Thesis, Oklahoma State University (1982).

Chan, W.S., Seapan, M.S., Crynes, B.L., and Al-Shaieb, Z., "Effect of Titanocene Dichloride on the Hydrotreatment of Coal-Liquids", PREPRINTS, ACS, Div. Petroleum Chem., 27(4), 816-825 (1982).

Chillingworth, R.S., Hastings, K.E., and Potts, J.D., "Alternative Modes of Processing SRC in an Expanded Bed LC-Finer to Produce Low Nitrogen Distillates", Ind. Eng. Chem. Prod. Res. Dev., 19, 34-38 (1980).

Cole, D.A., Herman, R.G., Simmons, G.W., and Klier, K., "Generation of Free Radicals in Partial Oxidation of Coal", Fuel, 64(3), 303-306 (1985).

Curtis, C.W., Guin, J.A., and Tarrer, A.R., DOE, Final Report, DE-FG22-82PC50793, May 1985.

Dack, S.W., Hobday, M.D., Smith, T.D., and Pilbrow, J.R., "EPR Study of Organic Free Radicals in Victorian Brown Coal", Fuel, 64(2), 219-225 (1985).

de Vlieger, J.J., Kieboom, A.P.G., and Van Bekkum, H., "Behaviour of Tetralin in Coal Liquefaction", Fuel, 63(3), 334-340 (1984).

Doraiswamy, L.K., and Tajbl, D.G., "Laboratory Catalytic Reactors", Catal. Rev., 10, 177-219 (1975).

Eppel', S.A., Matveev, B.I., Lane, K.K., and Kharlampovich, G.D., "Commercial Experience in Chemical Processing of Coal", translated from Khimiha i Tekhologiya Topliva i Masel, 3, 8-10 (1984).

Feldman, U.S. Patent 4,404,002, Sept. 13, 1983.

Filby, R.H., et al., DOE Topical Report, DOE/FE/496-T17 (1976).

Garg, D., and Givens, E.N., "Relative Activity of Transition Metal Catalysts in Coal Liquefaction", Fuel Processing Technology, 8, 123-134 (1984).

Garg, D., and Givens, E.N., "Catalyst Performance in Hydroprocessing Solvent-Refined Coal", Fuel Processing Technology, 9, 29-42 (1984).

Girgis, M.J., And Gates, B.C., "High-Pressure Catalytic Hydroprocessing of a Simulated Coal Liquid", PREPRINTS, ACS, Div. Petroleum Chem. 30(4), 697-703 (1985).

Gorewit, B., and Tsutsui, M., "Sigma-Pi Rearrangements and Their Role in Catalysis", Advances in Catalysis, 27, 227-263 (1978).

Graham, S.W., and Brinen, J.S., DOE, Topical Report, DOE/PC/40091-T11.

Graham, W.R.M., "The Study of Metal Species in Petroleum and Tar Sands Using the EPR and FTIR Techniques", PREPRINTS, ACS, Div. Petroleum Chemistry, 31(2), 608-612 (1986).

Hallie, H., "Experience Reveals Best Presulfiding Techniques for HDS and HDN Catalysts", Oil and Gas Journal, 12/20/82, 69-74 (1982).

Hamshar, J.A., and Potts, J.D., DOE, Quarterly Report, DOE/PC/60047-T4, July 1984.

Haynes, Jr., H.W., DOE, Quarterly Report No. 1, DOE/PC/70812-1, Decemeber 1984.

Hertan, P.A., Larkins, F.P., and Jackson, W.R., "Regeneration Studies on Nickel Molybdate Catalysts Used for the Upgrading of Coal-Derived Liquids", Fuel Processing Technology, 10, 121-130 (1985).

Hillebrand, W., Hodek, W., and Kolling, G., "Steam Cracking of Coal-Derived Oils and Model Compounds: (1) Cracking of Tetralin and t-Decalin", Fuel, 63(6), 756-761 (1984).

Iskander, F.Y., and Filby, R.H., "Formation of Anatase from Titanium(IV) Preasphaltenes Complexes under Coal Liquefaction Conditions", Fuel, 63(2), 280-282 (1984).

Jones, F.A., Rindt, J.R., and Radonovich, L.J., "Catalytic Upgrading of Solvent-Refined Lignite Using Hydrogen Sulfide and Iron Oxide-Supported Catalysts", PREPRINTS, ACS, Div. Petroleum Chemistry, 30(3), 521-529 (1985).

Jones, J.F., and Friedman, L.D., "Char Oil Energy Development Final Report", Office of Coal Research Report No. 56, 25 (1970).

Kissin, Y.V., "Free Radical Cracking of High Molecular Weight Branched Alkanes", PREPRINTS, ACS, Div. Petroleum Chemistry, 30(4), 652-657 (1985).

Kim, S.S., Jarand, M.L., and Durai-Swamy, K., "Quench Solvent Evaluation: An E.S.R. Study", Fuel, 63(4), 510-512 (1984).

Krichko, A.A., Yulin, M.K., Maloletnev, A.S., and Petrov, Y.I., "Production of Engine Fuels from Coals of the Kansk-Achinsk Basin", translated from Khimiya i Tekhologiya Topliv i Masel, 3, 5-8 (1984).

Kukes, S.G., Aldag, A.W., and Parrott, S.L., "Hydrodemetallization with Phosphorous Compounds Over Aluminas in a Trickle Bed Reactor", PREPRINTS, ACS, Div. Petroleum Chem. 31(2), 615-622 (1986).

Labinger, J., "Titanium, Zirconium and Hafnium Annual Survey Covering the Year 1978", Journal of Organometallic Chemistry, 180, 187-203 (1979).

Lynch, A.W., "Titanium Deposition on Coal Liquefaction Catalysts", PREPRINTS, ACS, Div. Petroleum Chemistry, 30(3), 446-453 (1985).

Maloletnev, A.S., Krichko, A.A., Yulin, M.K., and Gyul'maliev, A.M., "Hydrogenation of Heteroatomic Compounds of Coal Distillates on Wide-Pore Catalysts", translated from Khimiya i Tekhnologiya Topliv i Masel, 11, 12-14 (1984).

Mochida, I., Sakanishi, K., Oishi, T., Korai, Y., and Fujitsu, H., "Catalytic Hydrotreatment of Heavy Liquids Prepared from Coals of Different Rank", Fuel Processing Technology, 10, 91-101 (1985).

Monnier, J., and Kriz, J.F., "Catalytic Hydroprocessing of Mixtures of Heavy Oil and Coal", PREPRINTS, ACS, Div. Petroleum Chemistry, 30(3), 513-520 (1985).

Mralidhar, G., Massoth, F.E., and Shabtai, J., "Catalytic Functionalities of Supported Sulfides: I. Effect of Support and Addivitives on the CoMo Catalysts", Journal of Catalysis, 85, 44-52 (1984).

Mralidhar, G., Massoth, F.E., and Shabtai, J., "Catalytic Functionalities of Supported Sulfides: II. Effect of Support on Mo Dispersion", Journal of Catalysis, 85, 53-62 (1984).

Muchnick, T.L., Kutzenco, P.D., and Preston, W.J., "Effect of Catalyst Pore Structure on Upgrading of Coal-Derived Resid", PREPRINTS, ACS, Div. Petroleum Chemistry, 30(3), 488-494 (1985).

Neuworth, M.B., and Moroni, E.C., "Development of a Two-Stage Liquefaction Process", Advances in Coal Utilaztion Technology, Inst. of Gas Technology, 345-358 (1979).

Newton, R.T., Jr., "The Effect of Composite Beds Containing Catalysts with Different Active Metals on the Upgrading of a Coal Liquid", M.Sc. Thesis, Oklahoma State University (1985).

Ouchi, K., Makabe, M., Yoshimoto, I., and Itoh, H., "Coking Reaction in Hydrogenation", Fuel, 63(4), 449-451 (1984).

Parera, J.M., Beltramini, J.N., Querini, C.A., and Figoli, N.S., "Hydrogenation of Methylcyclopentadiene on Pt, Re, and Pt-Re/Al2O3 Involvements on Coke Formation During Reforming", PREPRINTS, ACS, Div. Petroleum Chem., 30(3), 532-536 (1985).

Pez, G.P. and Armor, J.N., "Chemistry of Titanocene and Zirconocene", Advances in Organometallic Chemistry, 19, 1-50 (1981).

Potts, J.D., Hastings, K.E., and Unger, H., "Expanded Bed Hydroprocessing of Solvent Refined Coal (SRC-I) Extract", presented at 5th International Conf. Coal Gasification, Liquefaction, and Conversion to Electricity, Pittsburgh, PA (1978).

Potts, J.D., Hastings, K.E. Chillingworth, R.S., and Unger, H., "LC-Fining of Solvent Refined Coal SRC-I and Short Contact Time Coal Extracts", ACS, Symp. Series No. 156, 153-173 (1981).

Pratt, K.C., and Christoverson, V., "Hydrogenolysis of Furan over Nickel-Molybdenum Catalysts", Fuel Processing Technology, 8, 43-51 (1983).

Rankel, L.A., "Degradation of Metalporphyrins in Heavy Oils Before and During Processing: Effects of Heat, Air, Hydrogen, and Hydrogen Sulfide on Petroporphyrin Species", PREPRINTS, ACS, Div. Petroleum Chem. 31(2), 625-632 (1986).

Retcofsky, H.L., Thompson, G.P., Hough, M., and Fridel, R.A., "Electron Spin Resonance Studies of Coals and Coal Derived Asphaltenes", Organic Chemistry of Coal, ed. J.W. Larson, ACS, Symposium Series, 71, 142-155 (1978).

Robison, W.E., and Filby, R.H., PREPRINTS, ACS, Div. Petroleum Chemistry, 30(3), 454-458 (1985).

Rudnick, L.R., and Sinclair, J.L., "Variable Temperature ESR of Commercial Coker Feeds", PREPRINTS, ACS 30(4), 720 (1985).

Rudnick, L.R., and Sinclair, J.L., "Variable Temperature ESR of Commercial Coker Feeds", poster presentation at ACS, 190th meeting (1985).

Rudnick, L.R., and Sinclair, J.L., "ESR Characterization of Commercial Coker Feeds", PREPRINTS, ACS, Div. Petroleum Chemistry, 30(2), 237-246 (1985).

Rudnick, L.R., and Tueting, D., "Investigation of Free Radcials Produced During Coal Liquefaction Using ESR", Fuel, 63(2), 153-157 (1984).

Salim, S.S. and Bell, A.T., "Effects of Lewis Acid Catalysts on the Hydrogenation and Cracking of Three-Ring Aromatic and Hydroaromatic Structures Related to Coal", Fuel, 63(4), 469-476 (1984).

Sapre, A.V., and Gates, B.C., "Hydrogenation of Aromatic Hydrocarbons Catalyzed by Sulfided CoO-MoO3/ -Al2O3: Reactivities, Reaction, Networks, and Kinetics", PREPRINTS, ACS, Div. Fuel Chemistry, 25(1), 66-77 (1980).

Scaroni, A.W., Jenkins, R.G., Utrilla, J.R., and Walker, Jr., P.L., "Lewis Acidity and Coking of Hydrodesulfurization Catalysts", Fuel Processing Technology, 9, 103-108 (1984).

Scaroni, A.W., and Jenkins, R.G., "Coking of Aromatics Over an HDS Catalyst", PREPRINTS, ACS, Div. Petroleum Chem., 30(3), 544-548 (1985).

Schweighardt, F.K., DOE, Quarterly Report No. 2, DOE/PC/60783-2, February 1984.

Schweighardt, F.K., DOE, Quarterly Report No. 5, DOE/PC/60783-5, October 1984.

Schindler, H.D., and Chen, J.M., DOE, Quarterly Report No. 9, DOE/ET/14804-9, April 1983.

Shell Chemical Company, "Presulfiding Procedure for Shell Hydrotreating Catalysts", Technical Bulletin SC:463-81 (1981).

Shah, Y.T., Gas-Liquid-Solid Reactor Design, McGraw-Hill (1979).

Smith, Jr., J.E., DOE, Final Report, DOE-FG22-84PC70814, April 1985.

Stenberg, V.I., DOE, Final Report, DE-FG22-82PC50814, April 1985.

Stenberg, V.I., Jones, M.B., and Suwarnasarn, N.J., "Radicals in Coals During Pyrolysis in Relation to Liquefaction Conversion", Fuel, 64(4), 470-474 (1985).

Sullivan, R.F., "Two-Stage Catalytic Hydrocracking of ITSL Oil for Jet Fuel and Naptha", PREPRINTS, ACS, Div. Petroleum Chemistry, 30(3), 503-512 (1985).

Suzuki, T., Yamada, O., Takahashi, Y. and Watanabe, Y., "Hydroliquefaction of Low-Sulfur Coals Using Carbonyl Complexes-Sulfur as Catalysts", Fuel Processing Technology, 10, 33-43 (1985).

Thompson, L.F., and Holmes, S.A., "Effect of Multistage Hydroprocessing on Aromatic and Nitrogen Compositions of Shale Oil", Fuel, 64(1), 9-14 (1985).

Tischer, R.E., Narain, N.K., Stiegel, G.J., and Cillo, D.L., "The Effect of Ni/Mo(W) Ratio on the Activity of Coal-Liquid Upgrading Catalysts", PREPRINTS, ACS, Div. Petroleum Chemistry, 30(3), 459-464 (1985).

Tscheikuna, J., "Effects of Titanocene Dichloride on Catalytic Hydrogenation of Hydrocarbons", M.Sc. Thesis, Oklahoma State University (1984).

Tscheikuna, J., and Seapan, M., "Effects of Titanocene Dichloride on Catalytic Hydrogenation of Hydrocarbons", PREPRINTS, ACS, Div. Petroleum Chemistry, 30(3), 438-445 (1985).

Vernon, L.W., "Free Radical Chemistry of Coal Liquefaction: Role of Molecular Hydrogen", Fuel, 59(2), 103-106 (1980).

Yamada, Y., Matsumura, A., Kondo, T., Ukegawa, K., and Nakamura, E., "Free Radicals Formed in Hydrotreated Coal Liquid and Influence of Oxygen", Liquid Fuels Technology, 2(2), 165-176 (1984).

Yokono, T., Kohno, T., and Sanada, Y., "Interaction Between Coal and Liquefaction Catalysts Studied by High Temperature Electron Spin Resonance", Fuel, 64(3), 411-413 (1985).

Yoshimoto, I., Itoh, H., Makabe, M., and Ouchi, K., "Pressure and Temperature Effects on the Hydrogenation of Coal-Derived Asphaltene", Fuel, 63(7), 978-983 (1984).

APPENDIX A

MAIN COMPONENTS OF THE SYSTEM

Reactor System

The reactor system consisted of two trickle-bed reactors connected in series, and equipped with temperature programmer/controllers and heating systems. In this study, only the top reactor was used.

Top reactor

The top reactor consisted of a 17-inch (43.2-cm) long, 0.5-inch (1.27-cm) outer diameter and 0.035-inch (0.089-cm) thick, 316 stainless steel tube, fitted with a 1/2-inch (1.27-cm) Swagelok cross at the top and 1/2-inch (1.27-cm) Swagelok union at the bottom. The effective reactor length was 16-inches (40.6-cm) as shown in Figure 59. Two 1/2-inch (1.27-cm) to 1/4-inch (0.64-cm) reducers were connected to both sides of the cross. A 1/8-inch (0.32-cm) outer diameter, 316 stainless steel tube with one end welded shut was used as a thermowell. The thermowell was secured in the middle of the reactor by a 1/4-inch (0.64-cm) to 1/8-inch (0.32-cm) reducing union which was drilled for inserting the thermowell. The reducing union was connected to the 1/2-inch (1.27-cm) cross by a 1/2-inch (1.27-cm) to 1/4-inch

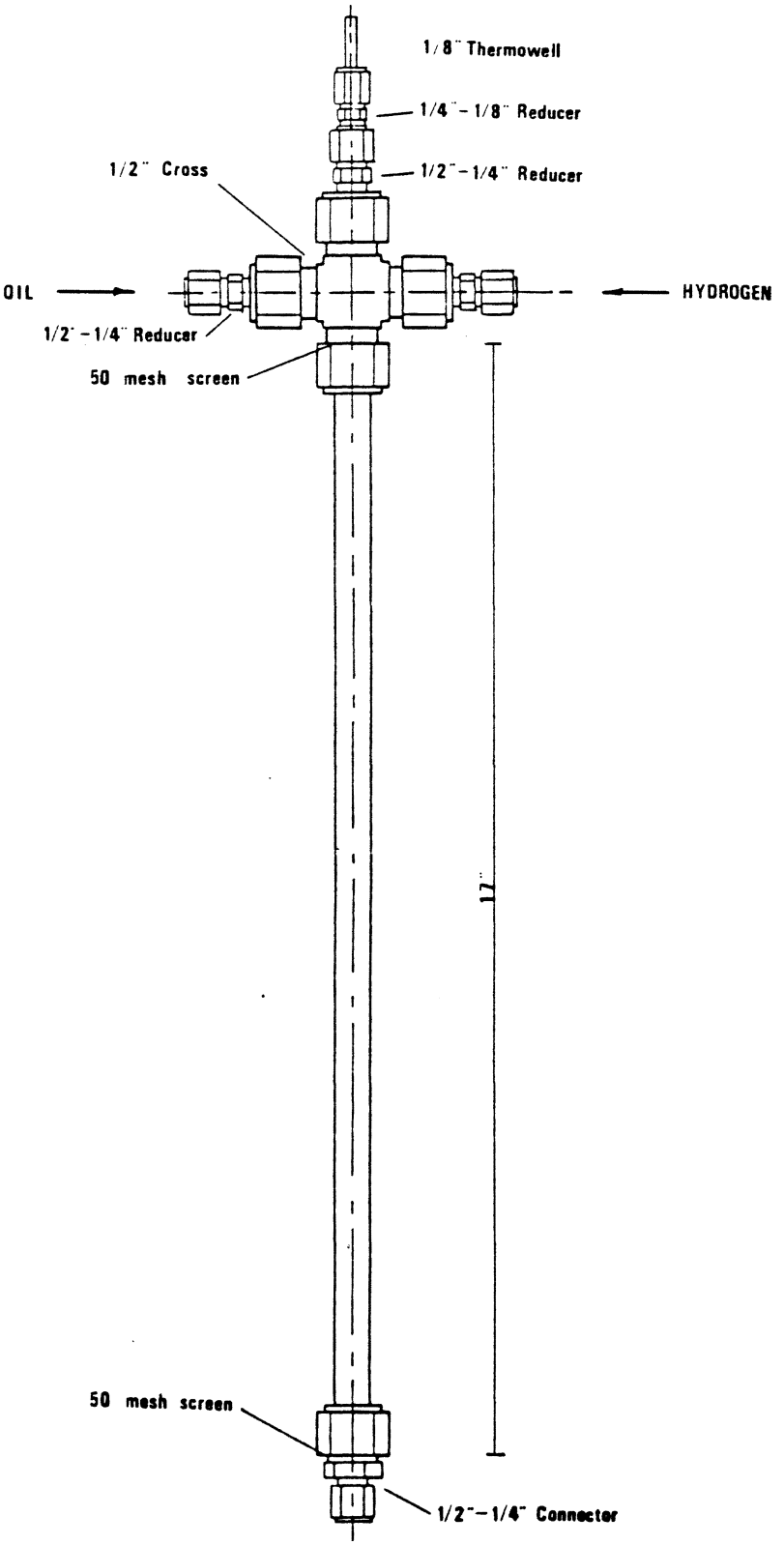

Figure 59. Top Reactor

(0.64-cm) reducing union. A stainless steel 50-mesh screen supported the catalyst bed. The bottom of the reactor was fitted with a 1/2-inch (1.27-cm) to 1/4-inch (0.64-cm) reducer to connect to the reducer to the interstage sampling system.

Reactor Heating System

A two-piece aluminum block, with grooves of reactor diameter running across the entire length was used as the heating block for the top reactor. The blocks were secured and bolted together around the reactor tube. The heating blocks were 14-inches (35.6-cm) long. The heating blocks were fitted with 3.5-inch (15.24-cm) heating bands rated at 300 watts placed around the assembled block. The power was supplied to the heating bands from either a temperature programmer/controller or a series of variable voltage suppliers (variacs). For the temperature programmer/controlloer, a platinum resistance thermocouple was placed in a hole drilled in the aluminum block, and used to give feedback to the temperature programmer/controller.

Felt material in the form of cylinders split down the middle were used to insulate the reactor. Fiberglass was also wrapped around the reactor

Oil Feed System

The oil feed system consisted of a tank, a Ruska positive displacement pump, and a rupture disk/safety line.

The feed tank was made of stainless steel and was 8 inches (20.32-cm) in diameter and 14 inches (35.56-cm) high. The feed tank could be pressurized, heated, and stirred to handle highly viscous fluids.

Liquid was fed to the reactor by the Ruska pump, which was operable up to 10,000 psig (68 MPa). The pump could be heated for easier flow along with the feed lines. In this study, neither the pump nor the feedlines was heated. Pump pressure was measure by pressure gauge 41 (refer to Figure 3 for gauge and valve numbers). The liquid feed rate was preset to the desired value before the pump was started.

To protect the oil feed system from excessive pressure, a switch set at 2500 psig (17 MPa) would shut off the Ruska pump when the pressure would exceed the 2500 psig pressure limit. A safety line, equipped with 2 rupture disks (rated at 2700 psig and 3200 psig) and a surge tank protected the system in case the safety switch would fail to operate.

Gas Feed System

Hydrogen or nitrogen gas flowed from cylinders through a manifold, which allowed the changing of gas cylinders without interrupting the run. The gas flow rate was metered by a high pressure gas rotameter which could be operated at pressures up to 5000 psig (34 MPa). The inlet gas pressure was regulated by the gas manifold regulator. A Heise pressure gauge was used to monitor the pressure.

An excessive gas flow check valve (installed close to

the manifold) would shut off the gas supply line in case of a line rupture. An emergency quarter-turn vavle was also installed to rapidly cut off the gas flow to the system in case of an emergency. Two flow-check valves were installed at the entrance to the reactor to prevent oil from flowing in the reverse direction.

Pressure and Flow Control

The upstream pressure of the system was monitored by a 0-3000 psig (0-20.8 MPa) Heise pressure gauge. The downstream pressures were indicated by pressure gauges 43 (connected to sample bomb 1) and 44 (connected to sample bomb 2). The Heise gauge measured the reactor pressure.

The gas flow rate was maintained by micrometer valve 10. The downstream gas flow was monitored by a low pressure flow meter, or by a 0-500-cm^3 bubble flow meter.

The exit gas was continuously scrubbed in an ethanolamine solution. Liquid traps, containing alumina spheres, were used to prevent liquid from flowing into the gas-measuring devices.

Temperature measurement

Temperatures were measured inside the catalyst bed and outside the reactor walls. Three iron-constatan J-type thermocouples, 1/8-inch (0.32-cm) in diameter, were used to monitor the reactor wall temperature. The reactor catalyst bed temperatures were measured by three thermocouples, each

0.001-inches (0.0025-cm) in diameter, which were placed at 3-inch intervals along the bed in the thermowell. An Omega digital temperature indicator, equipped with a multipoint temperature selector switch, was used to read the temperatures sent from the thermocouples.

Sampling System

Two different sampling systems were used in this study: the product sampling system, and the interstage sampling system.

The product sampling system consisted of four sample bombs: two of them were used to trap the liquid product; the other two were used to knock out any liquid entrainment in the gas outlet line.

The first sample bomb, 180-cm^3 in volume, was connected to the bottom of the second reactor with a 1/4-inch (0.64-cm) stainless steel tube. The top of the sample bomb was connected to the gas outlet line. The bottom of the first sample bomb was connected to the top of the second sample bomb by a high pressure valve. This valve was kept shut during sampling to keep from interrupting the system.

Liquid and gaseous products flowed into the second sample bomb of 600-cm^3 capacity, where the two phases were separated. The gaseous phase flowed into the third sample bomb, where the condensed vapors were collected and separated. The third sample bomb connected to the second

through a bottom line and valve 7 to return the collected liquids into the second sample bomb.

The gas from the third sample bomb flowed into the fourth sample bomb, where any entrained liquid was removed. This sample bomb could be kept in an ice bath to help knock out any liquid particles entrained in the gas phase.

The gas from the fourth sample bomb flowed through a metering valve, a gas scrubber, and a low pressure rotameter before exhausting to the atmosphere.

Interstage Sampling System

The interstage sampling system was installed between the top and bottom reactors. It was designed to collect from 3 to 5-cm^3 of liquid sample without disturbing the normal operation of the system. The interstage sampler consisted of a three-way valve, a pressure gauge, and a high-pressure liquid-sample holder (see Figure 60).

Gas and liquid from the top reactor normally flow through the three-way valve into the top of the bottom reactor. During sampling, the valve was closed and the liquid product was allowed to accumulate in the bottom part for 5 to 10 minutes. The flow was then diverted into the liquid-sample holder where the liquid sample was collected. The liquid-sample holder was depressurized after the flow was diverted back to its normal path.

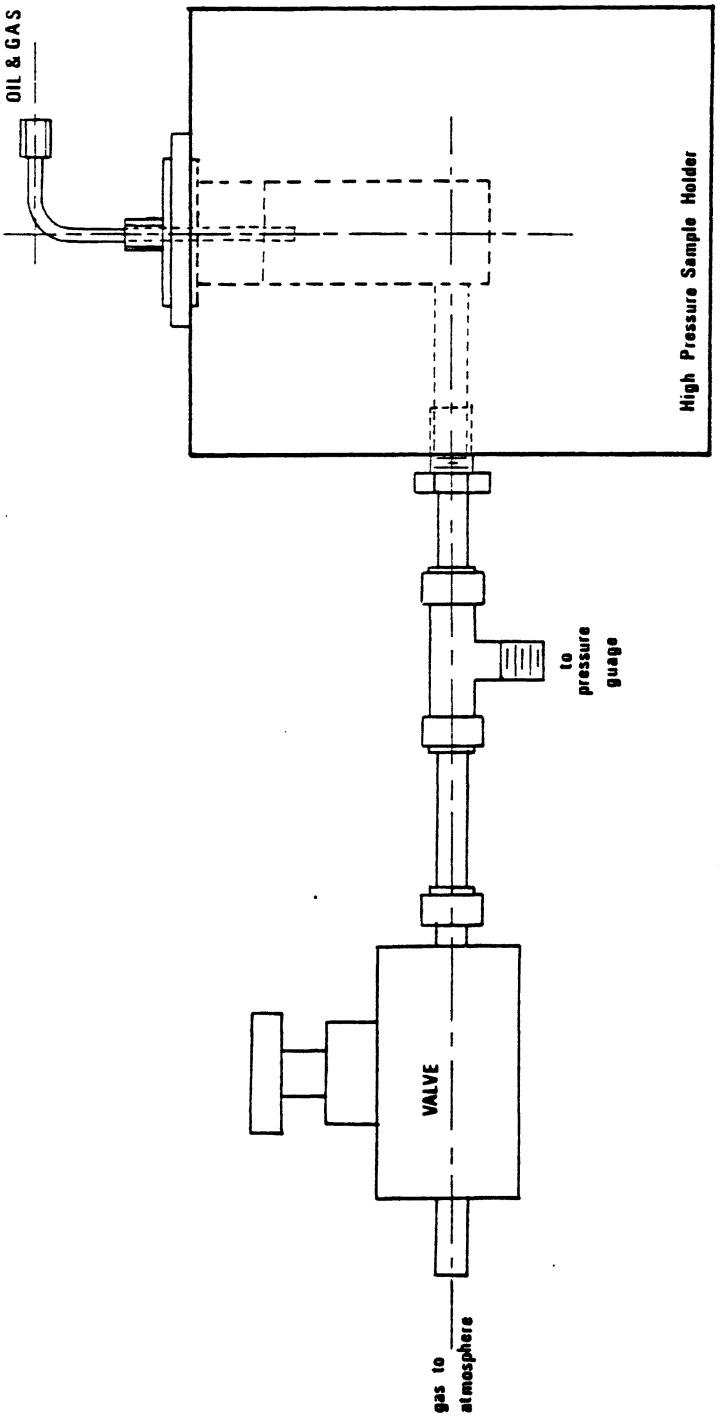

Figure 60. Interstage Sampler

Gas Detector

A combustible gas detector, MSA Model 501, was used to monitor the hydrogen concentration of the laboratory. A portable hydrogen sulfide detector was also used during catalyst sulfiding. The warning alarm would sound when the lab's hydrogen sulfide concentration exceed 17-20 ppm. The detector provided a digital readout of the present, average, and maximum hydrogen sulfide concentrations during a specified time interval.

Inert Gas Purging Facility

During sampling, the liquid product sample was purged with nitrogen gas in sample bombs 2 and 3 to remove any gases that were dissolved in the liquid sample. Nitrogen gas was also used to pressurize the sample bomb in order to remove the liquid sample. The nitrogen was supplied directly to the bottom of sample bomb 2 from the supply cylinder; the pressure was set by the pressure regulator of the cylinder. The nitrogen gas flowed through a flow-check valve into the sample bomb and was vented to the atmosphere through valve 8.

APPENDIX B

PROCEDURES

Refer to Figure 3 for valve and gage numbers.

Calcination

1) Close valves 2,3,13,14,24,32,35, and 51. Open valves 1,11,12,15,31,33,34,36, and 50.

2) Start the nitrogen flowing through the system at 250 to 300 psig and 400 cm^3/minute.

3) Turn on the temperature controller and control the heating rate at 2 C/minute.

4) When the reactor reaches 400 C, set the controller at isothermal for 1 hour.

5) After that hour has passed, set the temperature controller at the desired sulfiding temperature.

6) After the desired sulfiding temperature is reached, cut off the nitrogen flow.

Catalyst Sulfiding

A mixture of 5 volume percent hydrogen sulfide in hydrogen is used to sulfide the catalyst.

1) Turn on the hydrogen sulfide detector.

2) Shut valve 1.

3) Open valve 2, and start the sulfide flow through the reactor. The regulator pressure should be 80 psig, and the gas flow rate 400 cm^3/minute.

4) When the sulfiding time limit is up, cut off the gas flow by closing the main valve on the hydrogen sulfide/hydrogen bottle.

5) If desired, allow all the gas to flow out of the system. Then flush the system with nitrogen gas at 250 to 300 psig, and 400 cm^3/minute for 20 minutes.

Startup Procedure

1) Set the temperature controller 10 degrees C lower than the desired operating temperature.

2) Charge the feedstock into the feedtank. Set the pump to the desired feed rate.

3) Charge the feedstock into the Ruska pump by opening valve 23, and then traversing the pump to suck the liquid feed into the pump.

4) Close valves 23 and 24.

5) Traverse out the pump until the pump pressure is 1500 psig.

6) Close valves 11 and 3.

7) Pressurize the reactor with hydrogen to 1500 psig.

8) Open valves 4, 9, and 13. Make sure that valves 5, 7, and 8 are closed.

9) Set the nitrogen purge cylinder to 1500 psig. Open valve 6 to pressurize the sample bombs to 1450 psig. Close

valves 4 and 6.

10) Open valves 1 and 3. Adjust the hydrogen flow rate to 400 cm^3/minute, using valve 10 and the bubble flow meter.

11) Start the Ruska pump and open valve 24.

12) Adjust the temperature controller to the desired operating temperature.

Normal Operation

Record the following once every hour:

1) the temperature profile of the reactor;

2) the temperature profile of the heating block;

3) pressure gage readings;

4) pump scale reading;

5) inlet and outlet gas readings;

6) gas manifold reading.

Valve Positions During Normal Operation

POSITION	VALVE NUMBER
Open	1,3,9,10,13,15,21, 22,24,31,33,34,36,50.
Closed	2,4,5,6,7,8,11,12, 14,20,23,32,35,51.

Sampling Procedure

Liquid Sampling

1) Place a jar under the spout in the sampling

compartment.

2) Raise the nitrogen pressure to 100 to 200 psig.

3) Close valves 3 and 9.

4) Slowly open valve 8 to drop the pressure in sample bomb 2 to atmospheric pressure. If the pressure in sample bomb 1 drops, tighten valve 3 down.

5) Open valve 4 and then slowly open valve 6 to pressurize sample bomb 2 to 100 to 200 psig. Allow the purge to continue for 5 minutes.

6) Shut valves 8 and 6, in that order.

7) Slowly open valve 5 to take the sample. Close valve 5.

8) After the sample has been taken, raise the nitrogen purge pressure to 1500 psig or the maximum pressure available, which ever is less.

9) Open valve 6 slowly to pressurize sample bomb 2 to 1450 psig. Close valve 6.

10) Shut valve 4. Open valves 3 and 9.

11) Transfer the sample to a clean jar, and label that jar.

ESR Sample

1) Swab the interstage sample tube (running out of valve 51) with a pipe cleaner.

2) Make sure that the valve on the interstage sampler is shut tight. Gently tighten the cover to the sampler. Connect the sampler to the reactor via valve 51.

3) Close valve 50.

4) Wait 5 minutes.

5) Slowly open valve 51 and allow liquid to leak into the interstage sampler.

6) Close valve 51.

7) Disconnect the interstage sampler from the reactor. Open the interstage sampler.

8) Inject 0.5 cm^3 of the liquid sample into a quartz ESR tube. Cap the tube. Label the tube.

9) Place the tube into the dewar filled with liquid nitrogen.

10) Clean the interstage sampler with acetone.

Shutdown Procedure

1) Turn off the feed pump.

2) Close valve 24.

3) Turn off the temperature controller.

4) Traverse back the feed pump until the pump pressure reading is 0 psig. Drain the pump by opening valve 20 and traversing the liquid out.

5) When the reactor cools down to 250 C, cut off the hydrogen flow.

6) Depressurize the reactor to 250 psig, and start the nitrogen flow to purge and cool the reactor.

7) Collect the last bottom sample after the reactor reaches room temperature.

8) Depressurize the reactor and then remove the

reactor insulation.

9) Pull off the heating block; disconnect the feed lines, 3-way valve, and sample bombs from the reactor.

10) Cut the reactor and separate the catalyst bed into 5 parts, from the top to the bottom of the catalyst bed.

11) Place the catalyst samples in clean jars and label the jars.

Clean Up

1) Drain the feed from the feed tank.

2) Wash the pump and oil feed line with acetone.

3) Wash the sample bomb system with acetone.

APPENDIX C

SULFUR ANALYSIS

Several problems were encountered when the Horiba SLFA-200 Sulfur Analyzer was used to analyze the amount of sulfur in the coal liquid oil samples. Readings for the same sample would increase over a period of days or weeks, and eventually, the concentration of sulfur in a hydrotreated oil sample would become greater than that for the original feed.

Two samples, E12-1 and E15-FEED, were analyzed occasionally over a period of months. The two samples were stored at room temperature on a lab bench between each analysis. Table XXII lists the results of these analyses, and Figures 61 and 62 plot the results. It can be seen that the sulfur concentration of each sample appears to have increased with time. This is partly due to evaporation of the lighter components of the sample, leaving the sulfur-rich heavier components in the sample container, thus increasing the sulfur concentraton of the sample. This was confirmed when it was noted that the volume of each sample would decrease with time spent on the lab bench.

However, long-term evaporation alone could not account for the erratic sulfur readings. There was still an unkown

TABLE XXII

EFFECT OF TIME ON SULFUR READINGS
FOR TWO SAMPLES

DATE*	E12-1 CONC. (WT %)	E15-FEED CONC. (WT %)
8/1/86	0.20	0.12
8/4/86	0.21	0.17
8/5/86	0.22	
8/6/86		0.18
8/11/86	0.26	0.20
8/14/86	0.26	
8/15/86		0.23
8/19/86	0.29	
8/20/86		0.23
8/22/86	0.28	
8/27/86	0.32	0.24
9/5/86	0.38	0.29
9/12/86	0.39	0.29
9/17/86		0.28
10/27/86	0.40	
10/29/86	0.35	0.26

*Samples were made on 7/29/86.

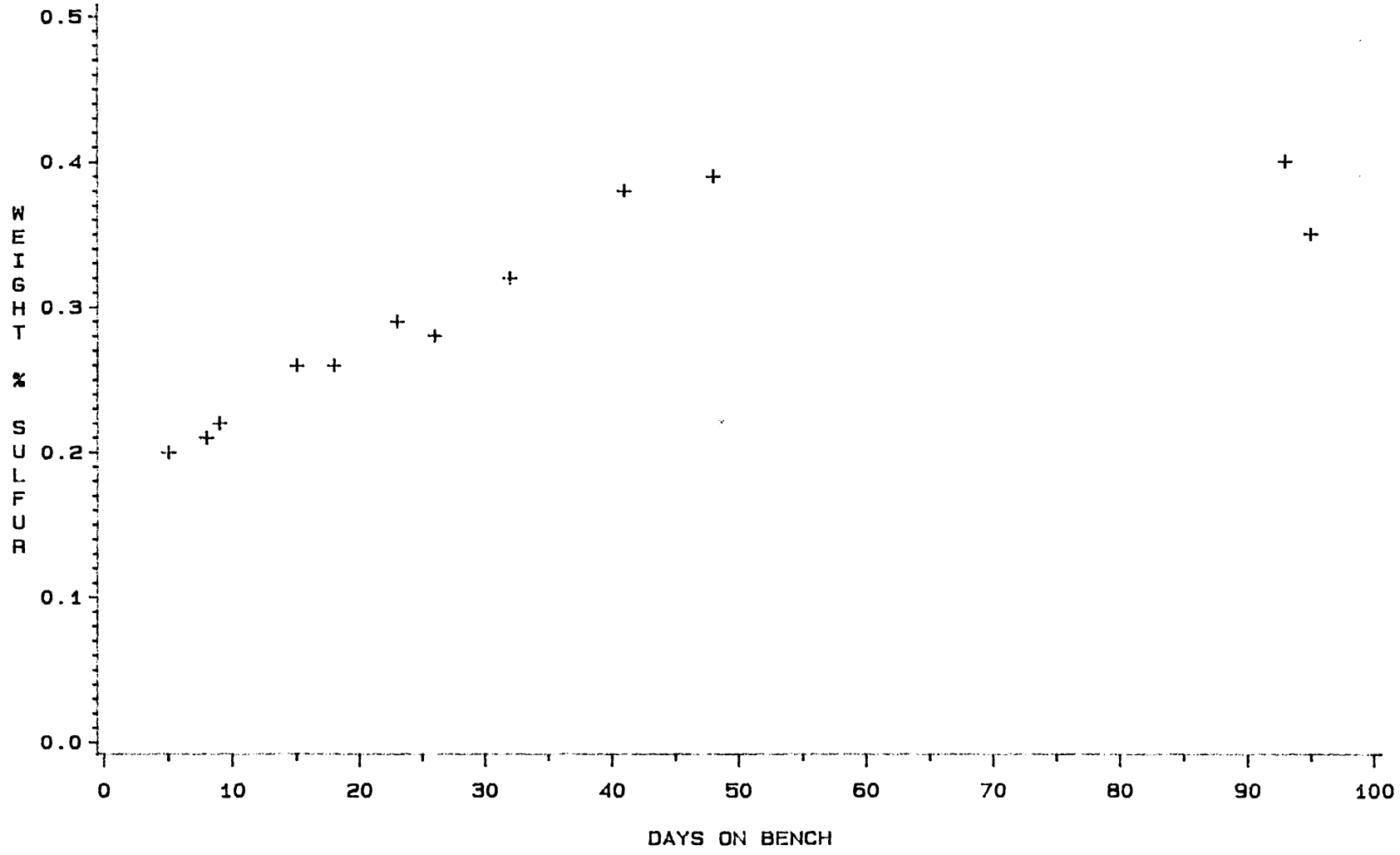

FIGURE 61. EFFECTS OF TIME ON SULFUR READING
FOR SAMPLE E12-1

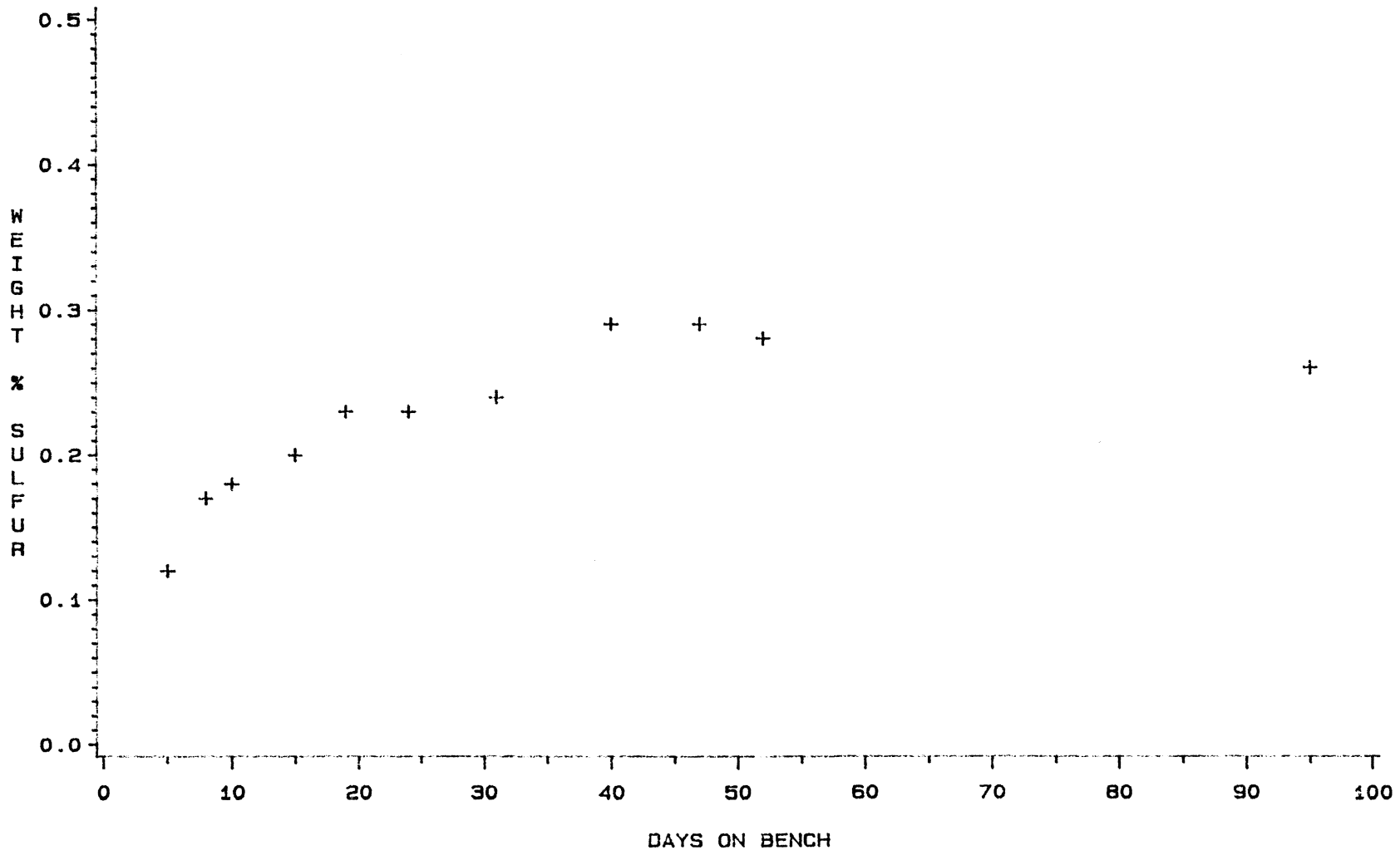

FIGURE 62. EFFECTS OF TIME ON SULFUR READING FOR SAMPLE E15-FEED

short-term effect on the apparent sulfur concentrations of the samples analyzed. At first, it was thought that a selective adsorption of the heterogenous sulfur compounds upon the mylar screen of the sample container was responsible for the sulfur discrepancy. However, a used mylar screen was reanalyzed, and there was no difference between the used and the new mylar screen. However, it was noted that whenever an old sample was shaken immediately before analysis, its apparent sulfur concentration would decrease and become consistent with previous readings. Thus, it appears that there was some settling of the heavier sulfur-rich compounds, which was read by the Horiba machine as an increase in sulfur concentration.

All oil samples were reanalyzed; each sample was reanalyzed immediately after preparation. Table XXIII presents the original and amended sulfur concentrations for all the oil samples analyzed. It is obvious that the amended readings are much more consistent and reproducible than those for the original readings, thus confirming that the earlier errors in sulfur concentration were due to long-term evaporation and also to short-term settling of the sample.

TABLE XXIII

COMPARISON OF OLD AND REANALYZED
SULFUR SAMPLES

SAMPLE	BEFORE	AFTER	SAMPLE	BEFORE	AFTER
E2-12	0.00	0.00	E11-3	0.21	0.13
E2-24	0.00	0.00	E11-4	0.04	0.11
E2-36	0.00	0.00	E11-5	0.37	0.15
E2-48	0.00	0.00	E12-1	0.20	0.14
E2-60	0.00	0.00	E12-2	0.34	0.15
E3-12	0.22	0.00	E12-3	0.14	0.14
E3-24	0.00	0.00	E12-4	0.08	0.00
E3-36	0.00	0.00	E12-5	0.13	0.10
E3-48	0.71	0.00	E13-1	0.17	0.12
E3-60	0.08	0.00	E13-2	0.18	0.11
E4-12	0.26	0.98	E13-3	0.15	0.11
E4-24	0.03	0.03	E13-4	0.16	0.12
E4-36	0.00	0.00	E13-5	0.60	*
E4-40	0.00	0.00	E14-1	0.25	0.17
E4-50	0.00	0.00	E14-2	0.28	0.13
E4-60	0.00	0.00	E14-3	0.17	0.11
E7-6	1.09	0.34	E14-4	0.15	0.12
E7-12	0.09	0.00	E14-5	0.17	0.10
E7-18	0.01	0.00	E14-6	0.17	0.12
E7-24	0.00	0.00	E14-7	0.16	0.12
E7-30	0.03	0.00	E14-8	0.27	0.19
E7-36	0.04	0.00	E15-1	0.20	0.15
E7-42	0.00	0.00	E15-2	0.14	0.15
E7-48	0.04	0.00	E15-3	0.21	0.12
E7-54	0.00	0.00	E15-4	0.16	0.12
E7-60	0.00	0.00	E15-5	0.18	0.12
E8-6	0.24	0.12	E15-6	0.00	0.11
E8-12	0.13	0.18	E15-7	0.14	0.11
E8-18	0.13	0.09	E16-1	0.24	0.14
E8-24	0.20	0.12	E16-2	0.18	0.13
E8-30	0.16	0.08	E16-3	0.17	0.13
E8-36	0.12	0.08	E16-4	0.18	0.18
E8-42	0.13	0.03	E16-5	0.20	0.10
E8-48	0.03	0.04	E16-6	0.19	0.12
E8-54	0.12	0.04	E16-7	0.18	0.13
E8-60	0.26	0.10	E17-1	0.15	0.17
E9-6	0.08	0.04	E17-2	0.19	0.08
E9-12	0.00	0.00	E17-3	0.19	0.13
E9-18	0.00	0.00	E17-4	0.18	0.11

TABLE XXIII (CONTINUED)

SAMPLE	BEFORE	AFTER	SAMPLE	BEFORE	AFTER
E9-24	0.00	0.00	E17-5	0.15	0.11
E9-30	0.00	0.00	E17-6	0.27	0.11
E9-36	0.00	0.00	E17-7	0.15	0.11
E9-40	0.00	0.00	E17-8	0.36	0.12
E9-50	0.00	0.00	E18-1	0.24	0.12
E9-55	0.11	0.00	E18-2	0.14	0.12
E9-60	0.00	0.00	E18-3	0.15	0.10
E10-1	0.03	0.05	E18-4	0.26	0.11
E10-2	0.05	0.05	E18-5	0.29	0.09
E10-3	0.09	0.06	E18-6	0.16	0.14
E10-4	0.06	0.13	E18-7-1&2	0.15	0.10
E10-5	0.28	0.08	E18-7-3	0.16	0.13
E11-1	0.10	0.10	E18-7-4	0.15	0.15
E11-2	0.13	0.11	E18-8	0.26	0.15

*Indicates sample not available for analysis.

APPENDIX D

HOMOGENOUS REACTION PRODUCT

When titanocene dichloride is dissolved in Tetralin, an insoluble homogenous reaction product is formed (Tscheikuna, 1984). This product was analyzed to determine the nature of the substance. Analysis methods included melting point determination, solubility tests, scanning electron microscopy, and elemental analysis.

The homogenous reaction product is a yellow, powdery solid. A micro-melting point apparatus was used to determine the melting poing of a small sample of the product. The sample was taken from room temperature to 350 C. The sample darkened gradually, turning light brown before 215 C, and dark brown before 250 C. The sample was char-black at 350 C. At no time during the test did any liquid form; therefore, it appears that the sample decomposed before reaching 350 C.

A study on the solubility of the homogenous reaction product in various solvents was made. The results of the study are shown in Table XXIV. Solvents of increasing polarity were tried, and only concentrated sulfuric acid was able to dissolve the product.

Scanning electron microscopy was used to examine the

TABLE XXIV

SOLUBILITY OF HOMOGENOUS REACTION PRODUCT IN VARIOUS SOLVENTS

Solvent	Solubility of product
Water (room temperature)	None
Water (75 degrees C)	None
n-Heptante	None
Pyridine	Very slight
Tetra-Hydro-Furan	Very slight
Chloroform	Very slight
Dilute Sulfuric Acid	None
Concentrated Sulfuric Acid	Very high

TABLE XXV

ANALYSIS OF HOMOGENOUS REACTION PRODUCT

Element	Weight percent	Mole percent
Carbon	28.8	31.3
Hydrogen	3.76	49.6
Titanium	33.3	9.14
Chlorine	34.1	12.5

physical structure of the product, and EDAX was used to determine if titanium and chlorine were present in the product. Figure 63 is an electron micrograph of the product, and Figure 64 is an electron micrograph of titanocene dichloride, the precursor of the homogenous reaction product. The reaction product appears highly amorphorous when compared to the crystalline structure of titanocene dichloride.

Figure 65 is an EDAX spectra of the product, and Figure 66 is one of titanocene dichloride. The presence of chlorine in the product was confirmed at a much lower concentration in the product than that in titanocene dichloride.

Carbon/hydrogen/nitrogen elemental analysis was used to determine the percentage of carbon (28.8 weight percent) and hydrogen (3.76 weight percent) in the product. Quantitative EDAX was used to determine the concentration of titanium (33.3 weight percent) present in the product. The balance of the product was assumed to be chloride (34.1 weight percent). Table XXV presents the quantitative analysis of the homogenous reaction product. Based upon these measurements, the empirical formula for the homogenous reaction product is $C_{10}H_{16}Ti_3Cl_4$. Further investigations are needed before a structural formula can be developed.

Earlier studies indicated the interference of titanocene dichloride with the catalyst activity and coking.

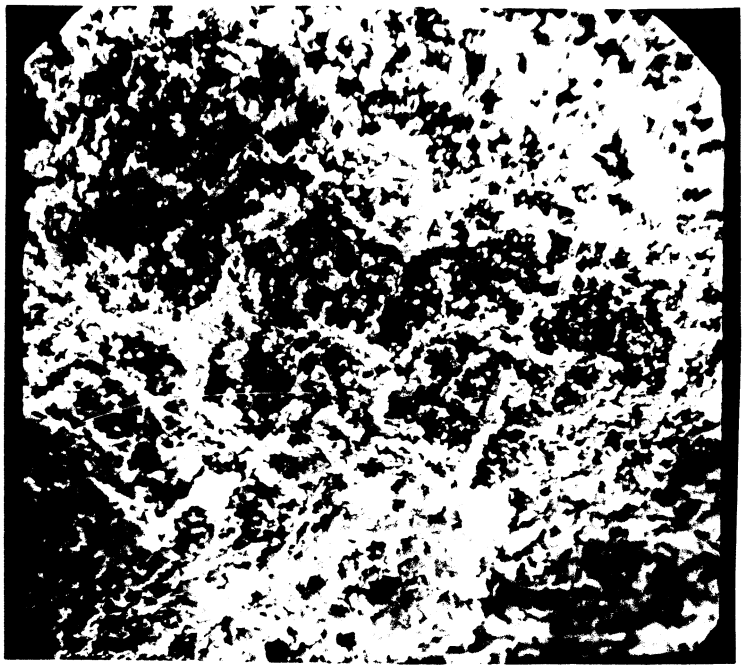

Figure 63. S.E.M. of Homogenous Reaction Product

Figure 64. S.E.M. of Titanocene Dichloride

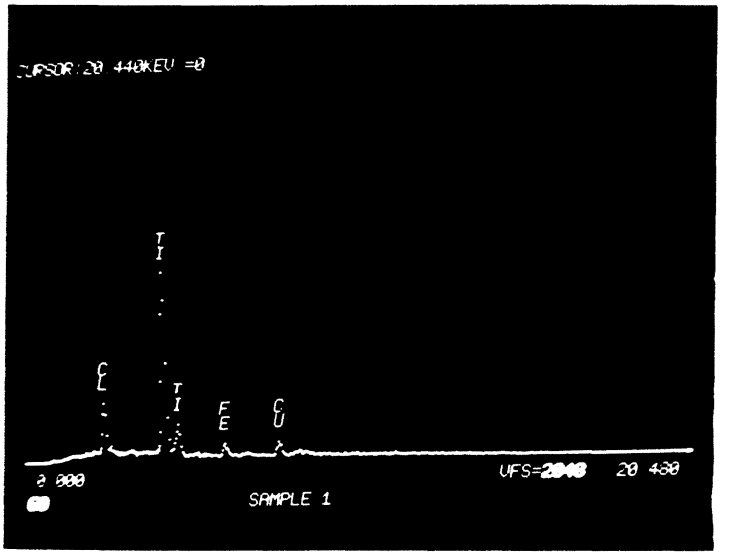

Figure 65. EDAX of Homogenous Reaction Product

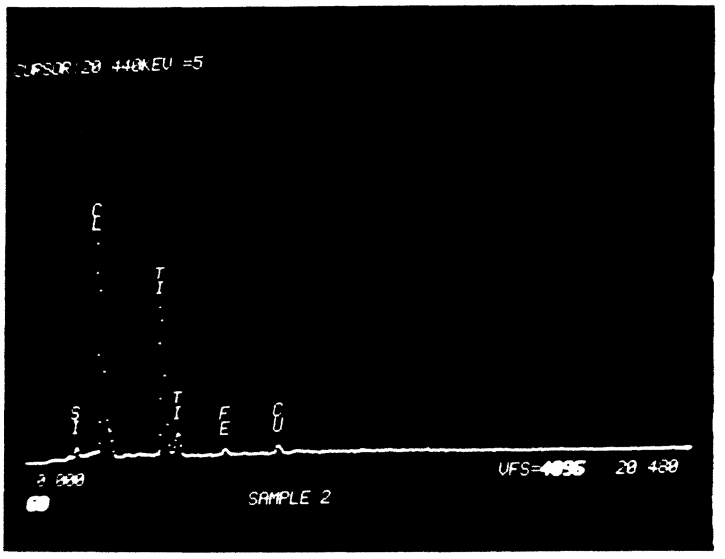

Figure 66. EDAX of Titanocene Dichloride

It was concluded that some intermediate compounds and/or free radicals were formed from the homogenous reaction of titanocene dichloride with Tetralin and could be responsible for the observed effects. In order to investigate the formation of free radicals from the homogenous reaction, e.s.r. spectroscopy was utilized.

A solution of 50 ppm of titanium as titanocene dichloride in Tetralin was prepared. The solution was allowed to react at room temperature. Samples of the solution were withdrawn 1-h, 24-h, AND 48-h after the solution was first allowed to react. The samples were analyzed by e.s.r. spectroscopy at room temperature, and at 77K.

At no time during the experiment were any free radicals detected. The threshold for the spectrometer was 1E12 to 1E15 unpaired spins; the spectrometer cavity window analyzed a sample approximately 0.17 cm^3 in volume; therefore, a free radical concentration of 9.8E-06 mol/liter was necessary for the spectrometer to detect any free radicals. However, no free radicals were detected; so if any free radicals were produced by the room temperature homogenous reaction, their concentration was less than 9.8E-06 mol/liter.

VITA

Harold Herbert Wandke

Candidate for the Degree of

Master of Science

Thesis: EFFECTS OF TITANOCENE DICHLORIDE ON THE FORMATION OF FREE RADICALS IN THE HYDROTREATMENT OF A COAL LIQUID

Major Field: Chemical Engineering

Biographical:

Personal Data: Born in Oklahoma City, Oklahoma, June 29, 1961, the son of John and JoAnn Dimmick. Married to Salli S. Sears on August 10, 1985.

Education: Graduated from Pioneer-Pleasant Vale High School, Waukomis, Oklahoma, in May, 1979; recieved Bachelor of Science Degree in Chemical Engineering from Oklahoma State University in May, 1984; completed requirements for the Master of Science degree at Oklahoma State University in December 1987.

Professional Experience: Student Engineer, Dow Chemical, Summer 1981; Research Assistant, School of Chemical Engineering, Oklahoma State University, June 1984 to July 1987.